INTEGRATED THEORETICAL AND EXPERIMENTAL STUDIES OF ORGANIC ATMOSPHERIC AEROSOLS

by

Michael Jacobson

A dissertation submitted in partial fulfillment of the requirements for the degree of

Doctor of Philosophy

University of Washington

1997

Approved by Robert Jay Charlson
Chairperson of Supervisory Committee

Program Authorized to Offer Degree Chemistry

Date December 18, 1997

Doctoral Dissertation

In presenting this dissertation in partial fulfillment of the requirements for the Doctoral degree at the University of Washington, I agree that the Library shall make its copies freely available for inspection. I further agree that extensive copying of this dissertation is allowable only for scholarly purposes, consistent with "fair use" as prescribed in the U.S. Copyright Law. Requests for copying or reproduction of this dissertation may be referred to University Microfilms, 1490 Eisenhower Place, P.O. Box 975, Ann Arbor, MI 48106, to whom the author has granted "the right to reproduce and sell (a) copies of the manuscript in microform and/or (b) printed copies of the manuscript made from microform."

Signature 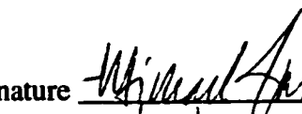

Date 12/18/97

University of Washington

Abstract

INTEGRATED THEORETICAL AND EXPERIMENTAL STUDIES OF ORGANIC ATMOSPHERIC AEROSOL

by Michael Jacobson

Chairperson of the Supervisory Committee: Professor Robert Charlson
Department of Chemistry

A combination of different projects are presented to (a) give the theoretical effects of organic aerosol on the nucleation and growth of cloud droplets and b) present measurements of organic aerosol material at a land-based site used to study the remote marine atmosphere.

The basis of the theoretical work is that organic aerosol material tends to have solubility in water that is lower than hygroscopic salts, but higher than other aerosol constituents such as mineral dust or elemental carbon (soot) particles. When present in an internal mixture with salt particles that deliquesce to form cloud droplets, the sparingly-soluble organic material would undergo gradual dissolution such that the critical supersaturation is lowered compared to droplets nucleated on salt particles alone. Results of an adiabatic cloud model are presented to show that the size distribution of activated droplets is shifted towards a smaller number of larger droplets as a result of this gradual dissolution. This effect is dependent on the amount and solubility of the organic material present in the particles, and would lower the reflectivity of clouds compared to the reference case of a cloud nucleated on purely hygroscopic aerosol. Atmospheric particle solubility therefore is a variable that influences the global radiative balance.

A thermal-optical carbon analyzer was built to measure ambient concentrations of organic and refractory carbon at Cheeka Peak, an atmospheric monitoring station on the

coast of the Olympic Peninsula of Washington State. Measurements took place continuously over the course of approximately one year, which is the largest data set of carbonaceous material for a site of this type. The instrument is described in detail, as well as the sampling methods used. The data shows that when quartz filters are used to collect atmospheric material in remote marine locations with very low concentrations of organic material, there is an organic vapor artifact that is approximately equal in mass to the amount of organic particles collected, adding to the uncertainty in the measurement. The average concentration of organic aerosol at this site is ca. 50 ng m^{-3}, compared with ca. 20 ng m^{-3} for refractory (black, soot) carbon.

TABLE OF CONTENTS

LIST OF FIGURES

LIST OF TABLES

ACKNOWLEDGMENTS

I would first like to thank my parents, William and Marilyn Jacobson for their encouragement of my scholastic development throughout my life. Their unfaltering belief in my capability of completing a Ph.D. and their enthusiastic assurance to me that years of being a poor graduate student were worth this goal has been a great inspiration to me to see my project to completion. Likewise, I am grateful for the support of my sister, Lisa Jacobson, who has managed to maintain a strong relationship with me despite the geographical distance that separates us. My friend Bodil Willumsen has been a great source of support since nearly the beginning of my graduate career, and has helped me solve both technical problems I have had in my research, and with the emotional ups and downs I have had as a graduate student. My many friends in Stockholm, Sweden have shown a surprisingly high level of interest in my work and progress towards my goals, even from so far away.

Professionally I have many people to thank for making my project happen. First is my advisor, Professor Robert Charlson, who has provided me with a paradigm for applying simple chemical concepts for investigating complicated scientific questions about the atmosphere. I have been strongly encouraged by his interest in my professional development, confidence in my scholastic abilities, and ability to recognize the importance of a discovery that at first seems to be a failure. Professor. David Covert and Dr. Tad Anderson have both been very valuable in teaching me the practical aspects of aerosol sampling and the many hours with them driving back and forth to Cheeka Peak as a beginning graduate student taught me a great deal about the field. Professor Richard Gammon has been a great help to me in both my laboratory work, providing me with the space to complete my tasks, and as a scientific mentor who has always been willing to listen to my concerns and provide valuable feedback. During my stay in Sweden, I learned a great deal from Professor Kevin Noone who has a very wide range of knowledge in the field, Professor H.C. Hansson, who is inspirational to me because of his

imaginative ideas about the hygroscopic properties of aerosols, and Professor Henning Rodhe, who is as involved in science policy as he is in scientific research. I would like to thank my collaborators Dr. Geert-Jan Roelofs who ran the cloud models for me in Utrecht, and Dr. Michelle Shulman with whom I first started thinking about solubility of organic compounds. Thanks also to Steve Gerst who analyzed my aerosol samples for carbon isotopes and helped me see the usefulness of this tool. I owe a great deal of thanks to Jordan Ferrier who put in endless hours driving to Cheeka Peak, analyzing my samples using the carbon analyzer while I was in Sweden. Jamie Wheeler has always been helpful providing computer data, and the occasional "attitude adjustment" when I have needed it. The other members of my group: Dr. Susan Harder, Dr. Mary Laucks, Tami Bond, and Sarah Doherty are all very talented scientists who have provided me with both encouragement and, occasionally, commiseration. Last but not least, I would like to acknowledge Professor William Hollingsworth at Carleton College, who got me interested in environmental chemistry in the first place.

CHAPTER 1: INTRODUCTION

Most aerosol particles in the atmosphere are invisible, tasteless, odorless, and generally not noticeable, but they are everywhere in the atmosphere. Even for those who study the particle-gas mixtures that comprise atmospheric aerosols, it is easy to forget that they exist. But aerosols, as I will refer to the particle phase of the mix, are extremely important atmospheric components. For such tiny individual pieces of material, their collective ubiquity causes some amazingly large effects on our planet. Clouds would not be able to form without a particulate mass with which water can condense. Entire mountain ranges can be hidden from view on otherwise cloudless days by hazes composed of particles. The radiative balance of our planet depends highly on the amount and type of particles present in the atmosphere [1-3]. Populations of large regions can become ill, find difficulty breathing, or experience eye irritation based on the particulate concentrations in the air, as seen recently in South-East Asia and Brazil, where forest fires have left the air thick with particles.

While most of the emphasis of the past decades has been on inorganics (sulfates, soils, inorganic elemental carbon), the focus of this dissertation is on atmospheric aerosols composed of organic compounds. Because of the extremely varied chemical and physical properties of organic compounds, and the elusiveness of particles themselves, these aerosols are especially challenging to characterize. This chapter illustrates the importance of studying the organic fraction in atmospheric aerosols and outlines the rest of the dissertation.

ATMOSPHERIC AEROSOLS: THE INCOMPLETE PICTURE

Fine particulate matter (diameter ≤ 2.0 μm) in the lower atmosphere is comprised of highly water-soluble inorganic salts, insoluble mineral dust, and carbonaceous material; this last fraction includes organic compounds ranging from very soluble to insoluble, plus elemental carbon. Fine particles are identified as a separate component of

the total aerosol because they are usually chemically different from coarse particles (>2μm), have different sources, much longer atmospheric lifetimes and very different effects. The water-soluble inorganic fraction of this aerosol, which is a mostly a mixture of various sulfate compounds [4, 5] has been studied extensively and several models of the geographical distribution and climatic effects of this group of compounds in the aerosol have appeared [5]. While somewhat less studied, the insoluble inorganic fraction has been analyzed, e.g. with nuclear methods and often consists of metal oxides, silicates, and clay minerals derived from soil dust. Unlike the salt and soil dust fractions, the organic compounds cover a very wide range of molecular forms, solubilities, reactivities, and physical properties which makes a complete characterization extremely difficult. The so-called "elemental" carbon (EC) aerosol has been studied extensively, but it is still not clear to what degree it is indeed elemental [graphitic, C(0)] material or high molecular weight refractory organic species or a combination of both. Consequently there is still no complete inventory of the chemical compounds that comprise the fine-particle organic aerosol from any site in the world, and only a limited understanding of the sources, sinks, transport, and transformation processes of these particles and their effects. Since organic compounds are usually the second most abundant component of fine aerosol after sulfates [4, 6, 7] our understanding of the numerous public health, climatic, and environmental issues surrounding atmospheric aerosols remain seriously hindered without more information on this fraction.

WHY ORGANIC AEROSOLS SHOULD BE STUDIED: THE ENVIRONMENTAL EFFECTS

While the organic fraction of the atmospheric aerosol is not well characterized there are a few outstanding examples of its environmental ramifications listed below that illustrate its potential importance. Furthermore, from the connection of these effects of organic aerosols to the molecular forms of the organic species, it will be seen that acquisition of a much fuller understanding of carbonaceous aerosols in general is justified.

DIRECT CLIMATE FORCING (REFLECTION OF SUNLIGHT BY AEROSOL PARTICLES)

Aerosol particles in the atmosphere directly influence climate by scattering and absorbing incoming solar radiation. The perturbation this causes in the global radiation budget (in units of watts per square meter) is called a climate forcing. The current estimate of total direct climate forcing from aerosol particles is -0.5 Wm^{-2}, averaged over the entire Earth [5]. This figure mostly represents the effects of sulfate aerosols, and does not take into consideration organics because of the general lack of knowledge on the concentrations of these components. However, given the ubiquity of carbonaceous aerosols, our understanding of the "direct effect" of aerosols on climate is certainly incomplete. Although there have been a few wide-ranging estimates of climate forcing by organic aerosols, such as that of Penner et al. [8] who report -2.0 Wm^{-2}, this estimate highly uncertain. Clearly, additional data on organic aerosols must be provided to better estimate changes in the Earth's radiative balance.

CLOUD NUCLEATION AND INDIRECT CLIMATE FORCING (CHANGES IN CLOUD REFLECTANCE)

Although standard cloud-nucleation theory is based on an assumption that cloud condensation nuclei (CCN) are composed of highly soluble inorganic salts [9], there are many highly- and slightly-soluble organic compounds which also can be cloud active [10]. Besides the essential role of providing solute for vapor-pressure depression, organics have often been mentioned as causing delays in droplet formation [11] or evaporation [12]. Such effects have long been suggested to result from organic films or coatings on incipient cloud droplets although both the physical and chemical data to support such ideas are meager to non-existent. Novakov and Penner [13], and Rivera-Carpio et al. [14] showed that organic aerosols can significantly contribute to the mass of cloud condensation nucleus particles (CCN), and Novakov and Corrigan [15] report that pure organic smoke from cellulose containing no salt component is able to form CCN without being associated with sulfates or other inorganic compounds. This indicates that organic compounds in smoke from biomass burning may be a significant source of CCN

and therefore indirect climate forcing [16]. For an in-depth discussion of the mechanism of indirect climate forcing see e.g. the review by Schwartz and Slingo [17].

RAINWATER CHEMISTRY AND ACIDIFICATION

Organic acids from C_1-C_{34} have been found in precipitation samples around the world, with formic and acetic acids generally predominating [18-25]. Although rainwater acidification generally is caused by sulfuric and nitric acid in areas affected by anthropogenic emissions, organic compounds found in aerosol particles (e.g. C_2 and higher diacids, formic, and acetic acids) may be major contributors to the acidity of rainwater in more remote regions where strong mineral acids are scarce [26-28]. The larger molecular weight acids are found in the low relative humidity atmosphere as aerosol particles, and are removed via incorporation into rain and cloud droplets.

TROPOSPHERIC OZONE AND PHOTOCHEMICAL SMOG

The only significant source of tropospheric ozone (O_3) is from the photolysis of NO_2 which produces atomic oxygen, leading to ozone after reaction with molecular oxygen (O_2). Organic compounds (both natural and anthropogenic) are involved in ozone production because organic peroxy radicals ($RO\cdot_2$) react with NO converting it to NO_2. Peroxy radicals are intermediate products resulting from initial reaction of organic compounds with hydroxyl radicals ($\cdot OH$). Thus ozone production is sensitive to the amount of organic material with respect to the amount of NO_x ($NO + NO_2$). Although discussion and research into this organic component has traditionally been linked to volatile (gaseous) compounds (VOCs), there is speculation that organic particulate matter is also involved in ozone production [29].

Since organic aerosols can also be a product of VOC oxidation by ozone, photochemical smog episodes have nearly always been associated with organic aerosols. This association has often been qualitative or even conjectural—since the chemical data sets are sparse for smog outside of Los Angeles, an area which is particularly rich in

organic materials [30-33]. Both primary (produced directly from sources) and secondary aerosols (from oxidation of gaseous species) are elevated in such episodes [31, 34, 35]. Important effects of the organic aerosol are visibility degradation (see below) and eye irritation where organic aerosols have often been alleged as the cause.

BIOGEOCHEMICAL CYCLING

There is evidence that organic aerosols are produced in significant quantities from the large amount of volatile organic compounds emitted naturally by vegetation [36-38]. The cycling of natural organic compounds play a large role in balancing the global carbon cycle and in the formation of oxidants (see description of tropospheric ozone above). Zimmerman and Chatfield [39] estimated that roughly 480 Tg per year of terpenes are emitted every year from natural sources. This figure is actually larger than the estimate of the total anthropogenic non-methane hydrocarbon emission rate of 60 Tg per year by Duce [40]. Terpenes are combinations of two units of isoprene, C_5H_8, which are joined together in either cyclic or acyclic ways. The double bonds in these compounds leave the molecule susceptible to oxidation by both ozone and the hydroxyl radical, yielding oxidized products that have very low vapor pressures compared to the parent compounds, and thus are usually found in the aerosol phase. Terpenes have been measured in the gas phase at many forested sites around the world including Scandinavia [41, 42], and in the rest of Europe [43]. The effect of terpenes on tropospheric ozone has also been modeled for a Swedish forest [44]. Went [45] first postulated that terpenoid compounds were responsible for the blue haze often associated with forested hilly areas, due to oxidative particle formation. Although it is clear that terpenes have a tendency to form particles when oxidized, this effect has not been investigated thoroughly in the natural atmosphere.

Incorporation of both natural and anthropogenic organic compounds into the particle phase is a principle mechanism of extraction from the atmosphere into other reservoirs. This cycling may take place by adsorption to large particles that are dry deposited, adsorption onto fine particles followed by wet deposition, or by dissolution

into solution droplets in clouds. The specific cycling process for any compound depends on properties governed by molecular form (vapor pressure, water solubility, etc.). Ballschmiter [46] provides a thorough review of biogeochemical cycling and fates of organic compounds.

VISIBILITY DEGRADATION

Aerosol particles, particularly those with sizes comparable to the wavelength of visible light, scatter and absorb light and thereby control the transmission of light through the atmosphere. Both primary and secondary aerosols are effective in this regard. White [6] has summarized calculations for apportionment of fine-particle scattering and reports that organics are sometimes responsible for as much as 60% of this scattering, especially in the urban areas of the western U.S. The average for the Eastern U.S. is 30%, while I am unaware of similar evaluations for Europe.

Colored (blue, yellow, brown, and black) smoke plumes from combustion sources utilizing fossil or biomass fuels have traditionally been targets for air pollution regulations. All such smokes have a significant organic content and can absorb light due to the presence of a variety of light-absorbing chromophores in the carbon-containing molecules. Some of the absorption is due to impure elemental carbon in graphitic form [47], although currently available analytical methods are not adequate for unambiguously apportioning light absorption to the organic/elemental carbon fractions. Wavelength dependent scattering, usually causing a smoke plume to appear blue, white, or gray (when scattered light is observed), or yellow to brown (when light transmitted through the plume is observed) is common with organic smokes due to the propensity of the molecular species that are involved to form submicrometer particles via condensation at elevated temperatures.

PHYSIOLOGICAL RESPONSE: TOXICITY

There are several types of highly toxic organic compounds found in the environment, but PAHs (polycyclic aromatic hydrocarbons), PCBs (polychlorinated biphenyls) and other organochlorine compounds have received the most attention as pollutants that occur in the aerosol phase. Man-made PCBs and organochlorines especially have been found in a very wide range of environments and matrices throughout the world, including arctic snows, seawater and myriad types of biological tissues [48-50]. Generally used as pesticides, these compounds are subject to long range atmospheric transport as both gases and particles [51], and are particularly damaging to Arctic ecosystems, which have very few species in the food chain. Arctic animals bioconcentrate these hydrophobic compounds because of the large amount of lipids in their tissues. PAHs are produced industrially and in biomass burning and are some of the most toxic and carcinogenic compounds known, even at extremely low concentrations [52, 53]. Bushby et al. [54] measured these and similar classes of compounds from wet and dry atmospheric deposition. The effectiveness of organic aerosols for physiological action is evident from the fact that aerosol forms are often selected for efficient delivery of medications on the one hand, and are used as chemical warfare agents on the other. It is unclear how the interaction of these compounds with water and other organic compounds affects their toxicological action.

GOALS OF THIS DISSERTATION AND OVERVIEW OF CONTENTS

This dissertation presents a tightly focussed and coordinated study of organic atmospheric aerosols in three distinct ways: A review of the chemical and physical properties that makes this aerosol fraction unique, a theoretical study of the effects some of these unique properties have on clouds and climate, and an experimental study of carbonaceous aerosols in a remote location. Using this approach, I have the following goals in mind:

1. **Provide a survey of recent literature illustrating the current state of knowledge about organic atmospheric aerosols.**

   The intention with the literature survey is not to be completely comprehensive, but rather to be illustrative and give a historical foundation for the theoretical and experimental sections that follow. Several comprehensive literature reviews have been produced [55, 56]. The recent review by Saxena and Hildemann [56] is particularly extensive and contains references to a large body of recent literature. I have attempted to select references that outline the major peculiarities of organic aerosols as atmospheric components and illustrate the limitations in our knowledge of their chemical and physical properties. This survey is in Chapter 2.

2. **Demonstrate theoretically that organic compounds may have large effects on clouds and planetary radiative balance.**

   Traditional theory of cloud formation describes droplets forming by condensation of water vapor on very highly soluble inorganic salts. It is becoming increasingly well accepted, however, that cloud droplets are also nucleated on particles that contain organic material. Because of their unique solubility properties, organics are not expected to dissolve into growing cloud droplets the same way that salt particles do. The ramifications of this dissolution process on droplet growth are calculated by utilizing an equilibrium thermodynamic droplet growth equation (the Köhler equation). Examination of these droplet growth effects on droplet growth is then extended to include consideration of cloud optical properties, and consequently climate. We also include a section discussing the phase characteristics of matter in growing droplets. This work is presented in Chapter 3. A published paper related to this work appears as Appendix A.

3. **Report the concentrations of organic and elemental carbon in the remote marine aerosol.**

Although continental aerosol has been fairly well surveyed for its content of carbonaceous material, the marine atmosphere is poorly represented in the literature for these types of studies. This is probably due to the cost of sampling from a shipboard platform, as well as very low aerosol concentrations that make sampling and analysis difficult for these aerosols. Data is presented here from filter samples of marine aerosol collected during on-shore flow at a mountaintop coastal site on the Olympic Peninsula in Washington State (Cheeka Peak). The inorganic components of the aerosol at this site have been characterized in previous studies but the contribution of carbonaceous materials has never been measured there. The study took place over the course of approximately one year and involved analysis for carbon using an instrument based on a thermal-optical method that was built for this study. This instrument is introduced in Chapter 4, and the data obtained with the instrument is presented in Chapter 5. A discussion of sampling artifacts due to gas phase adsorption and aerosol volatilization is discussed as it relates to this site, also in Chapter 5.

4. **Explore how the sampling and analysis techniques currently in use influence what we know about atmospheric organic aerosols.**

   Perhaps to a larger extent than for any other component of the atmospheric aerosol, what we find in the organic fraction is to a large extent determined by how we look. This is the theme of the conclusion chapter (Chapter 6) and includes a discussion of what can be done to help alleviate the important gaps in our knowledge of atmospheric aerosols.

In addition to the above information, I will report late breaking data on the ^{13}C and ^{14}C signatures for carbonaceous material in the marine atmosphere as measured at Cheeka Peak. These data have the potential to help determine the likely sources of the aerosol, and help confirm the existence of sampling artifact problems associated with quartz filter sampling. This material is presented in Appendix B.

NOTES TO CHAPTER 1

1. Charlson, R.J., J.J. Langner, H. Rodhe, C.B. Leovy, and S.G. Warren, *Perturbation of the Northern Hemisphere Radiative Balance by Backscattering from Anthropogenic Sulfate Aerosols.* Tellus, 1991. **43B**: p. 152-163.

2. Charlson, R.J., S.E. Schwartz, J.M. Hales, R.D. Cess, J. J.A. Coakley, J.E. Hansen, and D.J. Hofmann, *Climate Forcing by Anthropogenic Aerosols.* Science, 1992. **255**: p. 423-430.

3. Charlson, R.J., J.E. Lovelock, M.O. Andreae, and S.G. Warren, *Oceanic phytoplankton, atmospheric sulphur, cloud albedo and climate.* Nature, 1987. **326**: p. 655-661.

4. USEPA, *Criteria Document on Fine Particles.* 1996.

5. IPCC, *Climate Change*, ed. J.T. Houghton. 1995, Cambridge: Cambridge University Press.

6. White, *Section 4 of Visibility: Existing and Historical Conditions--Causes and Effects, J.C. Trijonis, ed.*, in *Acid Deposition: State of Science and Technology*, P.M. Irving, Editor. 1990, U.S. National Acid Precipitation Assessment Program: Washington, D.C. p. 85-102.

7. Heintzenberg, J., *Fine particles in the global troposphere. A review.* Tellus, 1989. **41B**: p. 149-160.

8. Penner, J.E., R.E. Dickenson, and C.A. O'Neill, *Effects of aerosol from biomass burning on the global radiation budget.* Science, 1992. **256**: p. 1432-1434.

9. Pruppacher, H.R. and J.D. Klett, *Microphysics of Clouds and Precipitation.* 1978, Dordrecht: D. Reidel.

10. Kulmala, M., P. Korhonen, T. Vesala, H.-C. Hansson, K. Noone, and B. Svenningsson, *The effect of hygroscopicity on cloud droplet formation.* Tellus, 1996. **48B**: p. 347-360.

11. Bigg, E.K., *Discrepancy between observation and prediction of concentrations of cloud condensation nuclei.* Atmos. Res., 1986. **20**: p. 82-86.

12. Gill, P.S., T.E. Graedel, and C.J. Weschler, *Organic films on atmospheric aerosol particles, fog droplets, cloud droplets, raindrops, and snowflakes.* Rev. Geophys. and Space Phys., 1983. **21**(4): p. 903-920.

13. Novakov, T. and J.E. Penner, *Large Contribution of Organic Aerosols to Cloud-Condensation-Nuclei Concentrations.* Nature, 1993. **365**: p. 823-826.

14. Rivera-Carpio, C.A., C.E. Corrigan, T. Novakov, J.E. Penner, C.F. Rogers, and J.C. Chow, *Derivation of contributions of sulfate and carbonaceous aerosols to cloud condensation nuclei from mass size distributions.* J. Geophys. Res., 1996. **101**(D14): p. 19,483-19,493.

15. Novakov, T. and C.E. Corrigan, *Cloud condensation nucleus actuivity of the organic component of biomass smoke particles.* Geophys. Res. Lett., 1996. **23**(16): p. 2141-2144.

16. Penner, J.E., C.C. Chuang, and C. Liousse. *The contribution of carbonaceous aerosols to climate change.* in *The Fourteenth International Conference of Nucleation and Atmospheric Aerosols.* 1996. Helsinki, Finland: Pergamon.

17. Schwartz, S.E. and A. Slingo, *Enhanced shortwave cloud radiative forcing due to anthropogenic aerosols*, in *Clouds, Chemistry and Climate*, P. Crutzen and V. Ramanathan, Editors. 1996, Springer-Verlag: Berlin-Heidelberg.

18. Likens, G.E., E.S. Edgerton, and J.N. Galloway, *The composition and deposition of organic carbon in precipitation.* Tellus, 1983. **35B**: p. 16-24.

19. Lunde, G., J. Gether, N. Gjos, and M.B.S. Lande, *Organic micropollutants in precipitation in Norway.* Atmos. Env., 1977. **11**: p. 1007-1014.

20. Matsumoto, G. and T. Hanya, *Organic constituents in atmospheric fallout in the Tokyo area.* Atmos. Env., 1980. **14**: p. 1409-1419.

21. Kawamura, K. and I.R. Kaplan, *Organic compounds in the rainwater of Los Angeles.* Envir. Sci. Technol., 1983. **17**: p. 497-501.

22. Galloway, J.N., G.E. Likens, and E.S. Edgerton, *Acid precipitation in the Northeastern United States: pH and acidity.* Science, 1976. **194**: p. 722-724.

23. Galloway, J.N., G.E. Likens, W.C. Keene, and J.N. Miller, *The composition of precipitation in remote areas of the world.* J. Geophys. Res., 1982. **87**: p. 8771-8786.

24. Guiang, S.F., III, S.V. Krupa, and G.C. Pratt, *Measurements of S(IV) and organic anions in Minnesota rain.* Atmos. Environ., 1984. **18**: p. 1677-1682.

25. Munger, J.W., J.J. Collett, B.C.J. Daube, and M.R. Hoffmann, *Carboxylic acids and carbonyl compounds in southern California clouds and fogs.* Tellus, 1989. **41B**(3): p. 230-242.

26. Chameides, W.L. and D.D. Davis, *Aqueous-phase source of formic acid in clouds.* Nature, 1983. **304**: p. 427-429.

27. Weathers, K.C., G.E. Likens, F.H. Bormann, S.H. Becknell, B.T. Bormann, B.C.J. Daube, J.S. Eaton, J.N. Galloway, W.C. Keene, K.D. Kimball, W.H. McDowell, T.G. Siccama, D. Smiley, and R.A. Tarrant, *Cloudwater chemistry from ten sites in North America.* Environ. Sci. Technol., 1988. **22**(9): p. 1018-1026.

28. Keene, W.C. and J.N. Galloway, *Organic acidity in precipitation of North America.* Atmos. Env., 1984. **18**(11): p. 2491-2497.

29. Council, N.R., *Rethinking the Ozone Problem in Urban and Regional Air Pollution.* 1991, Washington, D.C.: National Academy Press. 489.

30.

31. Hidy, G.M., P.K. Mueller, D. Grosjean, B.R. Appel, and J.J. Wesolowski, eds. *The Character and Origins of Smog Aerosols.* Advances in Environmental Science and Technology, ed. J.N.J. Pitts and R.L. Metcalf. Vol. 9. 1980, John Wiley & Sons: New York.

32. Rogge, W.F., M.A. Mazurek, L.M. Hildemann, G.R. Cass, and B.R.T. Simoneit, *Quantification of urban organic aerosols at a molecular level: Indentification , abundance and seasonal variation.* Atmos. Env., 1993. **27A**(8): p. 1308-1330.

33. Hildemann, L.M., M.A. Mazurek, G.R. Cass, and B.R.T. Simoneit, *Seasonal trends in Los Angeles ambient organic aerosol observed by high-resolution gas chromatography.* Aer. Sci. Technol., 1994. **20**: p. 303-317.

34. Husar, R.B. and W.R. Shu, *Thermal analysis of the Los Angeles smog aerosol.* J. Appl. Meteorol., 1975. **14**: p. 1558-1565.

35. Gray, H.A., G.R. Cass, J.J. Huntzicker, E.K. Heyerdahl, and J.A. Rau, *Characteristics of atmospheric organic and elemental carbon particle concentrations in Los Angeles.* Environ. Sci. Technol., 1986. **20**: p. 580-589.

36. Graedel, T.E., *Terpenoids in the Atmosphere.* Rev. Geophys. and Space Phys., 1979. **17**(5): p. 937-947.

37. Fehsenfeld, F., J. Calvert, R. Fall, P. Goldman, A.B. Guenther, C.N. Hewitt, B. Lamb, S. Liu, M. Trainer, H. Westberg, and P. Zimmerman, *Emissions of volatile organic compounds from vegetation and the implications for atmospheric chemistry.* Global Biogeochem. Cycles, 1992. **6**(4): p. 389-430.

38. Duce, R.A., V.A. Mohnen, P.R. Zimmerman, D. Grosjean, W. Cautreels, R. Chatfield, R. Jaenicke, J.A. Ogren, E.D. Pellizzari, and G.T. Wallace,

Organic material in the global troposphere. Rev. Geophys. Space Phys., 1983. **21**(4): p. 921-952.

39. Zimmerman, P.R. and R.B. Chatfield, *Estimates of the production of CO and H2 from the oxidation of hydrocarbon emissions from vegetation.* Geophys. Res. Lett., 1978. **5**: p. 679-682.

40. Duce, R.A., *Speculations on the budget of particulate and vapor phase non-methane organic carbon in the global troposphere.* Pure Appl. Geophys., 1978. **116**: p. 244-273.

41. Janson, R., *Monoterpene concentrations in and above a forest of scots pine.* J. Atmos. Chem., 1992. **14**: p. 385-394.

42. Janson, *Monoterpene emissions from scots pine and Norwegian spruce.* J. Geophys. Res., 1993. **98**(D2): p. 2839-2850.

43. Simpson, D., A. Guenther, C.N. Hewitt, and R. Steinbrecher, *Biogenic emissions in Eruope 1. Estimates and uncertainties.* J. Geophys. Res., 1995. **100**(D11): p. 22,875-22,890.

44. Johansson, C. and R.W. Janson, *Diurnal cycle of O3 and monoterpenes in a coniferous forest: Importance of atmospheric stability, surface exchange, and chemistry.* J. Geophys. Res., 1993. **98**(D3): p. 5121-5133.

45. Went, F.W., *Blue hazes in the atmosphere.* Nature, 1960. **187**: p. 641-643.

46. Ballschmiter, K., *Transport and fate of organic compounds in the global environment.* Angew. Chem. Int. Ed. Engl., 1992. **31**(5): p. 487-515.

47. Rosen, H., A.D.A. Hansen, L. Gundel, and T. Novakov, *Identification of the opticaly absorbing component in urban aerosols.* Appl. Optics, 1978. **17**(24): p. 3859-3851.

48. Tanabe, S., H. Tanaka, and R. Tatsukawa, *Bioaccumulation of PCBs, DDT and HCH isomers in the North Pacific ecosystem.* Arch. Environ. Contam. Toxicol., 1984. **13**: p. 731-738.

49. Tanabe, S. and R. Tatsukawa, in *PCBs and the Environment*, J.S. Waid, Editor. 1986, CRC Press: Florida. p. 143-161.

50. Hinckley, D.A., T.F. Bidleman, and C.P. Rice, *Atmospheric organochlorine pollutants and air-sea exchange of hexachlorocyclohexane in the Bering and Chukchi Seas.* J. Geophys. Res., 1991. **96**(C4): p. 7201-7213.

51. Patton, G.W., M.D. Walla, T.F. Bidleman, and L.A. Barrie, *Polycyclic aromatic and organochlorine compounds in the atmosphere of Northern Ellesmere Island, Canada.* J. Geophys. Res., 1991. **96**(D6): p. 10,867-10,877.

52. Payne, K., *Chemistry and Toxicology of PCDDs.* Chem. Ind., 1982. **9**: p. 298-300.

53. Stanley, J., R. Ayling, P. Cramer, K. Thornburg, J. Remmus, J. Breen, J. Schwemberger, H. Keng, and K. Watanabe, *PCDD and PCDF levels in human adipose tissue in the continental US collected between 1971 and 1987.* Chemosphere, 1990. **20**(7-9): p. 895-903.

54. Bushby, B., A. Fernandes, D. Wallace, and M. Kibblewhite, *Determination of Trace Organic Micropollutants in Atmospheric Deposition.* The Science of the Total Environment, 1993. **135**: p. 81-94.

55. Hahn, J. *Organic constituents of natural aerosols.* in *Aerosols: Anthropogenic and Natural, Sources and Transport.* 1979. New York: The New York Academy of Sciences.

56. Saxena, P. and L.M. Hildemann, *Water-organics in atmospheric particles: A critical review of the literature and application of thermodynamics to identify candidate compounds.* J. Atmos. Chem., 1996. **24**: p. 57-109.

CHAPTER 2: DESCRIPTION OF ORGANIC AEROSOL

INTRODUCTION

This chapter describes what is known and what is not known about carbonaceous atmospheric aerosols. The main points are:

1) There is evidence that organic compounds are a significant and ubiquitous aerosol component, but the distribution and molecular forms of these particles globally have only recently begun to be quantified. These studies carry very large uncertainties.

2) Organic aerosols come from a very wide variety of sources and although many of these sources have been identified, their relative importance is a matter of debate. The chemical composition of these particles depends largely on the sources and the conditions under which the particles were produced.

3) There are major uncertainties concerning the gas-particle partitioning of atmospheric organics, adding to the problem of apportioning sources and how to correctly sample organic aerosols.

4) Organic aerosols are involved in growth of water droplets in the atmosphere, although the ways this occurs depends on chemical form of the organic particle.

5) Organic aerosols are involved in chemical reactions in the atmosphere and their chemical form may change, possibly altering their effects.

In all, organic aerosols are an important, albeit extremely complicated atmospheric component, and most research presented thus far seems to generate as many new questions as it attempts to answer. What follows are the specifics of what has been learned.

SPATIAL DISTRIBUTION OF CARBONACEOUS AEROSOL

Carbon-based aerosols may be organic compounds, elemental carbon, or carbonate minerals. The latter are almost exclusively found as a remnant of soil dust in supermicrometer particles and will not be discussed further. Elemental (black) carbon in the atmosphere is generally internally mixed with organic compounds, and therefore a complete conceptual separation of the two chemical classes is not possible. Elemental, also called refractory carbon or soot, is nearly always linked to organics, but organic aerosols may exist independently of elemental carbon. The worldwide distribution of these aerosols is not well known because data are sparse, and what data do exist have usually been collected for short sampling durations. Liousse et al. [1] have collected available measurements and developed a model to describe the global distribution of carbonaceous aerosol. Their model relies on emission inventories of fuel usage and natural combustion, as well as natural sources of organic particulate. They report calculated average organic submicrometer particulate concentrations of 1-2 $\mu g\ m^{-3}$ for the eastern U.S., 0.5-1.0 $\mu g\ \ m^{-3}$ for the southwestern U.S., and as high as 10-12 $\mu g\ m^{-3}$ in central Europe, the Amazon basin, West-Central Africa, Eastern China, and Northern Australia. Marine estimates for organic particulate are mostly in the range 0.1-2.0 $\mu g\ m^{-3}$. These estimates appear to correlate well with the data that are available, although there are large uncertainties in both the emission factors and ambient measurements, which are in themselves hard to quantify. It has been shown that different types of biomass fuel sources lead to different black carbon to total carbon ratios in the product aerosol [2]. This complicates the problem of estimating the production of black versus organic carbon. White [3] has also surveyed the composition of fine particles in the U.S. That study indicates that organic compounds comprise approximately 30% of fine particulate mass in the eastern U.S. (both in urban and rural locations), between 20%-40% mass in the rural western United States, and 30%-80% mass in urban areas of the western U.S. Similar results are reported by Heintzenberg [4], who reviewed studies that included measurements of both total suspended fine particle (TSP) mass and chemical analysis from sites around the world. Reported averages of percentage of TSP that is organic are

31% in urban areas, 24% in non-urban continental areas, and 11% in remote regions. Although these studies do not report on the variability of organic contribution to fine particle mass, they do show that organic material is a ubiquitous and significant constituent of fine aerosol.

SOURCES

The source of particles determines both the chemical composition of the aerosol and the size distribution. Organic particles may be either directly emitted into the atmosphere (primary) or developed *in situ* by chemical reactions of gas phase compounds (secondary). The relative contribution of these two source processes depends on the local types of emissions as well as the meteorological and atmospheric chemical conditions in the area. Both primary and secondary aerosols can be of anthropogenic or natural origin. Depending on the type of formation, aerosols may be limited to the geographic region where they formed or possibly transported over very long distances before they become their final forms and are removed from the atmosphere.

Although the source strengths of organic and black carbon atmospheric particles are very uncertain, Liousse et al. [1] have estimated the following inventory of yearly emissions of submicrometer carbonaceous particles in Table 1. No uncertainty ranges were given for modeled results in the article, and forest fires are not considered "natural."

Table 2-1 Estimated source strengths of carbonaceous aerosols.

Source	Organic particulate (Tg/yr)	Black carbon particulate (Tg/yr)
Biomass Burning	44.6	5.63
Fossil Fuel	28.5	6.64
Natural Sources	7.8	0
Total	**81**	**12.3**

Biomass burning sources include burning of savannas, tropical forests, agricultural fires, and the burning of domestic fuels such as wood, charcoal, and dung. Determination of emissions and amount of biomass burned is extremely difficult, and these figures are subject to future revision. Fossil fuel sources are more easily estimated because of record keeping of the amount of fuel sold and studies on emissions from different sources. The only significant natural source of organic aerosol considered in this estimate is from photochemical oxidation of gaseous terpene emissions from vegetation. Direct emission of particles from plants was not included.

PRIMARY SOURCES

Plant Material

One form of natural primary organic aerosol results from the mechanical disintegration and dispersion of plant material fragments. Particles from this source are generally in the super-micrometer size range and have a distinctive n-alkane signature that has a predominance of compounds with an odd number of carbons from C_{27} to C_{33} [5-8]. Long range transport of this aerosol has been described by Folger [9] and Simoneit et al. [7], especially as part of aeolian dust in the Atlantic, downwind of Africa. Hildemann et al.[5] have recently determined the n-alkane profile of the waxes found on leaves in the Los Angeles area and correlated this profile with ambient samples. It was found that primary vegetation-derived aerosols account for less than 3% of the total fine aerosol burden in this urban area, but other studies have indicated that in remote locations this source may be more important [10]. Marty and Saliot [11] studied the odd-even carbon number preference as a function of particle size in the western equatorial Atlantic and reported that terrestrial sources were the dominant source of n-alkanes for particles larger than 1 μm. Smaller particles appeared to have an oceanic source. In other work, Schneider et al. [12] and Schneider and Gagosian [13] found that n-alkanes with an odd carbon number preference (land plant wax or soil origin) were predominant for all

particle sizes off the coast of Peru, but that this trend was more pronounced for the largest particle size fractions. For smaller particles, n-alkanes containing an even number of carbons became increasingly important. These compounds were attributed to anthropogenic sources but the authors do state the possibility of marine phytoplankton and bacteria as potential sources.

Viable Biological Particles

Primary production is responsible for the presence of viable biological microbes such as bacteria, viruses, and fungal spores, which are ubiquitous in the atmosphere and cover a very large size range from viruses (about 1 nm diam.) to pollen (up to 300 μm diameter) [14]. These particles are generally produced on the surface of plants and may be transported over very long distances [15], although Fuzzi et al. [16] recently measured biological particle populations in fogs and hypothesizes that fog droplets themselves can be favorable growth media for bacteria and yeasts.

By collecting particles on impactor plates that are coated with dyes that react with proteins in biological particles, larger biological particles (>2 μm) can be identified and counted using a light microscope, while smaller particles can be identified as biological on the basis of their morphology as seen in a scanning electron microscope (SEM) and by their elemental composition as analyzed by energy-dispersive X-ray detection (EDX) [17, 18]. Air masses that are influenced by rural areas generally have a large amount of giant biological particles such as pollen spores, whereas in urban and industrial air there is a higher concentration of smaller biological particles such as bacteria [19].

Bubble Bursting at the Ocean Surface

It has long been known that primary production over the oceans is caused at least in part by the ejection and dispersion of salt-water droplets from bursting bubbles at the sea surface [20]. The sea-salt aerosol that results may have an organic coating resulting from scavenging of surface active material from seawater, although the importance of this process as a source of marine organic aerosol remains speculative. Duce [21]

estimated that 1.4 Tg per year of fine mode particulate carbon is injected into the atmosphere from the ocean, which compares with about 10% of the total estimated anthropogenic source. Hoffman and Duce [22] investigated the factors that affect the amount of organic material that is deposited on particles emitted during bubble bursting and found that the distance the air travels in seawater before breaking at the surface is important, as well as the quantity and type of organic and surfactant material present in the seawater. The bubble-breaking mechanism is very complicated both from a physical and chemical point of view, which makes it difficult to generalize. To my knowledge there has not been subsequent work in this area or other attempts to estimate primary organic marine aerosol production.

There may be other mechanisms at work in producing marine organic particulate matter. Noone et al. [23] used single particle and x-ray excitation analysis and observed particles in marine aerosol that contained both carbon and chlorine, but no sodium. Sodium would be expected if the particles were sea-salt derived, and the authors suggest that this may be the result of a natural marine source of organohalogens. Indeed, several halogenated terpene compounds and other organohalogen compounds with low vapor pressures have been identified as having biological marine sources [24]. These compounds may be an underestimated marine organic aerosol.

Biomass and Fuel Combustion

Biomass and fossil fuel burning is one of the most important sources of primary organic particles globally, and combustion processes are in general the sole source of black carbon in the atmosphere [1, 25]. The amount of organic material compared to black carbon produced seems to depend on the type of material that is burned and the temperature of combustion [2]. Most of the work in identifying compounds originating from biomass burning sources has concentrated on polycyclic aromatic hydrocarbons (PAH's), which are toxic, and easily analyzed with GCMS. These types of compounds exist in both the gas and particle phase, which has been described by Ligocki and Pankow [26]. The concentrations and size of PAH molecules emitted in burning episodes

depends highly on the efficiency of burning, and does not seem to be affected by the type of plant being burned [27]. Oxygenated organic compounds also are produced by high temperature oxidation in biomass burning, some of which have vapor pressures that are sufficiently low to be found in the particle phase. Novakov and Corrigan [28] recently reported that the burning of cellulose, the molecule common to all wood species, produces smoke particles that are nearly 100% water soluble, which they have analyzed to be mostly carboxylic acids. Andreae et al. [29] analyzed particles produced in biomass-burning plumes in Brazil for monocarboxylic acids and methanesulfonic acid and found that all of the organic acid ions they searched for were significantly enriched. Very little additional work, however, has gone into sampling of ambient fires to determine the quantity and molecular forms of oxygenated, water-soluble organics produced in biomass burning. Particles derived from fossil fuel combustion have not been examined at all in this respect.

In urban areas, automobile emissions account for a significant amount of primary fine particulate matter. Rogge et al. [30] estimates that this figure is 21% of total particulate matter in Los Angeles. Car engine emissions of particles depend on a wide range of parameters relating to the type, size, and age of the engine, as well as the fuel and lubrication used. In the analysis by GCMS performed by Rogge et al. [30] on samples direct from automobile exhaust, it was found that of the 20% of the total amount of organics could be resolved in the GC spectrum, there were found n-alkanes, n-alkanoic acids, benzoic acids and a host of other cyclic, polycyclic, and aromatic compounds. Other unresolved fractions probably contained mostly branched alkane and cyclic alkane compounds.

SECONDARY ORGANIC AEROSOLS—AEROSOL FORMATION FROM THE GAS PHASE

Oxidation Reactions

Organic aerosols that are formed from the reactions of gases in the atmosphere are thought to be the result of oxidation of gaseous species by one of three electrophilic gases

present in trace amounts in the atmosphere: The hydroxyl radical (OH), ozone (O_3) and the nitrate radical (NO_3). These oxidizers are produced photochemically, and are active as reactants at only certain times of the day. O_3 is active both day and night, but OH is produced in large quantities only during the day from the photolysis of O_3. This produces singlet-D oxygen (an excited state of oxygen), which reacts with water vapor:

$$O_3 + h\nu \rightarrow O_2 + O(^1D) \qquad \text{(Eq. 2-1)}$$

$$O(^1D) + H_2O \rightarrow 2\ OH \qquad \text{(Eq. 2-2)}$$

NO_3 radical is only active at night because it photolyzes readily in the presence of sunlight.

The oxidized forms of gaseous organic compounds generally have vapor pressures much lower than the reduced compound. This is illustrated in Figure 2-1, which shows that vapor pressure is dependent both on the number of carbon atoms in the molecule and also on the number and type of polar functional groups.

In order for secondary aerosol formation to occur, the gas phase products of oxidation reactions must be produced in sufficiently high concentrations to condense either onto existing particles or to nucleate into a condensed form. The thermodynamics governing the gas-particle partitioning of organic compounds is covered in the next section, but generally speaking particle production will not occur if either the oxidation reaction is too slow or if the vapor pressure of the product is higher than that of the reduced form [31].

Laboratory Studies of Particle Formation

Most of the information on sources of secondary organics comes from controlled laboratory smog-chamber experiments where gases that have been measured in the atmosphere are introduced into a chamber and allowed to react with an oxidant. Usually a set of seed particles is provided in these experiments as surface for heterogeneous nucleation of the oxidized organics. The resultant aerosols are then examined using a

variety of methods including gravimetric analysis to determine aerosol yield, nephelometry to examine light scattering properties, differential mobility analysis and optical particle counting as sizing techniques, and carbon analysis to determine the amount of carbon transferred to the particle phase. It is not clear how much particle nucleation actually takes place in this manner and how much is based on homogeneous nucleation in the ambient atmosphere.

Organic Parent Gases

Based on a literature search of studies using reaction chambers, Grosjean and Seinfeld [32] have put together a remarkably short list of reactive organic gases (ROGs) that have been measured in the ambient atmosphere and have significant aerosol producing potential (i.e. those that have over a 10% conversion to aerosol in the presence of realistic atmospheric oxidant concentrations). These gaseous compounds are listed in Table 2-2. Although the chemistry of available precursor ROGs may be quite simple, dozens of aerosol and oxidized gas products can result from a single ROG because of differences in possible reaction pathways [33].

The anthropogenic gases listed in Table 2 are mostly found in automobile exhaust [32], whereas the terpenes are emitted naturally by trees [34]. One of the more studied product groups of ROG oxidation is dicarboxylic acids. These compounds are abundant in photochemical smog [33, 35, 36] and appear to be the products of the oxidation of cyclic and aliphatic diolephins, especially by reaction with ozone [33, 37-39]. There is strong evidence that the gaseous precursors of these aerosols can travel long distances and photochemically produce particles at locations very far away from the sources. This has been seen in several studies in Japan [40, 41], where there is a clear diurnal variation in the concentration of these species. These compounds have even been measured in the Arctic atmosphere at polar sunrise [42]. The presence of these aerosols affects visibility and climate through scattering of solar radiation, and also have effects on cloud droplet processes, which are discussed in more detail in Chapter 3.

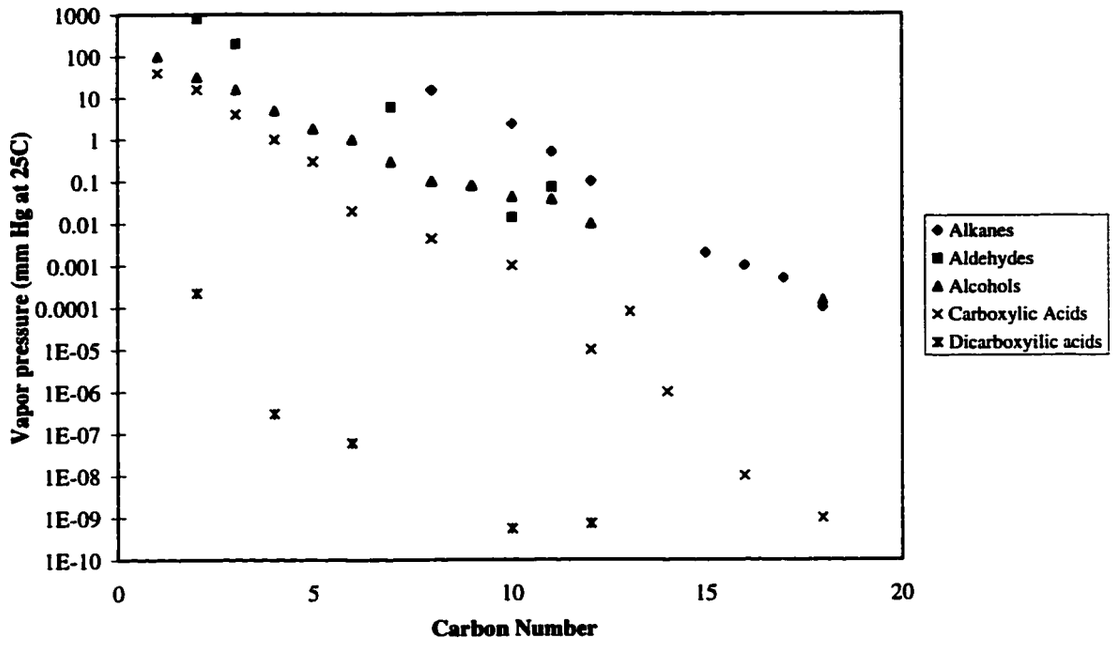

Figure 2-1 Vapor pressures of organic compounds as a function of carbon number and functionality. Data taken from Grosjean [33].

A goal in using information on the formation and transport of secondary aerosols is to be able to make models that predict the spatial distribution of particles and their chemistry, based on knowledge of gaseous emissions, weather patterns, and oxidant levels. Pandis et al. [43] made the first attempt to make such a model, and applied the calculations to sites in California where concurrent measurements were being made of organic and elemental carbon particulate [44]. Although the contribution of secondary organic aerosol to total carbonaceous aerosol can be roughly estimated by examining the correlation between the diurnal variations of organic carbon and elemental carbon [44], the lack of complete chemical analysis techniques for organic aerosols prevents any reliable method of apportioning carbonaceous material to primary or secondary emissions; thus it is difficult to compare the model results to a parameter measured directly in the atmosphere. The model inputs such as gas-phase emission rates and aerosol yields have high uncertainties, as well as the physical processes discussed in the next section that control the formation of the secondary aerosol. These shortcomings, pointed out by Pandis et al. [43] currently limit the usefulness of such models.

Table 2-2 Organic compounds that have aerosol yield greater than 10%

Anthropogenic ROGs	Molecular Forms and References
Phenols	Ortho cresol [45]
	4-hydroxy-2-nitrotoluene [45]
Diolefins	1,5 hexadiene [46]
	1,6 heptadiene [47]
	2-Methyl-1,5-hexadiene [46]
	1,7 octadiene [48]
	Cyclopentadiene [48]
Natural ROGs (terpenes)	α-pinene [47, 49]
	Limonene [50]

PHASE CHARACTERISTICS OF ORGANIC AEROSOLS

Since atmospheric organic compounds are found in both the gas and condensed phases, a compound's partitioning characteristics must be considered to understand its distribution, lifetime, removal mechanisms, and the effects the compound has on light scattering, cloud drop formation, and health. For secondary aerosols and some of the products of combustion, the gas-particle partitioning determines the yield of aerosol mass that forms from the gaseous products of atmospheric reactions. Partitioning is also an important consideration when sampling organic aerosol to understand the possible positive and negative artifacts inherent in sampling semivolatile material. In general, partitioning of a compound towards particles depends on its vapor pressure (controlled by the *molecular form*) as well as the amount *and chemical nature* of particles available as condensation sites, and temperature.

In a scenario for the formation of aerosol from the gas phase, a semivolatile organic compound (SOC) is produced either through photochemical oxidation in the atmosphere or is emitted by a combustion source. The SOC remains in the gas phase until its concentration reaches a point that it sorbs onto available existing particles until there is thermodynamic equilibrium between the gas and particle phases. An equation that parameterizes the partitioning is [51-55]:

$$K_p = \frac{c_p}{c_g(TSP)} \qquad \text{(Eq. 2-3)}$$

where K_p ($m^3\ \mu g^{-1}$) is the temperature-dependent equilibrium partitioning constant, TSP ($\mu g\ m^{-3}$) is the concentration of total suspended particulate and c_p and c_g are the concentrations of the SOC in the particle and gas phases, respectively. The distribution c_p/c_g can be measured by collecting particles on a filter with an adsorbent such as Tenax beads downstream to catch the gas-phase portion. This technique has especially been used in cities to measure partitioning of polycyclic aromatic hydrocarbons (PAH's),

alkanes, phthalate esters, fatty acids, and organohalogens [26, 51, 56] and more recently applied to the partitioning of PAH products of biomass burning [27]. Vapor phase information has also been acquired using gas chromatographic retention data for polychlorobiphenyls (PCB) compounds [57] in order to predict gas/particle distributions. I am unaware of studies of this type pertaining to secondary aerosol species, which are more highly oxidized and more difficult to analyze than these non-polar compounds listed. Interestingly, it appears that K_p values for a single SOC in the urban atmosphere are very similar even when measured from city to city.

One of the goals of using gas-particle partitioning theory is to develop realistic models of the production of secondary aerosol and to be able to predict which reactive gas emissions are most important in the production of particulate pollution. These models rely on inputs of the emission rates of reactive organic gases (ROGs), concentrations of oxidant species, and the fractional aerosol yield for each ROG calculated as:

$$Y = \frac{\Delta M_o}{\Delta ROG} \qquad \text{(Eq. 2-4)}$$

where Y (dimensionless) is the fractional aerosol yield, ΔM_o is the organic aerosol mass concentration ($\mu g\ m^{-3}$) produced from ΔROG, the amount of ROG reacted ($\mu g\ m^{-3}$). These aerosol yields usually come from smog chamber measurements, but traditionally it has been difficult to obtain a single value for aerosol yield from a single ROG with low uncertainty. As pointed out by Pandis et al. [43], reported aerosol yields may differ by more than an order of magnitude. It may be that a factor causing these discrepancies is a poor assumption on how the products of the oxidation reactions partition between the gas and particle phases. Odum et al. [58] investigate gas-particle partitioning assumptions to see how they affect Y.

Odum et al. [58] rely on an analysis by Pankow [54], who points out that although K_p is constant for a single compound at a single temperature, it does not state anything

about the mechanism involved in the sorption of the gas into or onto the existing particles. Traditionally, this problem has been treated according to a simple Langmuir isotherm, so that the gas is assumed to simply physically *adsorb* on the surface of the particles [51, 52, 59]. In this case, K_p would be predicted by theory to be [52]:

$$K_p = \frac{N_s a_{tsp} T e^{(Q_1 - Q_v)/RT}}{1600 p_L^o} \qquad \text{(Eq. 2-5)}$$

where N_s (sites cm^{-2}) is the surface concentration of sorption sites, a_{tsp} ($m^2 g^{-1}$) is the specific surface area of the existing particulate matter, T is temperature (K), Q_1 (kJ mol^{-1}) is the enthalpy of desorption from the particle surface, Q_v (kJ mol^{-1})is the enthalpy of vaporization of the adsorbing compound from the liquid phase (sub cooled if necessary), R is the universal gas constant, and p_L^o is the vapor pressure of the adsorbing compound as a liquid (sub cooled, if necessary). Note that this equation predicts that the degree of sorption is independent of the amount of material already sorbed to the particles. However, Pankow [55] suggests that the partitioning process for organic compounds may have an *absorption*, or chemisorption component, and may even dominate the sorption process. This would happen if there were organic material present in particles for organic gases to dissolve into, and thus as more organic material is added to particles, the partitioning characteristics would change. If this absorption is the only mechanism for partitioning, with no adsorption component, then theory would predict that [55]:

$$K_p = \frac{f_{om} 760 RT}{MW_{om} \zeta_i 10^6 p_{L,i}^o} \qquad \text{(Eq. 2-6)}$$

where f_{om} is the weight fraction that is the absorbing organic material in the particles, R is the universal gas constant, T is temperature (K), MW_{om} is the mean molecular weight of the absorbing organic material (g mol^{-1}), ζ_i is the activity coefficient of compound i in the organic material, and $p^o_{L,i}$ is the vapor pressure (torr) of the absorbing compound as a liquid at the temperature of interest.

Odum et al. [58] take Pankow's work one step further, pointing out that the expression for $K_{p,i}$ in Equation 6 changes as more organic is dissolved into the particles. They define instead a partitioning coefficient for species *i* in terms of both the fraction of compound *i* dissolved into the particles ($F_{i,om}$) and the total organic mass concentration in the particles (M_o):

$$K_{om,i} = \frac{F_{i,om}}{A_i M_o} = K_{p,i} / f_{om} \qquad \text{(Eq 2-7)}$$

This equilibrium partitioning coefficient will be constant as long as the total mass of absorbing organic (M_o) increases as $F_{i,om}$ increases. Odum et al. [58] go on to define an expression for overall semivolatile organic aerosol yield that is equivalent to the expression in equation 4, but based on the partitioning coefficient given in equation 2-7:

$$Y = M_o \sum_i \left(\frac{\alpha_i K_{om,i}}{1 + K_{om,i} M_o} \right) \qquad \text{(Eq. 2-8)}$$

where α_i is a proportionality constant relating the concentration of the ROG that reacts to the total concentration of product *i* that is formed. It depends on both the molecular form of the ROG and the temperature:

$$1000 \alpha_i \Delta ROG = C_i \qquad \text{(Eq. 2-9)}$$

By comparing yields predicted by Equation 2-8 and data from a variety of smog chamber experiments, Odum et al. [58] show that the absorption model for partitioning seems to fit. Furthermore, experiments performed by other groups were rationalized by analysis using the absorption model.

A picture of gas-particle partitioning as it stands now is that a combination of adsorption and absorption may drive partitioning, so that the partitioning coefficient can be written as [55]:

$$K_{p,i} = \frac{1}{p^{o}_{L,i}}\left[\frac{N_s a_{tsp} T e^{(Q_1 - Q_v)/RT}}{1600} + \frac{f_{om} 760 RT}{MW_{om}\zeta_i 10^6}\right] \qquad \text{(Eq.2-10)}$$

Current work seems to indicate that the second term in the brackets (the absorption term) may be more important, as was suggested by Odum et al. [58]. Storey et al. [60] also evaluated the relative importance of the two terms. They performed experiments using model semivolatile organic compounds (alkanes and PAH's) in the gas phase to determine the degree they adsorb onto the surface of clean quartz, as a model for adsorption to mineral dust in the atmosphere. Their results show that their model compounds adsorb less to quartz than the attachment that is seen in the ambient atmosphere. They suggest that *ab*sorption to the organic component of urban particulate is probably a more important mechanism in the partitioning of these compounds, but that in a rural environment where there is a considerable amount of soil and non-inorganic continental mineral dust, adsorption still may be important. These hypotheses have not yet been tested on more polar compounds found in atmospheric particulate matter.

Influence of Relative Humidity on Partitioning

By far the most ubiquitous condensable gas in the atmosphere is water vapor, which is responsible for the formation of fog and cloud droplets by condensation onto aerosol particles. The question of how water vapor in the mole fraction range of 10^{-6} (e.g. for the stratosphere and antarctic) to 10^{-2} (e.g. in the tropics) affects the gas-particle partitioning of organics has not been studied in depth, although there is evidence that relative humidity (RH) affects the adsorption of organic vapors to aerosol particles. SOC partial pressure has been observed to increase over particles as relative humidity increases, indicating that water molecules may preferentially sorb to the same sites on the particle that an organic compound would [61, 62]. Thibodeaux et al. [63] drew upon the aerosol/vapor adsorption partitioning equations of Junge [59] to develop a competition model of both water vapor and organic vapors adsorbing to the same particle. They suggest that at low relative humidity, organic adsorption should decrease with increasing RH due to competition with water for sites on the particle surface. At some intermediate

'damp' humidity, the water molecules on the particle begin to touch, forming a liquid layer at the surface. This represents maximum crowding of water molecules and is the point when the smallest amount of SOC would be expected to occupy the particle surface. After the liquid water layer forms, the organic can sorb to or into the water film, thus at this point adsorption increases with increasing RH. This scenario implies that aerosol particles associated with the most SOC are either completely dry or are completely covered by a film of liquid water.

Although competition with water vapor may affect condensation of organic species, the opposite question arises of how organic compounds affect the condensation of water vapor to the surface of aerosol particles. This complementary issue is covered in the next section, and has ramifications for the removal processes of organic particulate matter, the hydrologic cycle, and the 'indirect climate forcing' effect of organic aerosols, as discussed briefly in the introductory chapter.

HYGROSCOPIC GROWTH

It appears that numerous organic compounds are at least present in cloud condensation nuclei [23, 64]. A major question is how these particles grow into droplets when exposed to water vapor. Although it had previously been assumed that organic compounds would need to be associated with inorganic salt compounds in order to nucleate cloud droplets, some organic compounds found in woodsmoke are hygroscopic enough by themselves in the absence of an inorganic salt to cause cloud droplet growth [28]. Another possibility is that surface active organics are present on a small droplet or dry particle as a film. The topic of surface organic films has been discussed in detail by Gill et al. [65]. Depending on the molecular structure of the organic coating and the type of particle it resides on, a film could conceivably help or hinder hygroscopic growth, affect evaporation of water vapor from the droplet, or simply change the equilibrium size to which a droplet might grow at a certain relative humidity. Some evidence that organic surface films exist on aerosol droplets in the ambient atmosphere is from electron

micrographs, such as those taken by Husar and Shu [66]. These pictures show desiccated particles that are wrinkled in appearance, thought to arise from evaporation of a volatile inner core (H_2O), leaving behind a relatively non-volatile organic coating.

The growth of droplets from organic-coated dry particles has been studied in the laboratory both using a tandem-differential mobility analyzer method (TDMA) [67, 68] and using suspended single particles in an electrodynamic balance [69, 70]. These studies have generally shown that the growth of normally hygroscopic particles such as NaCl and $(NH_4)_2SO_4$ is hindered by the presence of a coating of an organic compound, although the work by Hansson et al. [67] showed that NaCl particles must be coated with very large amounts of hydrophobic organic material in order to significantly affect water uptake. This is probably because even hydrophobic organic coatings are susceptible to cracks where the hygroscopic salt is exposed. On the other hand, particles that are normally hydrophobic (e.g. soot) may experience increased affinity for water if certain organic coating types are present [70]. This behavior has also been seen in ambient aerosols [71], where in a non-urban location (Grand Canyon), the presence of organic compounds *enhanced* water absorption by particles, accounting for 25-40% of total water uptake on average, but in Los Angeles particles, water uptake was *depleted* by the presence of organic compounds by 25-35%.

Experiments dealing with organic coatings and their effects raise the question of the type of mixing present in atmospheric particles, and how much of the organic material in a set of particles is associated with other materials. Junge [72] first described the concept of two limiting cases of aerosol particle mixing: *Internal* mixtures where each particle is a uniform combination of several chemical species together, and *external* mixtures where each particle is composed of a single chemical compound. Realistically, most atmospheric aerosols are probably between these two extremes, with each particle containing a different mixture of chemical compounds. To identify the type of mixing in an aerosol sample requires either examination of individual particles (single particle analysis, e.g. electron microscopy) or conditioning ambient aerosol in a certain way to

cause a change to only one type of particle (e.g. TDMA using humidification between the two size classifiers). Using a combination of single particle analysis, TDMA analysis, and chemical analysis on size fractionated samples, Zhang et al. [73] found that aerosols collected in Los Angeles and at the Grand Canyon were externally mixed as a non-hygroscopic fraction with a fraction that was more hygroscopic. This behavior has also been seen in other locations [74]. It appeared that in Los Angeles and at the Grand Canyon, the fraction of particles that was found to be less hygroscopic was too small to account for all of the carbon measured by chemical analysis, indicating that organic compounds are in both modes. This was confirmed by single particle analysis by scanning electron microscopy (SEM) combined with x-ray analysis. There appeared to be particles that contained carbon or carbon and oxygen only, particles that contained sulfur, and particles that contained both sulfur and carbon together. Because of their different chemical compositions, these particles would be expected to also have different hygroscopic properties of the type seen with the TDMA method. The concept that organic material could be associated with either hygroscopic or hydrophobic particles is consistent with the rich and varied chemistry of organic compounds.

The exact mechanism for differences in the apparent hygroscopic properties of a particle as seen by TDMA at this point remains unclear. TDMA experiments such as those discussed could be affected by the amount of time aerosol particles are exposed to humid air, in which case particles that do not appear hygroscopic might not have had time to interact with the water vapor in order to dissolve fully. Lowering of the surface tension of the droplet solution is another mechanism that needs to be explored. Such a change in surface tension arises from the presence at the particle-air interface of molecules having one or more polar functional groups on the end of a carbon chain. The molecules are lined up so that the polar ends are in the water while the non-polar (hydrophobic) ends are repelled into the air, away from the surface of the droplet. The amount of surface tension lowering varies according to the molecular structure of the organic, the amount of surfactant present, and the degree to which the organic molecule partitions to the aerosol droplet surface, as opposed to being dissolved in the liquid.

Shulman et al. [75] showed that this last parameter is related in some cases to the solubility of the organic compound.

The effects on cloud droplet growth due to lowered surface tension by dicarboxylic acids is discussed by Shulman et al. [75]. They measured surface tension for five straight-chain organic diacids, phthalic acid, and cis-pinonic acid, all of which have been measured in the ambient atmosphere, and are probably the products of secondary aerosol formation (see next section: Chemical Transformations). It was found that there is a general decrease in surface tension with increasing organic concentration, and that the decrease in surface tension is greater for organic compounds with higher carbon number. The solubililties of these compounds were also measured in various concentrations of ammonium sulfate solutions, and it was found that in many realistic cases, these compounds would experience complete dissolution only after droplet growth had taken place past deliquescence. The effects of slight solubility of organic compounds on the growth of water droplets is the subject of Chapter 3.

CHEMICAL TRANSFORMATIONS

Since the majority of organic aerosol mass remains poorly characterized, the study of chemical reactions involving organics in the condensed phase is sparse, especially in the ambient atmosphere. However, since the typical water content of particles in the lower-atmosphere is about 30-50% by mass, Graedel and Weschler [76] point out that theoretical and laboratory study of reaction chemistry in the atmospheric condensed phase can be approximated in part as taking place in aqueous solutions, assuming that organic compounds have dissolved into the aqueous solution. Under these idealized conditions, the most reactive atmospheric species are oxidants, such as the hydroxyl radical, atomic oxygen, ozone, and molecular oxygen. Graedel and Weschler [76] go through the reactivities and physical properties of the main groups of organic compounds that have been successfully identified in the atmosphere. In general, if organic compounds are reactive, they become smaller and more polar through oxidative

cleavage and addition of oxygen. If non-polar coatings or organic gases become associated with cloud droplets, many reactions may take place that provide the source of new organic particles, since clouds form and evaporate on the same CCN several times before precipitating. This process may be responsible for a large fraction of low molecular weight, polar organics in the atmosphere.

Dicarboxylic acids are once again a good example of a class of compounds that illustrate reactivity trends of organic material in the atmosphere. As mentioned in section IIB2, laboratory experiments show that larger dicarboxylic acids ($>C_6$) are formed by photochemical oxidation of alkenes, especially cyclic alkenes [33, 38, 39]. Also, as shown in Figure 1, their vapor pressures are low, even at low carbon number which causes them to partition into the aerosol phase. Numerous studies have shown that the most abundant dicarboxylic acid is oxalic acid, the smallest (C_2) diacid species, followed by malonic (C_3) and succinic (C_4) acids [42, 77, 78]. These three species account for more than 80% of the diacids found in arctic regions, which are far away from the source of reactive gases. This distribution suggests that when the longer chain dicarboxylic acids form, they remain photochemically labile, continuing to cleave to successively smaller carbon chains.

One area that condensed phase organic compounds may play an important role is in the oxidation and reduction of transition metals in cloud and fog droplets. The oxidation of aldehydes to carboxylic acids takes place through the reduction of Fe(III) to Fe(II) [79-82]. Ions such as oxalate can also act as ligands, forming transition metal complexes, and appear to also be involved in the redox chemistry of iron. Although the studies involving metals have focused on the oxidation state of the metal, the interaction with organic compounds may be an important parameter in controlling the acidity of the solution droplets. Reactions such as these can also affect solubility of gas-phase atmospheric components, which could further affect droplet growth, as discussed in Chapter 3.

NOTES TO CHAPTER 2

1. Liousse, C., J.E. Penner, C. Chuang, J.J. Walton, H. Eddleman, and H. Cachier, *A global three-dimensional model study of carbonaceous aerosols.* J. Geophys Res., 1996. **101**(D14): p. 19,411-19,432.

2. Cachier, H., M.-P. Bremond, and P. Buat-Menard, *Carbonaceous aerosols from different tropical biomass burning sources.* Nature, 1989. **340**: p. 371-373.

3. White, *Section 4 of Visibility: Existing and Historical Conditions--Causes and Effects, J.C. Trijonis, ed.*, in *Acid Deposition: State of Science and Technology*, P.M. Irving, Editor. 1990, U.S. National Acid Precipitation Assessment Program: Washington, D.C. p. 85-102.

4. Heintzenberg, J., *Fine particles in the global troposphere. A review.* Tellus, 1989. **41B**: p. 149-160.

5. Hildemann, L.M., W.F. Rogge, G.R. Cass, M.A. Mazurek, and B.R.T. Simoneit, *Contribution of primary aerosol emissions from vegetation-derived sources to fine particle concentrations in Los Angeles.* J. Geophys. Res., 1996. **101**(D14): p. 19,541-19,549.

6. Sicre, M.-A., J.-C. Marty, and A. Saliot, *n-Alkanes, fatty acid esters, and fatty acid salts in size fractionated aerosols collected over the Mediterranean sea.* J. Geophys. Res., 1990. **95**(D4): p. 3649-3657.

7. Simoneit, B.R.T., R. Chester, and G. Eglinton, *Biogenic Lipids in Particulates from the Lower Atmosphere over the Eastern Atlantic.* Nature, 1977. **267**: p. 682-685.

8. Gagosian, R.B., O.C. Zafiriou, E.T. Peltzer, and J.B. Alford, *Lipids in Aerosols From the Tropical North Pacific: Temporal Variability.* J. Geophys. Res., 1982. **87**(C13): p. 11,133-11,144.

9. Folger, D.W., *Wind transport of land-derived mineral, biogenic and industrial matter over the North Atlantic.* Deep Sea Res., 1970. **7**: p. 337.

10. Mazurek, M.A., G.R. Cass, and B.R.T. Simoneit, *Biological input to visibility-reducing aerosol particles in the remote arid southwestern United States.* Environ. Sci. Technol., 1991. **25**: p. 684-694.

11. Marty, J.-C. and A. Saliot, *Aerosols in Equatorial Atlantic Air: n-Alkanes as a Function of Particle Size.* Nature, 1982. **298**(8 July): p. 144-147.

12. Schneider, J.K., R.B. Gagosian, J.K. Cochran, and T.W. Trull, *Particle size distributions of n-alkanes and 210-Pb in aeorols off the coast of Peru.* Nature, 1983. **304**: p. 429-432.

13. Schneider, J.K. and R.B. Gagosian, *Particle Size Distribution of Lipids in Aerosols off the Coast of Peru.* J. Geophys. Res., 1985. **90**(D5): p. 7889-7898.

14. Duce, R.A., V.A. Mohnen, P.R. Zimmerman, D. Grosjean, W. Cautreels, R. Chatfield, R. Jaenicke, J.A. Ogren, E.D. Pellizzari, and G.T. Wallace, *Organic material in the global troposphere.* Rev. Geophys. Space Phys., 1983. **21**(4): p. 921-952.

15. Edmonds, R.L., ed. *Aerobiology: The Ecological Systems Approach.* . 1979, Dowden, Hutchinson & Ross: Stroudsburg, PA.

16. Fuzzi, S., P. Mandrioli, and A. Perfetto, *Fog droplets--An atmospheric source of secondary biological aerosol particles.* Atmos. Env, 1996. **In press**.

17. Matthias-Maser, S. and R. Jaenicke, *A method to identify biological aerosol particles with radius > 0.3 um for the determination of their size distribution.* J. Aerosol Sci., 1991. **22**(Supp 1): p. S849-S852.

18. Matthias-Maser, S. and R. Jaenicke, *Examination of atmospheric bioaerosol particles with radii > 0.2um.* J. Aerosol Sci., 1994. **25**(8): p. 1605-1613.

19. Matthias-Maser, S. and R. Jaenicke, *The size distribution of primary biological aerosol particles with radii > 0.2 um in an urban/rural influenced region.* Atmos. Resch., 1995. **39**: p. 279-286.

20. Woodcock, A.H., *Salt nuclei in marine air as a function of altitude and wind force.* J. Meteorol., 1953. **10**: p. 362-271.

21. Duce, R.A., *Speculations on the budget of particulate and vapor phase non-methane organic carbon in the global troposphere.* Pure Appl. Geophys., 1978. **116**: p. 244-273.

22. Hoffman, E.J. and R.A. Duce, *Factors influencing the organic carbon content of marine aerosols: A laboratory study.* J. Geophys. Res., 1976. **81**(21): p. 3667-3670.

23. Noone, K.J., E. Ostrom, R.A. Pockalny, L. de Bock, and R. Van Grieken. *The size distribution and chemical compposition of cloud droplet residual particles in marine stratocumulus clouds observed during the MAST experiment.* in *Fourteenth International Conference on Nucleation and Atmospheric Aerosols*. 1996. Helsinki, Finland: Pergamon.

24. Gribble, G.W., *Natually occurring organohalogen compounds--a survey.* J. Nat. Prod., 1992. **55**(10): p. 1353-1395.

25. Andreae, M.O., *Biomass burning: Its history, use, and distribution and its impact on environmental quality and global climate*, in *Global Biomass*

Burning: Atmospheric, Climatic, and Biospheric Implications, J.S. Levine, Editor. 1991, MIT Press: Cambridge, MA. p. 3-21.

26. Ligocki, M.P. and J.F. Pankow, *Measurements of the gas/particle distributions of atmospheric organic compounds.* Environ. Sci. Tech., 1989. **23**: p. 75-83.

27. Jenkins, B.M., A.D. Jones, S.Q. Turn, and R.B. Williams, *Particle concentations, gas-particle partitioning, and species intercorrelations for polycyclic aromatic hydrocarbons (PAH) emitted during biomass burning.* Atmos. Environ., 1996. **30**(22): p. 3825-2835.

28. Novakov, T. and C.E. Corrigan, *Cloud condensation nucleus actuivity of the organic component of biomass smoke particles.* Geophys. Res. Lett., 1996. **23**(16): p. 2141-2144.

29. Andreae, M.O., E.V. Browell, M. Garstang, G.L. Gregory, R.C. Harriss, G.F. Hill, D.J. Jacob, M.C. Pereira, G.W. Sachse, A.W. Setzer, P.L. Silva Dias, R.W. Talbot, A.L. Torres, and S.C. Wofsy, *Biomass-burning emissions and associated haze layers over Amazonia.* J. Geophys. Res., 1988. **93**(D2): p. 1509-1527.

30. Rogge, W.F., L.M. Hildemann, M.A. Mazurek, G.R. Cass, and B.R.T. Simoneit, *Sources of fine organic aerosol. 2. Noncatalyst and catalyst-equipped automobiles and heavy-duty diesel trucks.* Environ. Sci. Technol., 1993. **27**(4): p. 636-651.

31. Grosjean, D., J.P. Smith, T.M. Mischke, and J.N. Pitts, Jr., *Chemical and physical transformations in urban-suburban transport of air pollutants.*, in *Atmospheric Pollution*, M.M. Benarie, Editor. 1976, Elvesier: Amsterdam. p. 549-563.

32. Grosjean, D. and J.H. Seinfeld, *Parameterization of the formation potential of secondary organic aerosols.* Atmos. Env., 1989. **23**(8): p. 1733-1747.

33. Grosjean, D. *Secondary Organic Aerosol: Identification and Mechanisms of Formation.* in *Carbonaceous Particles in the Atmosphere.* 1978. Berkely, CA.

34. Zimmerman, P.R. and R.B. Chatfield, *Estimates of the production of CO and H2 from the oxidation of hydrocarbon emissions from vegetation.* Geophys. Res. Lett., 1978. **5**: p. 679-682.

35. Cronn, D.R., *Analysis of Atmospheric Aerosols by High Resolution Mass Spectrometry*, in *Civil Engineering*. 1975, University of Washington: Seattle.

36. Appel, B.R., S.M. Wall, and R.S. Knights, *Characterization of carbonaceous materials in atmospheric aerosols by high-resolution mass*

spectrometric thermal analysis. Adv. Envir. Sci. Technol., 1980. **9**: p. 353-365.

37. Grosjean, D., *Aerosols. Chapter 3*, in *Ozone and Other Photochemical Oxidants*. 1977, National Academy of Sciences: Washington, D.C.

38. Hatakeyama, S., T. Tanonaka, J. Weng, H. Bandow, H. Takagi, and H. Akimoto, *Ozone-cyclohexene reaction in air: quantitative analysis of particulate products and the reaction mechanism.* Envir. Sci. Technol., 1985. **19**: p. 935-942.

39. Hatakeyama, S., M. Ohno, J. Weng, H. Takagi, and H. Akimoto, *Mechanism for the formation of gaseous and particulate products from ozone-cycloalkene reactions in air.* Envir. Sci. Technol., 1987. **21**: p. 52-57.

40. Satsumabayashi, H., H. Kurita, Y. Yokouchi, and H. Ueda, *Mono- and di-carboxylic acids under long-range transport of air polution in central Japan.* Tellus, 1989. **41B**(3): p. 219-229.

41. Satsumabayashi, H. and H. Kurita, *Photochemical formation of particulate dicarboxylic acids under long-range transport in central Japan.* Atmos. Env., 1990. **24A**(6): p. 1443-1450.

42. Kawamura, K., H. Kasukabe, O. Yasui, and L.A. Barrie, *Production of dicarboxylic acids in the artic atmosphere at polar sunrise.* Geophys. Res. Lett., 1995. **22**(10): p. 1253-1256.

43. Pandis, S.N., R.A. Harley, G.R. Cass, and J.H. Seinfeld, *Secondary organic aerosol formation and transport.* Atmos. Environ., 1992. **26A**(13): p. 2269-2282.

44. Turpin, B.J. and J.J. Huntzicker, *Secondary formation of organic aerosol in the Los Angeles Basin: A descriptive analysis of organic and elemental carbon concentrations.* Atmos. Environ., 1991. **25A**: p. 207-215.

45. McMurray, P.H. and D. Grosjean, *Photochemical Formation of Organic Aerosols: Growth Laws and Mechanisms.* Atmospheric Environment, 1985. **19**(9): p. 1445-1451.

46. Prager, M.J., E.R. Stephens, and W.E. Scott, *Aerosol formation from gaseous air pollutants.* Ind. Eng. Chem., 1960. **52**: p. 521-524.

47. O'Brien, R.J., J.R. Holmes, and A.H. Bockian, *Formation of photochemical aerosol from hydrocarbons--Chemical reactivity and products.* Environ. Sci. Technol., 1975. **9**(6): p. 568-576.

48. Grosjean, D. and S.K. Friedlander, *Formation of organic aerosols from cyclic olefins and diolefins*, in *The Character and Origins of Smog Aerosols*, G. Hidy, Editor. 1979, John Wiley and Sons: New York. p. 435-473.

49. Zhang, S.-H., M. Shaw, J.H. Seinfeld, and R.C. Flagan, *Photochemical aerosol formation from alpha-pinene and beta-pinene.* J. Geophys. Res., 1992. **97**(D18): p. 20,717-20,729.

50. Schuetzle, D. and R.A. Rasmussen, *The molecular composition of secondary aerosol particles formed from terpenes.* J. Air Pollut. Cont. Assoc., 1978. **28**: p. 236-240.

51. Yamasaki, H., K. Kuwata, and H. Miyamoto, *Effects of ambient temperature on aspects of airborne polycyclic aromatic hydrocarbons.* Environ. Sci. Technol., 1982. **16**(4): p. 189-194.

52. Pankow, J.F., *Review and comparative analysis of the theories on partitioning between the gas and aerosol particulate phases in the atmosphere.* Atmos. Environ., 1987. **21**(11): p. 2275-2283.

53. Pankow, J.F., *A Simple Box Model for the Annual Cycle of Partitioning of Semi-Volatile Organic Compounds Between the Atmosphere and the Earth's Surface.* Atmospheric Environment, 1993. **27A**(7): p. 1139-1152.

54. Pankow, J.F., *An Absorption Model of the Gas/Aerosol Partitioning Involved in the Formation of Secondary Organic Aerosol.* Atmospheric Environment, 1994. **28**(2): p. 189-193.

55. Pankow, J.F., *An Absorption Model of Gas/Particle Partitioning of Organic Compounds in the Atmosphere.* Atmospheric Environment, 1994. **28**(2): p. 185-188.

56. Cautreels, W. and K. Van Cauwenberghe, *Experiments on the distribution of organic pollutants between airborne particulate matter and the corresponding gas phase.* Atmos. Env., 1977. **12**: p. 1133-1141.

57. Falconer, R.L. and T.F. Bidleman, *Vapor pressures and predicted particle/gas distributions of polychlorinated biphenyl congeners as functions of temperature and ortho-chlorine substitution.* Atmos. Env., 1994. **28**(3): p. 547-554.

58. Odum, J.R., T. Hoffmann, F. Bowman, D. Collins, R.C. Flagan, and J.G. Seinfeld, *Gas/particle partitioning and secondary organic aerosol yields.* Environ. Sci. Technol., 1996. **30**: p. 2580-2585.

59. Junge, C.E., *Basic considerations about trace constituents in the atmosphere as related to the fate of global pollutants*, in *Fate of Pollutants in the Air and Water Environments*, I.H. Suffet, Editor. 1977, John Wiley: New York. p. 7-25.

60. Storey, J.M.E., W. Luo, L.M. Isabelle, and J.F. Pankow, *Gas/solid partitioning of semivolatile organic compounds to model atmospheric solid surfaces as a function of relative humidity. 1. Clean quartz.* Environ. Sci. Technol., 1995. **29**: p. 2420-2428.

61. Spencer, W.F., W.J. Farmer, and W.A. Jury, *Review: Behavior of organic chemicals at soil, air, water interfaces as related to predicting the transport and volatilization of organic pollutants.* Envir. Toxicol. Chem, 1982. **1**: p. 17-26.

62. Chiou, C.T., D.E. Kile, and R.L. Malcolm, *Sorption of vapors of some organic liquids on soil humic acid and its relation to partitioning of organic compounds in soil organic matter.* Envir. Sci. Technol., 1988. **22**: p. 298-303.

63. Thibodeaux, L.J., K.C. Nadler, K.T. Valsaraj, and D.D. Reible, *The effect of moisture on volatile organic chemical gas-to-particle partitioning with atmospheric aerosols--competitive adsorption theory predictions.* Atmos. Environ., 1991. **25A**(8): p. 1649-1656.

64. Novakov, T. and J.E. Penner, *Large Contribution of Organic Aerosols to Cloud-Condensation-Nuclei Concentrations.* Nature, 1993. **365**: p. 823-826.

65. Gill, P.S., T.E. Graedel, and C.J. Weschler, *Organic films on atmospheric aerosol particles, fog droplets, cloud droplets, raindrops, and snowflakes.* Rev. Geophys. and Space Phys., 1983. **21**(4): p. 903-920.

66. Husar, R.B. and W.R. Shu, *Thermal analysis of the Los Angeles smog aerosol.* J. Appl. Meteorol., 1975. **14**: p. 1558-1565.

67. Hansson, H.-C., M.J. Rood, S. Koloutsou-Vakakis, K. Hameri, D. Orsini, and A. Wiedensohler, *NaCl aerosol particle hygroscopicity dependence on mixing with organic compounds.* Journal Atmospheric Chemistry (submitted), 1997.

68. Hansson, H.-C., A. Wiedensohler, M.J. Rood, and D.S. Covert, *Experimental determination of the hygroscopic properties of organically coated aerosol particles.* J. Aerosol Sci., 1990. **21S**(1): p. s241-s244.

69. Rubel, G.O. and J.W. Gentry, *Measurement of water and ammonia accommodation coefficients at surfaces with adsorbed monolayers of hexadecanol.* J. Aerosol Sci., 1985. **16**(6): p. 571-574.

70. Andrews, E. and S.M. Larson, *Effect of surfactant layers on the size change of aerosol particles as a function of relative humidity.* Environ.Sci.Technol., 1993. **27**: p. 857-865.

71. Saxena, P., L.M. Hildemann, P.H. McMurry, and J.H. Seinfeld, *Organics alter hygroscopic behavior of atmospheric particles.* J. Geophys. Res., 1995. **100**(D9): p. 18,755-18,770.

72. Junge, C., *Das Wachstum der Kondensationskerne mit der relativen Feuchtigkeit.* Ann. Met., 1950. **3**: p. 129-135.

73. Zhang, X.Q., P.H. McMurry, S.V. Hering, and G.S. Casuccio, *Mixing characteristics and water content of submicron aerosols measured in Los Angeles and at the Grand Canyon.* Atmos. Environ., 1993. **27A**(10): p. 1593-1607.

74. Svenningsson, B., H.-C. Hansson, A. Wiedensohler, K.J. Noone, J. Ogren, A. Hallberg, and R. Colvile, *Hygroscopic growth of aerosol particles and its influence on nucleation scavenging in cloud: Experimental results from Kleiner Feldberg.* J. Atmos. Chem., 1994. **19**: p. 129-152.

75. Shulman, M.L., M.C. Jacobson, R.J. Charlson, R.E. Synovec, and T.E. Young, *Dissolution behavior and surface tension effects of organic compounds in nucleating cloud droplets.* Geophys. Res. Lett., 1996. **23**(3): p. 277-280.

76. Graedel, T.E. and C.J. Weschler, *Chemistry within aqueous atmospheric aerosols and raindrops.* Rev. Geophys. and Space Phys., 1981. **19**(4): p. 505-539.

77. Kawamura, K., S. Steinberg, and I.R. Kaplan, *Concentrations of monocarboxylic and dicarboxylic acids and aldehydes in southern California wet precipitations: Comparison of urban and nonurban samples and compositional changes during scavenging.* Atmos. Env., 1996. **30**(7): p. 1035-1052.

78. Sempere, R. and K. Kawamura, *Low molecular weight dicarboxylic acids and related polar compounds in the remote marine rain samples collected from the western Pacific.* Atmos. Env., 1996. **30**(10/11): p. 1609-1619.

79. Cunningham, K.M., M.C. Goldberg, and E.R. Weiner, *The aqueous photolysis of ethylene glycol adsorbed on goethite.* Photochem. Photobiol., 1985. **41**: p. 409-416.

80. Faust, B.C. and M.R. Hoffmann, *Photoinduced reductive dissolution of hematite by bisulfite.* Environ. Sci. Technol., 1986. **20**: p. 943-948.

81. Erel, Y., S.O. Pehkonen, and M.R. Hoffmann, *Redox chemistry of iron in fog and stratus clouds.* J. Geophys. Res., 1993. **98**(D10): p. 18,423-18,434.

82. Pehkonen, S.O., R.L. Siefert, Y. Erel, S. Webb, and M.R. Hoffmann, *Photoreduction of iron oxyhydroxides in the presence of important atmospheric organic compounds.* Environ. Sci. Technol., 1993. **27**: p. 2056-2062.

CHAPTER 3 : SENSITIVITY OF CLOUDS AND CLIMATE TO THE SOLUBILITY OF ORGANIC CLOUD CONDENSATION NUCLEI CONSTITUENTS

INTRODUCTION

Some of the most quoted scientists in the popular press are climate modelers. Our society's realization that human activities may be able to cause changes in climate has caused the modelers and their models to receive a great deal of scrutiny; we look to them to predict the climatic future of our planet--something that affects every living thing on earth. Although the climate system is much too complex for even the fastest computers to simulate accurately, we can gain a better understanding of the way the entire system works by researching the individual parts. The effects of clouds on planetary radiative balance remains as a large uncertainty, both in terms of the large scale reflective and insulating effects of cloud cover, and how these larger properties are affected by cloud droplet growth, and the chemistry and size of the particles that nucleate cloud droplets. This chapter addresses the issue of how the chemical composition of particles in the atmosphere, through their solubility, affect the size distribution of cloud droplets they nucleate. The optical effects of these changes are calculated, along with an estimate of the sensitivity of the planetary radiative balance to these effects. The intent is that this theory will someday be included in climate models, as more data on the amount and chemical forms of cloud condensation nuclei (CCN) becomes available.

THEORETICAL BASIS FOR DESCRIBING THE CLOUD NUCLEATING PROPERTIES OF MULTIPLE-PHASE CCN: PHASE RULE CONSIDERATIONS

Concepts describing the way aqueous solutes allow cloud droplet nucleation were first delineated in the 1920's by Köhler [1], and have remained in essentially that form since that time. The fundamental equation in its simplest form describes the competition

between the Kelvin effect due to the high curvature of small droplets with the vapor pressure depression by solutes (Raoult effect) [2]:

$$P_{H2O}/P^{\circ}_{H2O} \approx 1 + A/r - B/r^3 \qquad \text{(Eq. 3-1)}$$

Where A/r, the Kelvin effect, describes the influence of surface tension and droplet radius on the saturation ratio, and B/r^3 describes the vapor pressure depression by solutes. This version of the equation explicitly assumes that all of the available solute is in the droplet even when P_{H2O}/P°_{H2O} is less than unity. In the 1970's, a modification of the equation was introduced allowing the existence of an insoluble "core" (e.g. "soot" or mineral dust particle), but once again assumed that all of the solute was dissolved and the amount was constant as the droplet grew. This formulation results in a definition of the volume or mass fraction of the original aerosol particle that is soluble, and common usage in the field of cloud physics considers the soluble fraction to mean only the portion of the mass that dissolves, once again at $P_{H2O}/P^{\circ}_{H2O} \leq 1$.

While used very widely, this formulation ignores the possibility or likelihood that some of the material in the aerosol particles may be of limited solubility, such that at $P_{H2O}/P^{\circ}_{H2O} \leq 1$, not all of the solute is dissolved. This failure to recognize slight solubility was brought to our attention during the studies of atmospheric organic aerosol particles, the molecular forms of which (e.g. oxygenated organics) often have limited solubility in water.

Before presenting a reformulation of the Köhler equations, it will be useful to describe the fundamental basis for describing phase relationships in multiple-phase systems. This brief treatment will illustrate the fact that aerosol particles which act as CCN can (and likely do) have different numbers of phases present as the droplets grow (or shrink). This then requires knowledge of the solubility of the compounds involved, defined by the properties of the saturated aqueous solution of each constituent. Owing to the fact that solubilities of slightly soluble compounds can depend strongly on the presence and concentrations of other solutes, it is further necessary to know the

solubilities of slightly soluble species (e.g. organics) in solutions of highly soluble substances (e.g. inorganic salts).

In the rest of this chapter, a reformulation of Eq. 3-1 that explicitly includes solutes of limited solubility is presented, followed with a discussion of how inclusion of these solutes may influence the optical properties of clouds. First I will discuss some thermodynamic considerations for droplet systems with multiple phases.

PHASE RULE CONSIDERATIONS FOR DROPLET GROWTH

The application of Equation 3-1 for use with solutes of limited solubility implicitly assumes that a droplet system must follow Gibb's Phase Rule for Mixtures. This thermodynamic rule represents the criterion for the number of phases that will coexist at equilibrium, stated mathematically in Equation 3-2:

$$F = C - P + N \qquad \text{(Eq. 3-2)}$$

Where C is the number of components present in the system and P is the number of phases those components are present as. N is the number of non-compositional variables, and is generally listed as 2 for temperature and pressure. F is the number of degrees of freedom that the system has, i.e. the number of variables such as temperature, pressure, and concentration that must be specified to completely describe the system. For simplicity's sake I would like to consider only isothermal systems in the examples that follow, thus N = 1 and the equation becomes:

$$F = C - P + 1 \qquad \text{(Eq. 3-3)}$$

In addition, since liquid water is essentially incompressible, the external pressure of the system (atmospheric pressure, which is more or less constant) affects only the vapor pressure of water and other condensable or soluble gases. Thus pressure as a variable will be considered only as vapor pressure, and not the total system pressure. Therefore for most of the examples, water vapor will be considered as the only gas

present. The examples I will discuss with respect to this equation are diagrammed in picture form in Figure 3-1. As a starting point, consider a deliquescing salt (case a). At the moment that the salt starts to dissolve, it exists in both the solid and solution phases. There are two components (water and salt), present in a total of three phases: the solid salt, the solution, and the gas above the droplet. By equation 3-3, there are no degrees of freedom, i.e. if any variable changes in the system, the equilibrium will relax to a different state. For example, if vapor pressure of water increases, the salt will dissolve completely. If the vapor pressure decreases, the condensed water will evaporate. An illustration of this effect can be seen in humidograms that show the change in light scattering of an aerosol as relative humidity is increased. Figure 3-2 shows the humidogram for sodium chloride. The rapid and large change that occurs as the aerosol material reaches the deliquescence point shows that the number of phases in the droplet changes instantaneously as relative humidity is increased by a very small amount. In the next example (case b), let the deliquescing salt completely dissolve into the solution. There are still two components, present in two phases (an aqueous phase containing water and dissolved salt, and a gas phase containing water vapor). Now $F = 1$, meaning that the system can be defined by either the concentration of salt or by the water vapor pressure alone. One variable forces definition of the other. Strictly speaking, there are other possible degrees of freedom, such as the concentration of water in the aqueous solution, but this also would define the system alone, under isothermal conditions.

The next simplest case is the inclusion of a completely insoluble core in the CCN, as considered by Hänel [3]. In this case (not diagrammed), if the core (mineral dust, or soot particle) is coated with highly soluble material, such as sulfuric acid, the critical supersaturation is lowered compared to another smaller particle containing the same amount of soluble salt. This is only because the dry particle size of

a) Deliquescing salt: 3 phases, 2 components. 0 degrees of freedom.

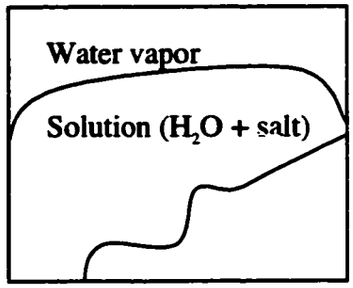

b) Droplet growing from deliquesced salt: 2 phases, 2 components. 1 degree of freedom, e.g. P_{H2O}

c) Droplet growing from deliquesced salt on a weakly soluble organic particle: 3 phases, 3 components. 1 degree of freedom.

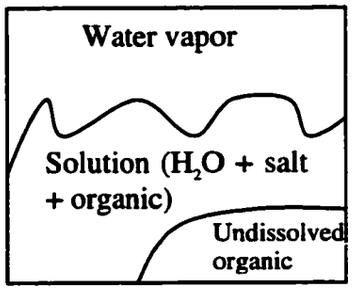

d) Same droplet as (c), but the weakly soluble material has dissolved: 2 phases, 3 components. 2 degrees of freedom.

e) Same droplet as (c), but with an added soluble gas component: 3 phases, 4 components. 2 degrees of freedom.

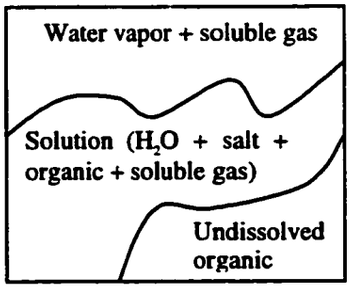

Figure 3-1 Gibbs phase rule applied to droplet systems

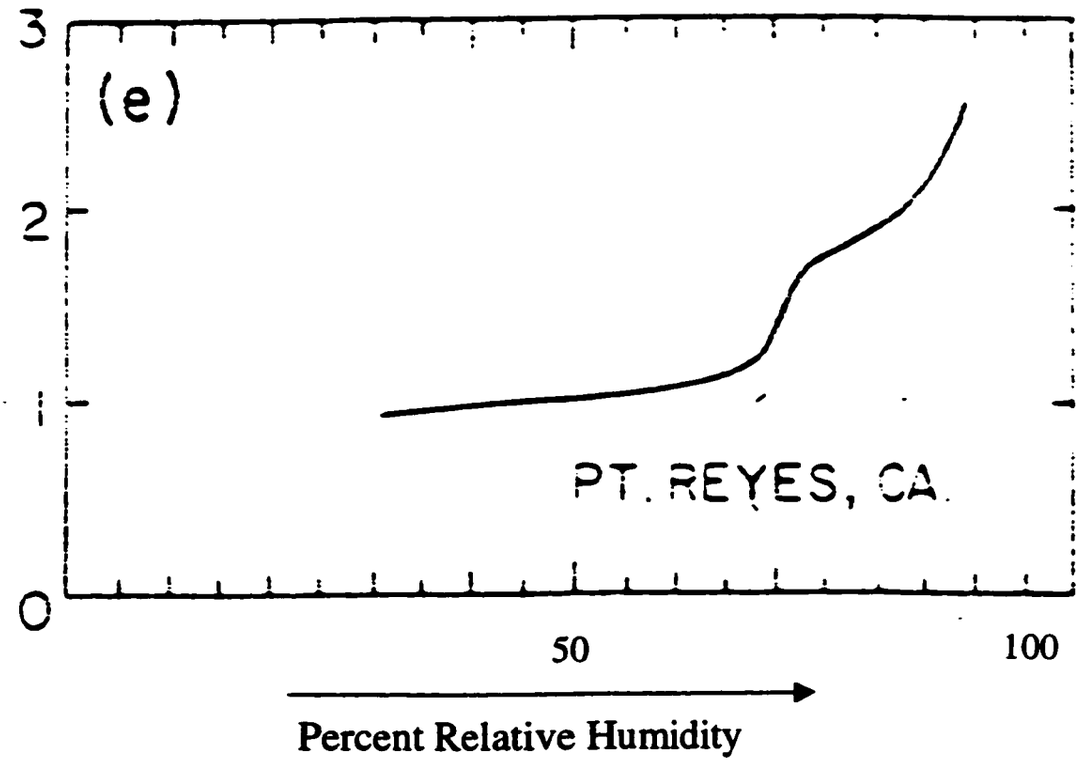

Figure 3-2 Humidogram from Point Reyes, CA, as evidence that deliquescence occurs in a state with no degrees of freedom. The y-axis is light scattering at the relative humidity listed on the x-axis, divided by light scattering at 30% R.H. The deliquescing salt is NaCl. Taken from Charlson, R.J., Covert, D.S., and Larson, T.V., *Observation of the effect of humidity on light scattering by aerosols.* In Hygroscopic Aerosols, edited by L.H.Ruhnke and A. Deepak, A Deepak Publishing, Hampton, VA, 1984.

the core-containing CCN is larger than that of the corresponding non core-containing particle. The number of degrees of freedom in this case is the same as the classical case discussed above because the core is chemically isolated from the rest of the system. The system has three phases (the solid, the solution, and the gas) and three components (the core material, the dissolved salt, and water). This system thus is thermodynamically equivalent to the case b and can be defined by a single variable. Another way to look at this situation is that the insoluble core is not thermodynamically part of the system at all.

The type of system considered in the rest of the chapter is a bit more complex (case c). There are initially three phases (gas, aqueous, and undissolved organic material) at the outset of droplet growth. As the slightly soluble organic compound dissolves, the solid phase disappears and P=2 (case d). There are always three components, however (water, the soluble salt, and the organic). Under isothermal conditions, the system has one degree of freedom at the beginning of the process. The only flexible variables in this case are the vapor pressure of water and the concentration of the salt. The concentration of the organic compound is fixed at its saturation concentration, so this system is in this sense thermodynamically equivalent to the two already listed. The only concentration changing is that of the salt, and the system can be completely described with the knowledge of this salt concentration *or* the water vapor pressure, since these variables affect each other. At the moment the organic dissolves fully into the droplet, however, two things that change the way the system is defined occurs. There is the loss of the undissolved phase, and the organic concentration now becomes a flexible variable, with the ability to decrease its concentration if more water is added to the system. There are now two degrees of freedom, among the variables of water vapor pressure, salt concentration, and organic concentration. In this sense, when the slightly soluble compound in this type of droplet fully dissolves it becomes thermodynamically different from the state it was in at the beginning of droplet growth. Furthermore, as the solid phase completely dissolves, the mole fraction of the organic is at its highest, affecting the vapor pressure the most at this point. The droplet size at which this occurs depends on the amount of organic material in the system and its solubility. As seen in the section on

cloud modeling, this characteristic can have large effects on the size distribution of cloud droplets and the corresponding optical properties.

Taking the example one step further (case e), Kulmala et al. [3] consider a system consisting of a hygroscopic salt, a weakly soluble core, water (liquid and vapor), as well as a highly soluble gas (nitric acid). The purpose of their treatment was to show that droplets under these conditions can become activated at a relative humidity of less than 100%, because the nitric acid dissolves into the immature droplet and contributes to the Raoult effect, diminishing the water vapor pressure. This system, like the one discussed in the last example has two regimes. The first is before full dissolution of the weakly soluble core. There are 4 components in 3 phases to start with, implying two degrees of freedom. The definable variables are the gas phase concentration of the soluble gas, the water vapor pressure, and the salt concentration. As before, the weakly soluble component has an unchanging concentration. When this component fully dissolves, there is an additional degree of freedom. The concentration of the weakly soluble component becomes a variable at this point.

DISSOLUTION BEHAVIOR OF PROXY ORGANIC MATERIAL IN NUCLEATING CLOUD DROPLETS

The basis for most of the material presented in this chapter is the article, *Dissolution behavior and surface tension effects of organic compounds in nucleating cloud droplets* by Shulman, Jacobson, Charlson, Synovec, and Young (Geophysical Research Letters, Vol. 23, No. 3, Pages 277-280). This article appears as an appendix to this dissertation as Appendix A, but the main features related to the work in this chapter are summarized in this section. To examine the effects that components with a range of solubilities from slight to high would have on the process of droplet growth, seven difunctional organic acids were chosen as proxy compounds for the hundreds of different types of material possible in atmospheric aerosol. The solubilities of these acids (oxalic, malonic, succinic, glutaric, adipic, phthalic, and cis-pinonic acids) were measured in

solutions of ammonium sulfate and ammonium bisulfate, with salt concentrations ranging from 0 to 3 molar. These salt concentrations were chosen because they represent the range that is present in the early stages of cloud droplet growth. The solubility of the organic acids were higher in the lower salt concentrations, and the compounds chosen had a range of solubilities from very soluble (malonic and glutaric acids) to very slightly soluble (phthalic and cis-pinonic acids). The solubility data is given in Table 3-1.

Table 3-1 Solubility of Slightly Soluble organic acids in Water, Ammonium Sulfate, and Ammonium Bisulfate

Compound	Solubility in H_2O (mol/L)	Solubility in Sulfate (mol/L)				Solubility in Bisulfate (mol/L)			
		0.01M	0.1M	1.0M	3.0M	0.01M	0.1M	1.0M	3.0M
Oxalic Acid	0.39	0.34	0.35	0.07	0.07	0.32	0.33	0.08	0.08
Malonic Acid	5.19	5.81	6.21	6.03	5.56	5.87	5.55	5.16	4.46
Succinic Acid	0.25	0.25	0.23	0.22	0.15	0.24	0.22	0.19	0.12
Glutaric Acid	2.26	2.37	2.47	2.07	1.04	2.30	2.15	1.65	1.70
Adipic Acid	0.05	0.05	0.05	0.04	0.02	0.05	0.05	0.04	0.02
Phthalic Acid	0.02	0.02	0.02	0.03	0.01	0.02	0.02	0.01	0.004
Cis-Pinonic Acid	0.02	0.02	0.02	0.007	0.0007	0.02	0.02	0.01	0.004

Using the solubilities listed in Table 3-1, the concentration of both the organic component and inorganic salt was simulated for droplets growing from a typical CCN. Figure 3-3 shows this simulation graphically.

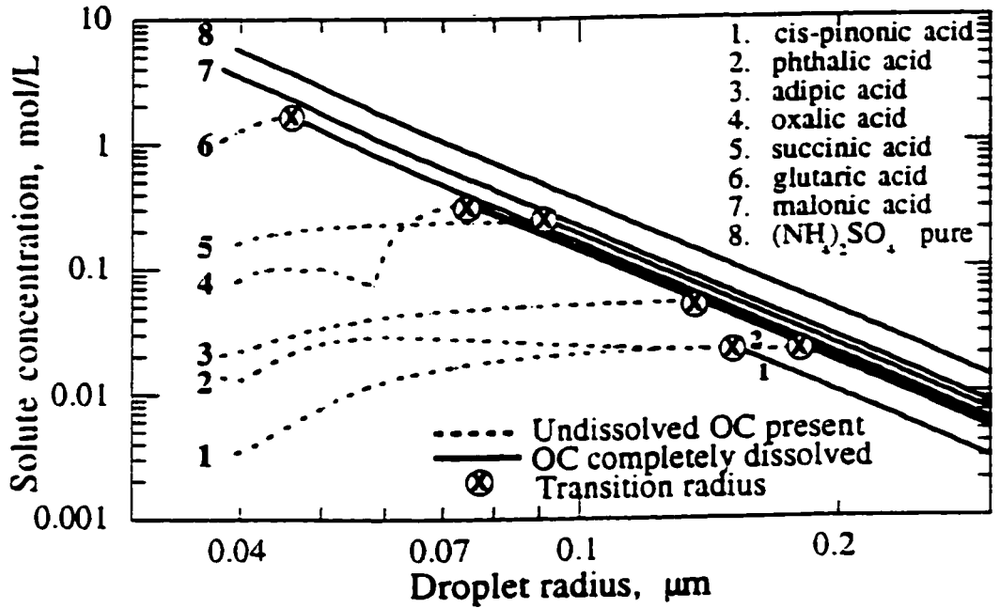

Figure 3-3 Concentration of organic compounds in a droplet as a function of radius. The dry particle radius is 0.03 μm, with mass 50% $(NH_4)_2SO_4$ for each of the seven aqueous systems containing an organic compound. The dry particle radius is 0.03 μm for the curve corresponding to pure sulfate. The size range in the plot is limited to 0.04 μm to just above 0.2 μm to focus on the radius where full dissolution takes place. Figure taken from Shulman et al., 1996 (Appendix A) [4].

The main feature of these simulations is that under realistic conditions, the features of case c in Figure 3-1 can be created, i.e. the organic compound is initially present in two phases (dissolved in saturated solution and undissolved) until the droplet has grown large enough to cause complete dissolution. The droplet size where this occurs depends on the solubility of the organic, the size of the dry particle, and the percentage of the total mass contributed by the organic material.

The results of the dissolution simulation were applied to a modified form Eq. 3-1 (the Köhler equation), listed as Eq. 3-4. This version of the Köhler equation includes a term describing the amount of a second, slightly soluble organic phase:

$$\frac{e'}{e_s} = 1 + \frac{2\sigma M_w}{kT\rho r^3} - \frac{3M_w\Phi}{4\pi\rho r^3}\left(\frac{\upsilon_{org}X_{org}m_{org}}{M_{org}} + \frac{\upsilon_{sulf}m_{sulf}}{M_{sulf}}\right) \qquad \text{(Eq. 3-4)}$$

where e' is the equilibrium vapor pressure of water over a solution droplet of a given radius (r) relative to the water vapor pressure over a plane surface of water (e_s), σ is the surface tension, M_w is the molecular weight of water, k is the Bolzmann constant, T is the temperature, ρ is the solution density, Φ is the osmotic coefficient of the aqueous solution, ν_{org} is the number of ions into which the organic dissociates when dissolved, m_{org} is the total mass of organic compound, m_{sulf} is the mass of the sulfate salt in the dry particle, M_{org} is the molecular weight of the organic, and M_{sulf} is the molecular weight of ammonium sulfate. Although we expressly refer to the material that gradually dissolves as organic matter, the same effect would be seen with any slightly soluble compound.

When Equation 3-4 is plotted as supersaturation vs. droplet size, as shown in Figure 3-4, there is a radius that corresponds to a maximum supersaturation on the curve. These values are the critical radius and critical supersaturation. This is the level of supersaturation and droplet size the droplet must experience in order to grow spontaneously, without any increase in super saturation of water vapor. These values depend on the dry particle size and chemical content of the particle, especially the solubility. The shape of the curve is also affected by the solubility of the constituents of

the particle, as shown in Figure 3-4, which has a curve for a pure salt, and curves for two different cases of organic compounds mixed with the salt. Figure 3-5 shows the effect of dry particle size on the curve.

The curve for the pure salt in Figure 3-4 exhibits a single maximum, while the curves for droplets containing organic material have a cusp and/or double peak, caused from the gradual dissolution of the organic material into the droplet as it grows. The magnitude of this effect is governed both by the solubility of the organic and the amount the organic material contributes to the mass of the dry particle. The critical supersaturation is increased with lower compound solubility, and with higher mass fraction of organic. For more details on these effects the reader is directed to Shulman et al. [4] (Appendix A). Figure 3-5 shows that the larger the size of the dry particle, the lower the critical radius and supersaturation (i.e. larger particles are easier to nucleate.) This is important for the next section, where the effects of changing critical radius and supersaturation on the size distribution of cloud droplets are explored.

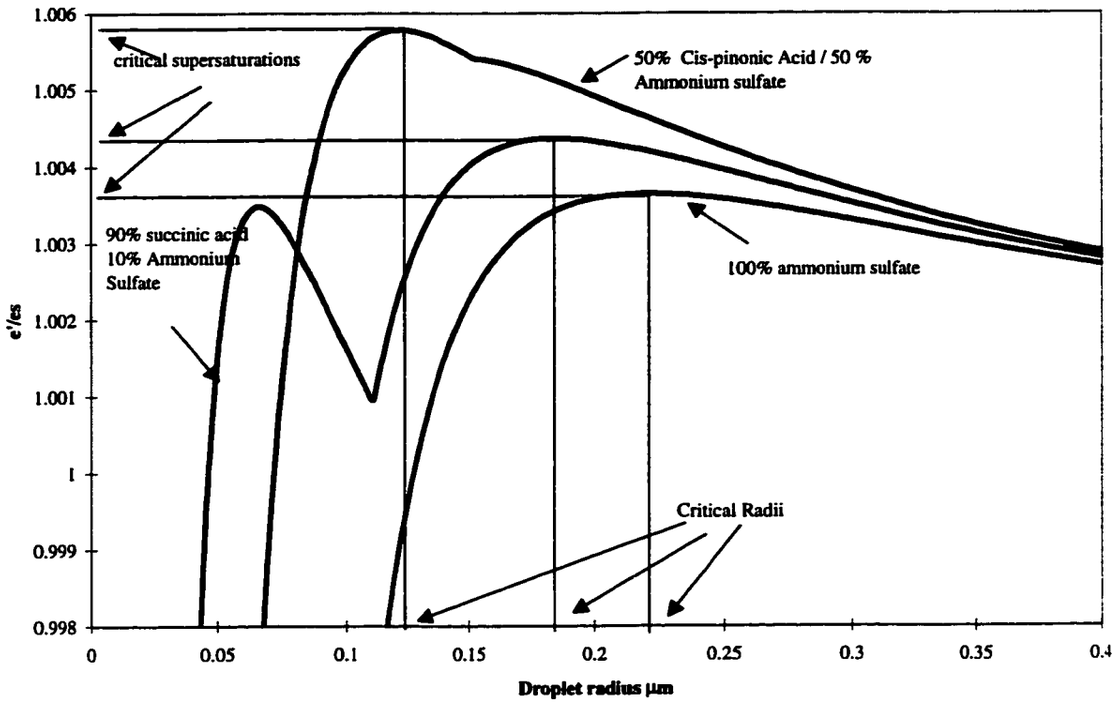

Figure 3-4 Köhler curves for droplets nucleated on pure ammonium sulfate, 90% succinic acid - 10% ammonium sulfate, and 50% cis-pinonic acid - 50% ammonium sulfate, all with a 0.03 µm dry particle radius. Droplet surface tension, temperature, and osmotic coefficient are assumed to be constant at 76 dynes/cm (the same as that for pure water), 273 K, and unity, respectively. The organic is assumed to dissociate into 2 ions, and the ammonium bisulfate into 3 ions. The size range in the plot is limited in order to focus on the region of droplet activation and cusp in the curves. Solubilities and other assumptions are as listed in Shulman et al., 1996.

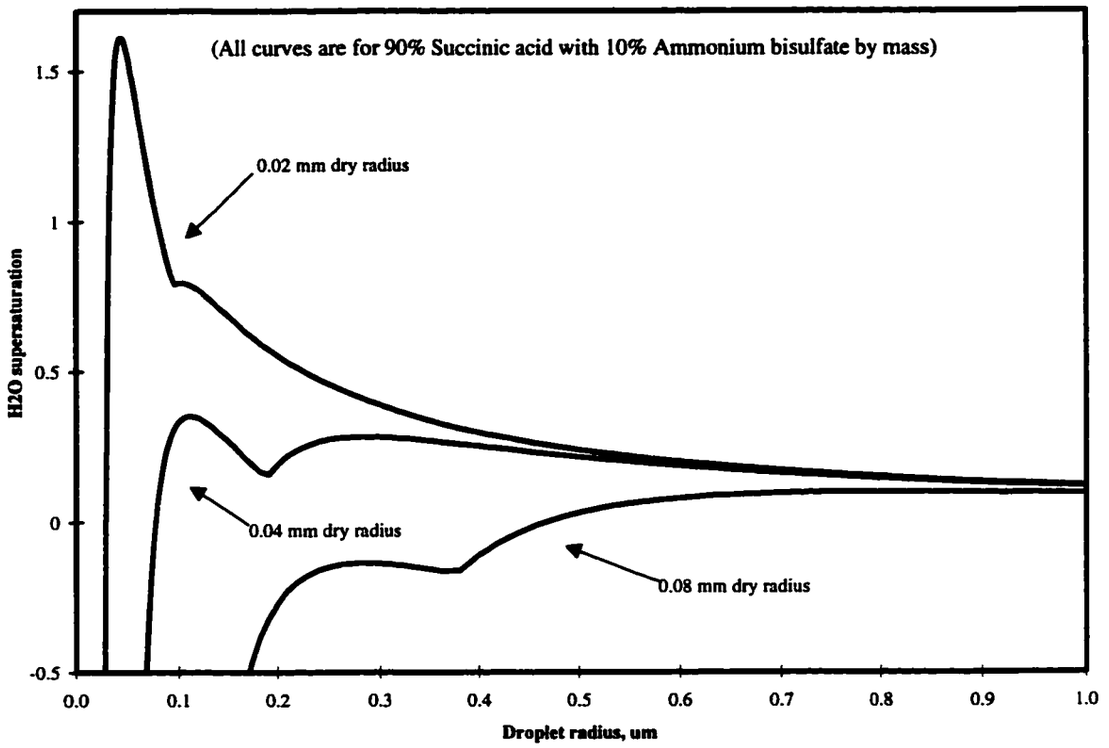

Figure 3-5 Köhler curves for droplets with different dry particle sizes. All curves are for droplets nucleated on 90% succinic acid – 10% ammonium bisulfate by mass. Other assumptions are as listed for Figure 3-4.

APPLICATION OF THE MODEL

Using a rising parcel model [2], the changes in the size distribution of droplets in a cloud due to the effects of organic material in CCN is calculated. The code for the computer model was formulated and run by Dr. Geert-Jan Roelofs of the University of Utrecht, The Netherlands. Two of the dicarboxylic acids are considered as model organic compounds with different solubilities; succinic acid with moderate solubility, and cis-pinonic acid with low solubility. Droplet growth is formulated using the solubility of one of the organic acids with ammonium bisulfate in a chemically homogeneous, internal mixture. The influence of the organic substance on surface tension and accommodation coefficient is neglected in order to examine the effect of solubility in isolation from other complicating factors. The initial size of the droplet at 99% RH is assumed controlled by the NH_4HSO_4 solute alone. In using the solubility characteristics of only two compounds, the intent was to provide a diagnostic of how the cloud droplet distribution would change under different solubility conditions. I do not mean to imply that these mixtures are necessarily realistic in the atmosphere, only that they are useful in qualitatively understanding the way the system reacts.

The cloud model dynamics are described by the equations for a simple rising air parcel [2]. Temperature and humidity profiles are taken from Lee et al. [5]. Initial height, radius, relative humidity, and upward velocity of the parcel are 1000 m, 350 m, 99%, and 1 m s^{-1} respectively. The time resolution of the parcel model is 0.05 seconds. The aerosol particles are initially given as a single dry lognormal distribution, with the shape and number concentration reflecting background continental conditions [6]. The initial mass concentration of this aerosol is 5.8 $\mu g\ m^{-3}$, for particles containing only ammonium bisulfate. The concentration is lower when the organic compounds are included because of their lower densities. Smallest and largest dry particle radii are 0.02 μm and 2 μm; this range is subdivided into 500 particle size bins. The particles are assumed to contain an internal mixture of ammonium bisulfate and an organic acid (i.e. each particle contains the same proportion of both substances), and to be equilibrated with the ambient RH =

99%. A linearized version of the droplet growth equation is used to calculate the condensational growth of the particles [2, 3] taking into account the limited solubility of the organic material. Development of the cloud is confined to a relatively small distance (approximately 250m) above the cloud base, so that entrainment can be neglected.

In order to check that the results are not simply a function of different molecular weight or solute considered in the CCN, one set of model calculations was run using the solubility of the organic acids in the model, while keeping all other physical constants the same as for ammonium bisulfate. The results for these runs were not significantly different than those using the actual physical data (density, molecular weight) of the model organic compounds.

CLOUD MODEL RESULTS

Figures 3-6 and 3-7 are number and surface area distributions (respectively) of activated droplets from the modeled growth of different compositions (percentages are by mass): 100% ammonium bisulfate, 50% cis-pinonic acid/50% ammonium bisulfate, 90% succinic acid/10% ammonium bisulfate, and 90% cis-pinonic/10% ammonium bisulfate. In each case, the distributions containing slightly soluble compounds are shifted to a smaller number of droplets with larger sizes than with the ammonium bisulfate nucleated droplet distribution. The size shift is dependent on both the molecular form and mass fraction of organic in the dry particles, with cis-pinonic acid at high mass fraction showing the largest deviation from the pure ammonium bisulfate case. Succinic acid, which is more soluble than cis-pinonic acid, shows less effect, even when it comprises a high mass percentage of the particles. For both organic acids, the more mass the organic contributes, the fewer and larger the resultant cloud droplets become. This effect can be qualitatively predicted by examining the Köhler curves shown in Figures 3-4 and 3-5. The critical supersaturation is determined both by the solubility of the solute (Figure 3-4) and by the size of the dry particle (Figure 3-5), with the larger, and more soluble particles exhibiting the lowest critical supersaturations. When material of lower solubility is

included as a fraction of aerosol mass, it becomes increasingly difficult for the smallest particles to activate because the critical supersaturation becomes higher than the ambient conditions determined in the rising parcel model.

As the resulting droplet size distribution is shifted towards larger droplets, there is a corresponding lowering in the total droplet surface area available to scatter light. Table 2 lists the total number, surface area, and volume for activated droplet distributions shown in figures 3-6 and 3-7. Since the largest shift in size is associated with droplets grown from cis-pinonic acid particles, this distribution has the lowest total surface area. The total volume of these three droplet distributions are equal, i.e. the liquid water content for these three cases are the same. Thus for the greatest changes in size distribution from the reference case, the largest particles activate and grow, absorbing water that would have otherwise been condensed on smaller droplets. Such shifts in cloud droplet size distribution imply changes in cloud optical properties [7].

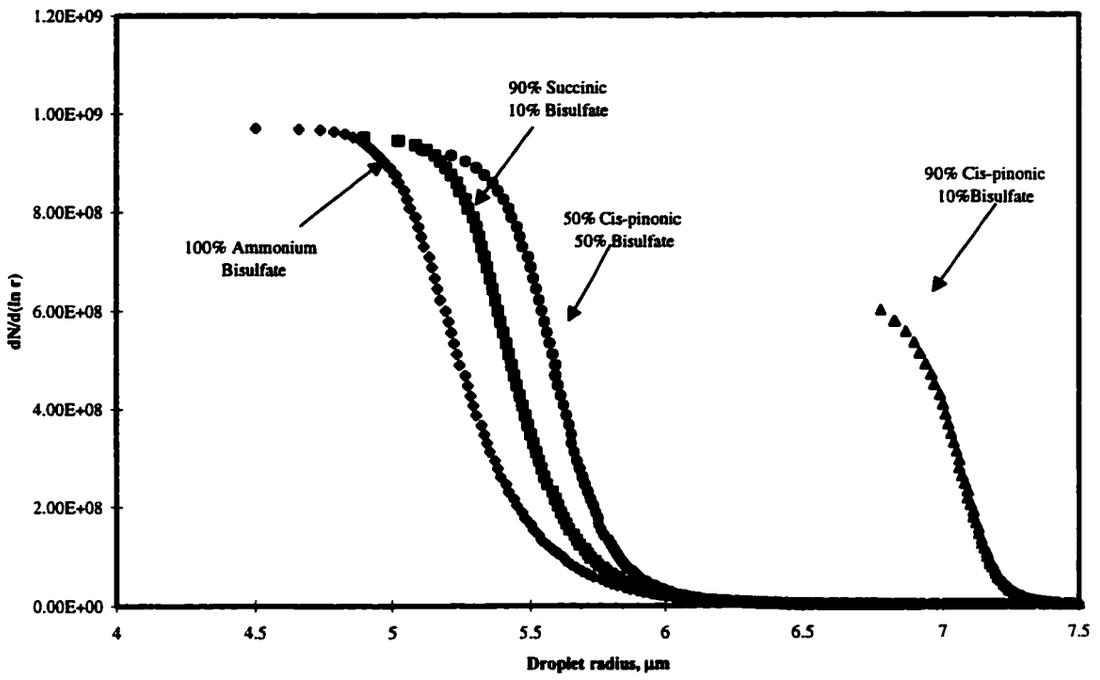

Figure 3-6 Number distributions of activated droplets grown from different chemical compositions of dry CCN, at a height of 1245 m, 1 m/s updraft speed. Chemical assumptions are as those listed for Figure 3-4.

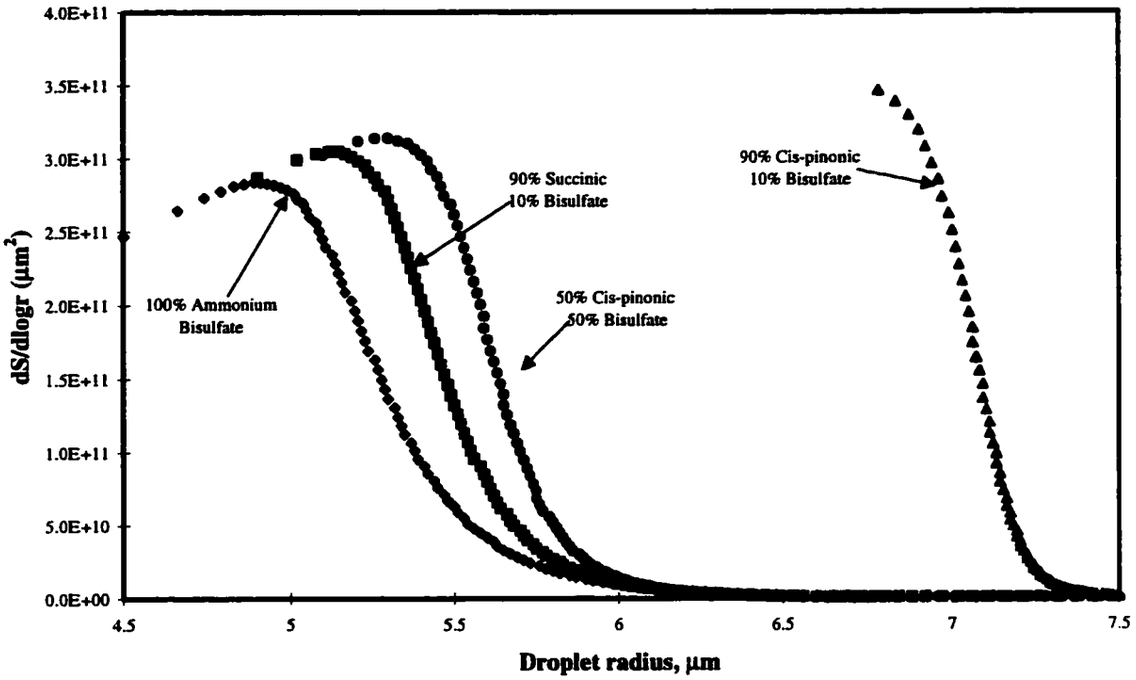

Figure 3-7 Surface area distributions of activated droplets. The conditions are the same as those listed for Figure 3-6.

Table 3-2 Total number, surface area, and volume for droplets grown from 100% Ammonium bisulfate, 90% Succinic Acid/10% Ammonium bisulfate, and 90% Cis-pinonic Acid/10% Ammonium bisulfate

CCN Composition (volume percent)	Total number activated droplets (m^{-3})	Total surface area of activated droplets (μm^2 m^{-3})	Total volume of activated droplets (g H_2O m^{-3})
100% Bisulfate	8.9×10^8	2.96×10^{11}	0.51
90% Succinic/10% Bisulfate	8.0×10^8	2.85×10^{11}	0.51
90% Cis-Pinonic Acid/10% Bisulfate	4.8×10^8	2.39×10^{11}	0.51

The sensitivity of change in cloud albedo caused by changing the mass percentage of organic matter in the dry CCN has been estimated using the approach followed by Twomey, 1977, [7], Charlson et al., 1987 [8], and Schwartz and Slingo, 1996 [9] where the droplet size distribution is compared with that of a reference cloud having a known albedo. The index for the distribution is the surface area-weighted average radius, (the effective radius, r_{eff}). Equation 3-5 uses the effective radius to give the difference in albedo from that of the reference cloud:

$$\Delta R_{ct} = -R^{\circ}_{ct}(1-R^{\circ}_{ct}) \ln(r_{eff}/r^{\circ}_{eff}) \qquad \text{(Eq. 3-5)}$$

where ΔR_{ct} is difference in cloud top albedo, R°_{ct} is the cloud-top albedo of the reference cloud, at a wavelength of 0.6 μm and solar zenith angle of 60°[8]. The terms r_{eff} and r°_{eff} are the effective radii of the model and reference clouds, respectively [8, 9]. The effective radius of the reference cloud with R°_{ct}=0.5 is taken from the case assuming pure ammonium bisulfate particles. The results of the calculation are shown graphically in Figure 3-8, as a function of the mass percent of organic material in the dry particles.

Assuming the chemical makeup of CCN could be shifted globally (e.g. by the addition of anthropogenic sulfate, or a transition between ice-age and interglacial times), we can estimate the planetary radiative forcing caused by the change in cloud-top albedo described above. For this calculation we assume a reference planetary albedo (R°_{p}) of 0.3, which is the average albedo of a planet half-covered with clouds (R°_{ct} =0.5) and an average non-cloud covered surface albedo of 0.1 (R_S):

$$R^{\circ}_{p} \simeq 0.5(R_S) + 0.5(R^{\circ}_{ct}) = 0.3 \qquad \text{(Eq. 3-6)}$$

The modified planetary albedo (R_p) is then calculated from the change in cloud albedo calculated in Eq. 3-5:

$$R_p = 0.5(R_s) + 0.5(R^{\circ}_{ct}-\Delta R_{ct}) \qquad \text{(Eq. 3-7)}$$

Forcing in Wm^{-2} (ΔF) can then be calculated as:

$$\Delta F = F_o(R^{\circ}_{p} - R_p) \qquad \text{(Eq. 3-8)}$$

where F_o is the average solar irradiance, assumed to be 300 Wm^{-2}. The results are shown on the second axis in Figure 3-8. Even the addition of 10% of a compound having the solubility of cis-pinonic acid would change cloud albedo by more than 0.003, causing a forcing of ca. -0.5 Wm^{-2}, a forcing that is significant considering the forcing due to anthropogenic CO_2 of ca. 1.5 Wm^{-2} [10].

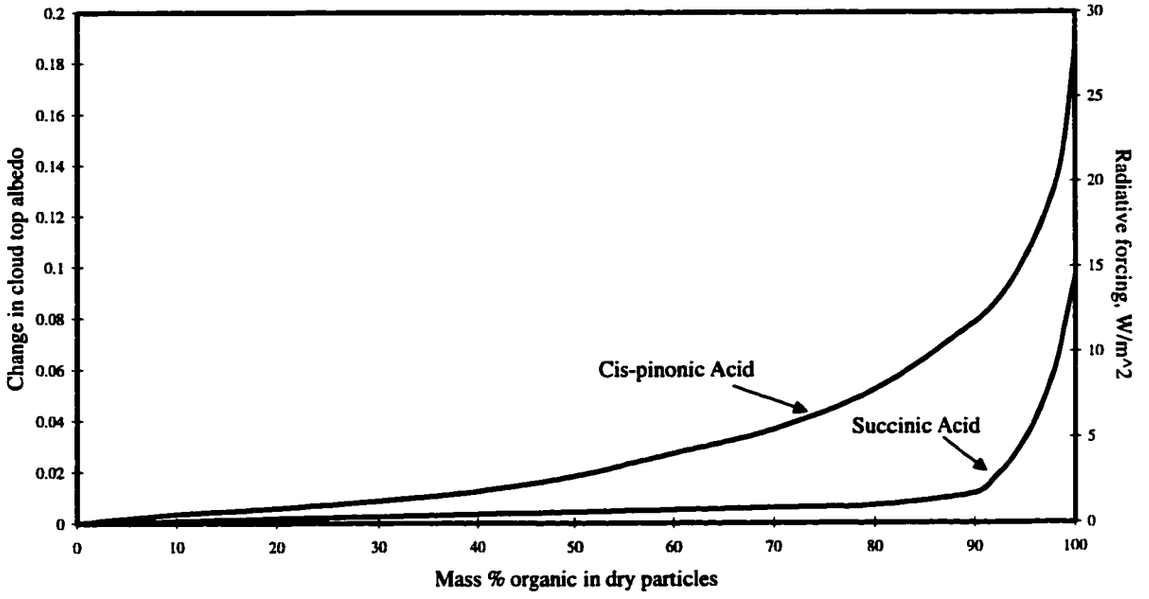

Figure 3-8. Lowering of cloud albedo from a reference albedo of 0.5, as calculated in Equation 3-5, as a function of mass percentage of organic in the dry particle. The balance of the dry mass is assumed to be ammonium bisulfate. Right axis: Corresponding radiative forcing caused by lowered cloud albedo, assuming a world-wide shift in chemical composition and albedo from the reference cloud conditions of 100% ammonium bisulfate CCN and 0.5 cloud top albedo; calculated from Equations 3-6 to 3-8. Due to its higher solubility, succinic acid has less effect on cloud albedo and radiative forcing than cis-pinonic acid.

IMPLICATIONS FOR CLIMATE

Even if atmospheric aerosol size distribution and concentration remained constant (e.g. via a population steady state [11], changing the solubility alone of CCN would affect cloud droplet size distributions, and therefore cloud optical properties and planetary radiative balance. The presence or absence of these organic materials may also influence surface tension and accommodation coefficient and could cause further changes in cloud droplet size distributions. However, the lack of data on organic aerosol forms and physical properties, as well as the difficulty and uncertainties involved in obtaining quantitative information on the effects of aerosols on cloud properties prevent a more thorough analysis or experimental confirmation of the findings at this time.

The concept that slight solubility can change the albedo of clouds has implications for differences in climate on the ice-age, interglacial and industrial time scales. Specifically, the proportions of slightly soluble organics, sulfates, sea-salt and mineral particles must have varied systematically between those periods, leading to differences in the fraction of particles acting as CCN. It is not possible to model such changes quantitatively, but it is clear that certain controlling factors must have been involved. During periods of glaciation, the current large area-vegetative sources of natural aerosol-genic alkenes (e.g. terpenes) and smoke from natural fires were greatly lessened due to ice cover [12], while the emission of DMS from the sea appears to have been at least as large as today [13], making it relatively more important to the total aerosol and perhaps the globally dominant source of CCN. During the pre-industrial, interglacial time, the boreal forests arose [12] and organic aerosols from the oxidation of terpenes and from natural fire were added into the mix, increasing the organic fraction over that present during the glacial time. The model results presented here suggest therefore a natural positive feedback process where the warmer temperatures of the preindustrial interglacial time caused a decrease in the average solubility of CCN, leading to clouds with lower albedo, and thus increased surface temperatures. If this feedback operated during the

transition from the glacial to the pre-industrial/interglacial time, the consequently lower cloud albedo could have been a factor hastening the end of the ice-age.

Industrialization subsequently has added large amounts of sulfates [14] and smoke from biomass and fossil fuel combustion, leading to a still different aerosol composition and the CCN that we observe today. Systematic changes in both the total aerosol number population and the fraction of it that act as CCN must have occurred, leading to corresponding changes in cloud microphysics and albedo. It is possible to speculate that higher fractions of the aerosol might act as CCN during the glacial and industrial periods relative to the pre-industrial interglacial time, due to the possibly higher fraction of soluble sulfates; however, evidence to demonstrate this is not available and would be difficult to acquire. Clearly, organic fraction, CCN, cloud microphysics, and therefore cloud albedo cannot be assumed to remain constant over such climatic time scales.

NOTES TO CHAPTER 3

1. Köhler, H., *The nucleus in the growth of hygroscopic droplets.* Trans. Far. Soc., 1936. **32**: p. 1152-1161.
2. Pruppacher, H.R. and J.D. Klett, *Microphysics of Clouds and Precipitation.* 1978, Dordrecht: D. Reidel.
3. Hänel, G., *The role of aerosol particles during the condensational stage of cloud: A reinvestigation of numerics and physics.* Beitr. Phys. Atmosph., 1987. **60**: p. 321-339.
4. Shulman, M.L., M.C. Jacobson, R.J. Charlson, R.E. Synovec, and T.E. Young, *Dissolution behavior and surface tension effects of organic compounds in nucleating cloud droplets.* Geophys. Res. Lett., 1996. **23**(3): p. 277-280.
5. Lee, I.Y., G. Hänel, and H.R. Pruppacher, *A numerical determination of the evolution of cloud drop spectra due to condensation on natural aerosol particles.* J. Atm. Sci., 1980. **37**: p. 1839-1853.
6. Jaenicke, R., *Aerosol physics and chemistry*, in *Landolt-Bornstein, Numerical Data and Functional Relationships in Science and Technology*, K.H. Hellwege, Editor. 1988, Springer-Verlag: Berlin.
7. Twomey, S., *Atmospheric Aerosols.* 1977, Amsterdam: Elsevier.
8. Charlson, R.J., J.E. Lovelock, M.O. Andreae, and S.G. Warren, *Oceanic phytoplankton, atmospheric sulphur, cloud albedo and climate.* Nature, 1987. **326**: p. 655-661.
9. Schwartz, S.E. and A. Slingo, *Enhanced shortwave cloud radiative forcing due to anthropogenic aerosols*, in *Clouds, Chemistry and Climate*, P. Crutzen and V. Ramanathan, Editors. 1996, Springer-Verlag: Berlin-Heidelberg.
10. IPCC, *Climate Change*, ed. J.T. Houghton. 1995, Cambridge: Cambridge University Press.
11. Baker, M.B. and R.J. Charlson, *Bistability of CCN concentrations and thermodynamics in the cloud-topped boundary layer.* Nature, 1990. **345**(6271): p. 142-145.
12. Prentice, I.C., M.T. Sykes, M. Lautenschlager, S.P. Harrison, O. Denissenko, and P.J. Bartlein, *Modelling global vegetation patterns and terrestrial carbon storage at the last glacial maximum.* Global Ecol. Biogeogr. Lett., 1993. **3**: p. 67-76.

13. Legrand, M.R., R.J. Delmas, and R.J. Charlson, *Climate forcing implications from Vostok ice-core sulphate data.* Nature, 1988. **34**: p. 418-420.

14. Mayewski, P.A., W.B. Lyons, M.J. Spencer, M.S. Twickler, C.F. Muck, and S. Whitlow, *An ice-core record of atmospheric response to anthropogenic sulphate and nitrate.* Nature, 1990. **346**: p. 554-556.

CHAPTER 4: THERMAL-OPTICAL CARBON ANALYSIS

INTRODUCTION

The message of the first three chapters was that organic aerosols are important constituents in the atmosphere that have unique physical characteristics controlled by molecular form that are poorly understood at this time. One of the most basic measurements that has only been done to a limited extent is determination of total organic and refractory (sometimes called soot) carbon concentration in a wide variety of atmospheric environments. This measurement is important not only for mass balance and modeling, as discussed in Chapter 2, e.g. the recent work by Liousse et al. [1], but also as a measure of the severity and type of environmental effects organic aerosols have been shown to have (e.g. those listed in Chapter 1). The studies presented in Chapter 3, especially the speculation of what percentage of CCN mass may be organic are also dependent on this basic information. There is, therefore, a demonstrated need for a simple and reliable method of measuring the concentration of organic aerosol. In this chapter I present an instrument that was built specifically for the project of attempting to measure the concentrations of organic aerosols on the coast of Washington State, as described in Chapter 5.

GENERAL DESCRIPTION AND HISTORICAL ASPECTS

The method presented here follows the same general concept as previous instruments used to measure particulate organic and refractory carbon [2-4]. It relies on the property of organic compounds to volatilize and oxidize at lower temperatures than refractory (usually thought to be elemental) carbon, especially in the absence of oxygen, and usually involves samples collected on quartz filters. The operation of these analyzers is to (1) volatilize organic compounds from a small piece of the sample filter by heating at various temperatures in an oxygen-free atmosphere, (2) convert these compounds to

carbon dioxide by passing the gases over an oxidizing catalyst, (3) quantify CO_2 either directly using an NDIR (non-dispersive infrared) measurement, or indirectly by transforming the CO_2 into methane with subsequent quantification by flame ionization detection (FID), (4) oxidize refractory carbon by introducing oxygen into the gas mixture with continued heating, and (5) measure elemental carbon as CO_2 or CH_4 as described in steps 2-3. In the first studies of ambient aerosol using analysis of this type, it was recognized that there was a darkening of the samples during the initial volatilization step due to carbonization (charring) of organic compounds while heating in the absence of oxygen [2, 3]. This process produces refractory, possibly elemental carbon at the expense of organic carbon, so that organic carbon is underestimated and refractory carbon is overestimated. A method of optically monitoring the darkening of the filter using a laser transmission and/or reflectance method was developed and added to the method for most subsequent generations of these analyzers [3, 4]. This optical correction was used in the method described in this chapter, and will be explained in detail in a later section.

The variations in the methods used for different instruments has been in the analysis time at each temperature, the rate of temperature increase in the first step, the atmospheric composition, the calibration standards, and the presence or absence of concurrent optical monitoring of the quartz filter for charring of organic carbon. All of analyzers produced to date have produced apparently reliable data on total carbon from ambient sites, but differ in the organic/refractory carbon ratio. The changes that have taken place in the designs of these analyzers have been attempts to better characterize this cutoff between organic and refractory carbon.

Chapter Overview

The organization for the rest of the chapter will be to first describe the instrument in detail in terms of the equipment used and the design of how it is put together. This is followed by a discussion of the computer program used to run the instrument and the sequence of events in a typical run. Finally I present a listing of the characteristics and

usefulness of the instrument, as well as some sample results and discussion of possible sources of error.

DESIGN OF THE CARBON ANALYZER

The design of the carbon analyzer used for this project was a combination of those designed and used by Cadle et al. At General Motors [2] and Chow et al., used at the Desert Research Institute in Reno, NV. [4]. Much of the equipment for the analyzer built here was donated by General Motors from the equipment described by Cadle et al. [2]. The Chow/DRI instrument was based mainly on instruments produced at Oregon Graduate Center by Huntzicker et al. [3]. Significant modifications were made to both of these basic designs. A block schematic for the instrument is shown in Figure 4-1. There is a valve network that is controlled by a personal computer. Gas flows are controlled by these valves so that the proper gas mix reaches a heated quartz combustion and oxidation cell where the chemical reactions take place. Heating of the cell is set by a computer using a feedback from a thermocouple, and controlled by a power amplifier run off a signal from the computer. Gas emerging from the cell is analyzed for CO2 as it passes through the NDIR analyzer. The signal from the NDIR is read by the computer and stored. The charring effect on the filters is monitored by the transmission of laser light (632.8 nm) and read by a photodetector. The photodetector signal is fed to an amplifier and sent to the computer. The main subsystems are described more detail in the sections that follow.

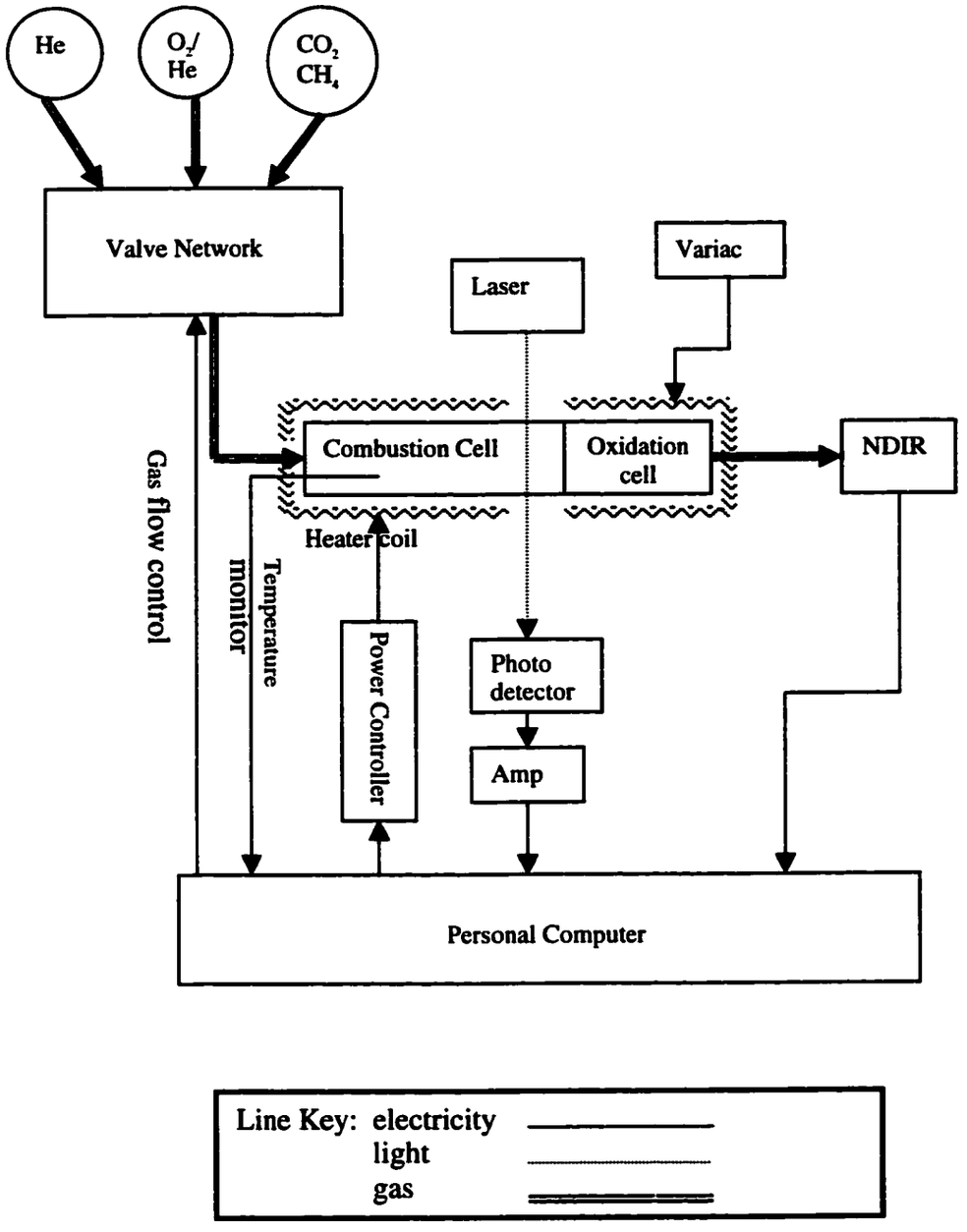

Figure 4-1 Block diagram of the carbon analyzer.

COMBUSTION CELL

A diagram of the combustion cell is given in Figure 4-2. There are two main sections of the cell, the volatilization zone and the oxidation zone. The sample on a quartz filter sits on a stainless steel platform within the volatilization zone where it is heated from ambient up to 800 °C in steps of 200 °C. Small dimples (thermal wells) are impressed into both zones to provide a port to measure temperature with thermocouples. Organic gases are liberated and carried by a gas flow into the oxidation zone, which is packed with an oxidizing agent (manganese dioxide). The MnO_2 is kept heated at approximately 900°C and is exposed to a constant flow of 0.1 L min^{-1} of 10% O_2 in helium. The organic gases are transformed into CO_2 at this point, which is carried off to the NDIR spectrometer. It was found that at the conditions used, the methane calibration gas mixture (10% in He) injected into the cell produced the same signal as the carbon dioxide standard, indicating complete oxidation of the most reduced form of carbon. Both zones are made of ½" O.D. quartz tubing, but there is a section of ¼" quartz tube between the two zones to increase the carrier gas velocity at this interface to reduce the possibility of oxygen bleeding into the volatilization zone. The front of the cell (the right side in Figure 4-2) is kovar metal (½" O.D.) which is fused directly to Pyrex glass (½" O.D.) (Larson Electronic Glass KP-050-T). The Pyrex is fused to quartz in front of the heated part of the cell. The entire remainder of the cell is made of quartz. This arrangement with a metal tube was chosen so that a Swagelok fitting could be tightened down on the tube without fear of breaking it. This seals the cell from the ambient air and provides a means of holding the sample platform in the tube at the proper place, as well as support for the entire cell assembly. The volatilization zone is wrapped with a 0.5 mm x 0.5 cm x 10 cm nichrome ribbon for heating. The oxidation zone is wrapped in a coil of nichrome wire. These heating elements and the glass parts of the cell were enclosed in an aluminum cylindrical shell that was packed with ceramic insulation material. This gives a fast temperature response and protects the operator from possible burns (the outer shell covering the cell remains cool to the touch, even at high operating temperatures. The only glass parts protruding from the shell are quartz tubes (1/4" diam) mounted

perpendicular to the rest of the cell. These tubes are mounted directly to the outside of the quartz tube comprising the volatilization zone, and do not protrude into the wall of the cell. They serve as alignment guides for the laser system used to monitor charring of material on the filter sample.

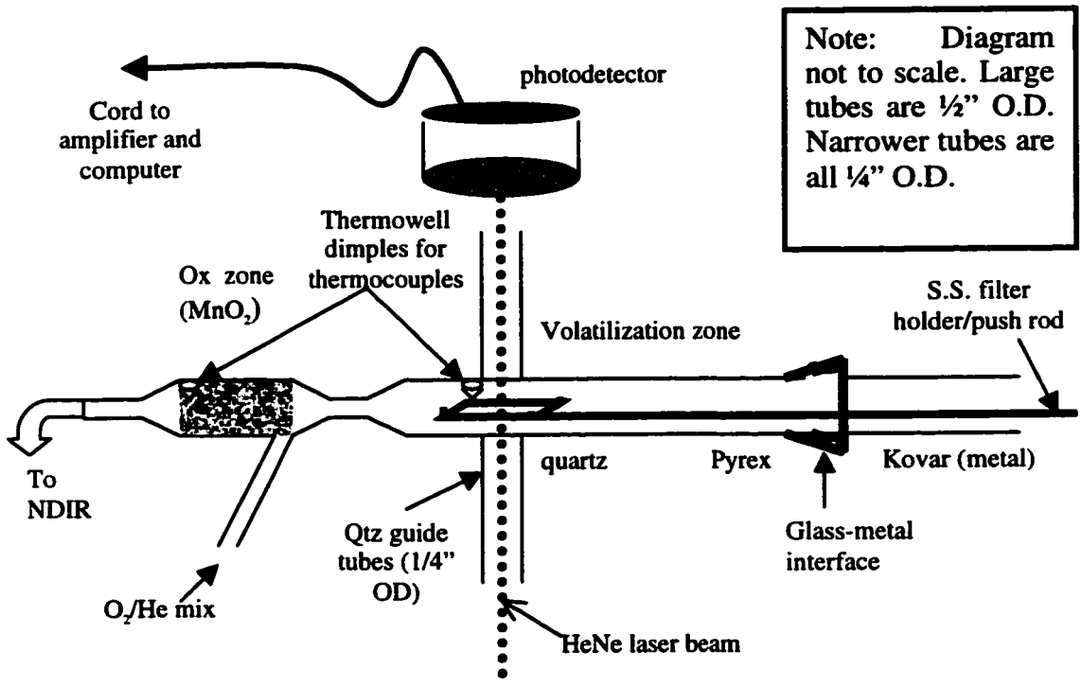

Figure 4-2 Combustion cell diagram.

PLUMBING AND VALVE NETWORK

Flow control

A diagram of the plumbing system is given in Figure 4-3. All gas flows are controlled using solenoid valves (Asco, 8262 series), which are all actuated by a TTL digital 5 volt signal by the computer. The system is designed so that there is always a flow rate of 1.0 L min^{-1} reaching the NDIR analyzer, regardless of the gas mixture. This is important because the NDIR measures the concentration of CO_2, not the absolute number of moles. The concentration of evolved CO_2 reaching the analyzer is dependent on the flow rate.

The main part of the flow is pure helium, which makes up either 90% or 80% of the total flow, depending on the section of the run. The other gas always flowing is a mixture of oxygen (10%) in helium. This O_2/He mix is either 10% or 20% of the total. At the beginning of analysis, the filter sample that is situated in the volatilization zone of the combustion cell is exposed to pure, oxygen free helium only. The helium that flows into this part of the cell is 90% of the total flow, and 100% of the flow into the volatilization zone, thus both solenoids 1 and 2 on this section are left open. Before being allowed to enter the combustion cell, the gas is passed through two oxygen scrubbers to prevent oxygen contamination in the volatilization zone. The first is a heated gas purifier (Supelco model 2-2398). This is followed by treatment through an indicating oxygen trap (Alltech model 4004) which indicates if the first trap is failing. The O_2 /He mix that flows into the oxidation zone of the cell makes up 10% of the total flow at this point, so solenoid 3 is open and solenoid 4 is left closed. When the gas mixture is to be changed so that the filter sample is exposed to oxygen (for measurement of refractory carbon), the 10% of the total flow that is helium is replaced with the O_2/He mix by closing solenoid 2 and opening solenoid 4. This gas mixture also continues to flow directly to the oxidation zone of the cell, at a flow rate of 10% of total. The gas composition during refractory carbon analysis therefore is 2% O_2 / 98% He at the filter sample, and at least 10% O_2 in the oxidation zone. Flow rates between 0.02 and 1.0 L min^{-1} were measured using rotameters accurate to within 0.001 L min^{-1} and controlled

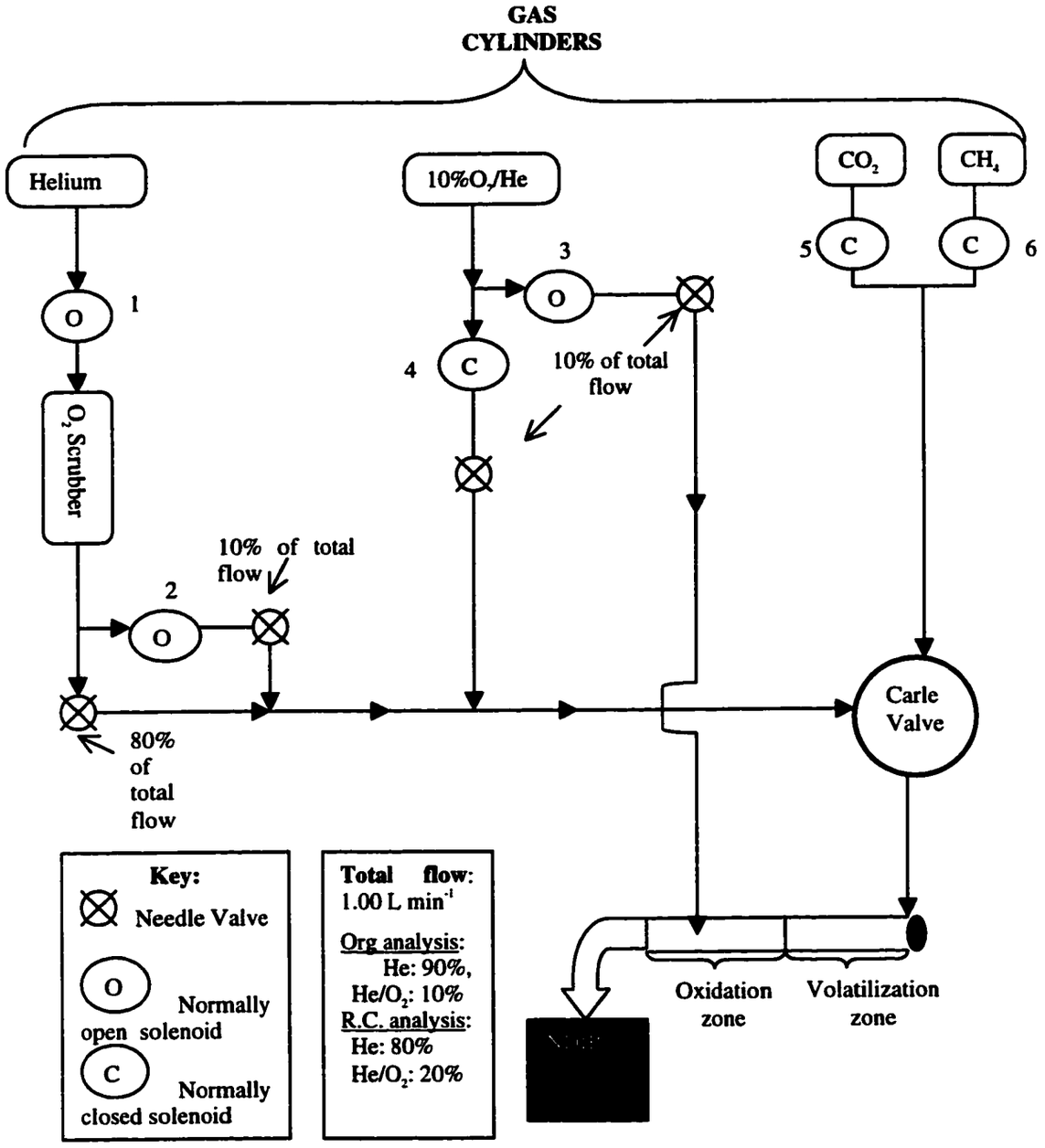

Figure 4-3 Carbon analyzer plumbing and valve system.

using needle valve flow controllers that deliver a set flow rate over a wide range of gas pressures introduced at the inlet of the valve (Condyne model 300). The entire valve network was plumbed using 1/8" stainless steel tubing with a 0.028" wall (Pac Stainless).

Calibration gas valve system

Automatic injection of calibration gas (10% methane in helium) was performed at the end of each instrumental run, using a Carle injection valve (Carle model 2918). A schematic of the valve is given in Figure 4-4. Gas from the main flow (90% of the volumetric flow rate as described above) enters the valve at port 6. During the "fill" step, port 5, which leads to the combustion cell, is connected to port 6. In this configuration, calibration gas enters the valve at port 2, and fills a loop, re-entering the valve through port 4, which is connected to the vent out of the instrument at port 3. In the "injection" configuration the main flow is allowed to sweep through the loop already containing calibration gas, carrying the calibration gas through to the combustion chamber out port 5 of the valve. Calibration gas still entering the valve at this point is directed out the vent through port 3. The Carle injection valve is actuated to move clockwise or counterclockwise using a 5V TTL high issued from the computer. The signal produced at the NDIR by injection of calibration gas from this valve was found to be precise to within 0.25%. This valve is equipped with a 50 μL loop.

TEMPERATURE CONTROL

Temperature at the oxidation zone is measured using a rigid K-type thermocouple with an inconel sheath (Omega, KMQIN 0.062" sheath diameter, 4" long, grounded), placed into a thermal well dimple impression in the quartz cell, protruding out from the aluminum shell of the combustion cell. The thermocouple wire is connected to the data acquisition system of the computer at a port on the screw terminal that is cold junction compensated. The temperature data is fed into a subroutine of the data acquisition and control program that acts as a proportional-integral-differential (P.I.D.) temperature controller. The output from this program is relayed out as an analog signal to the power

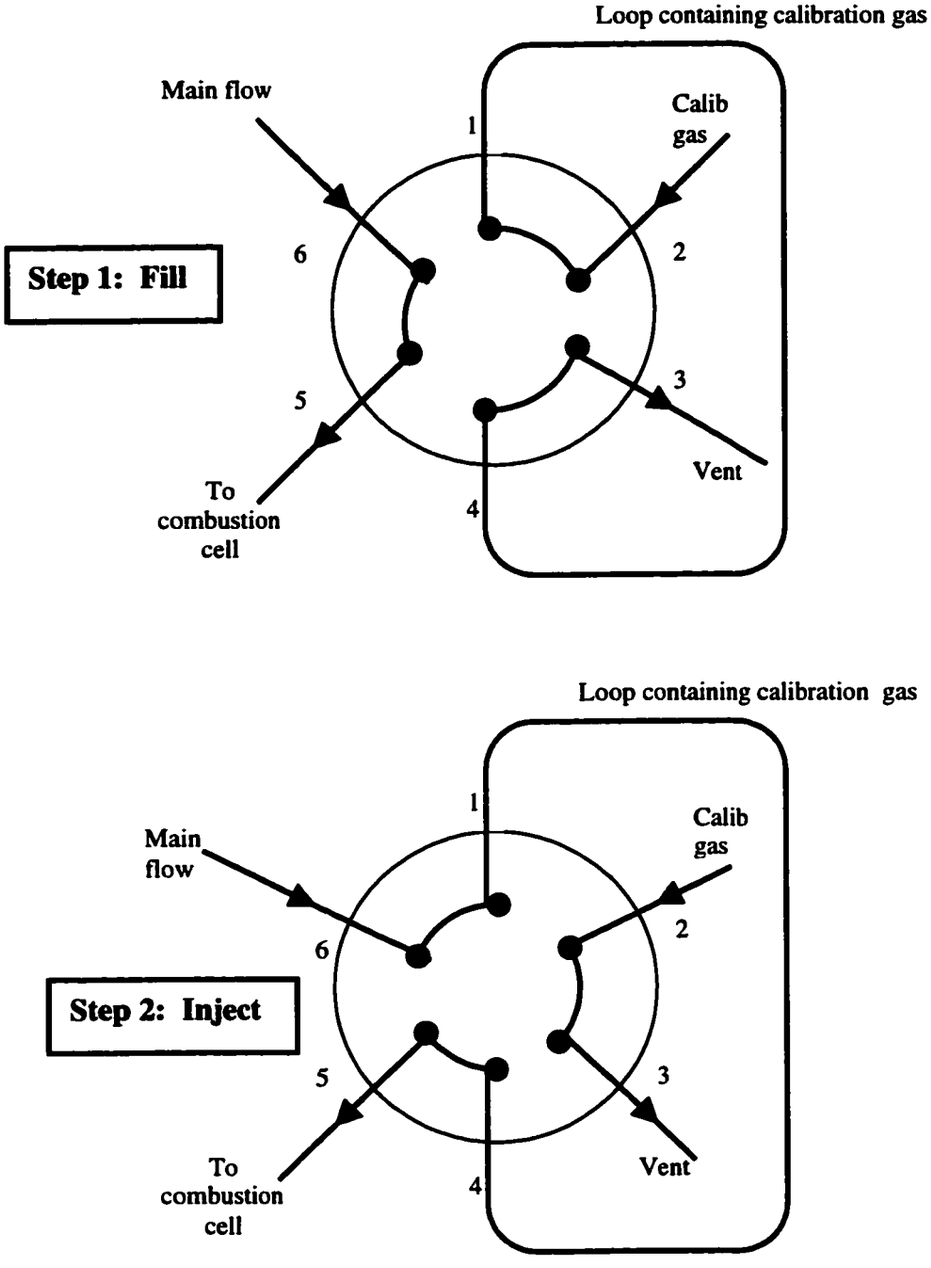

Figure 4-4 Carle valve schematic

controller (Barber Colman series 401). The power controller provides a controlled voltage source (up to about 110 V) that is proportional to a computer signal acting as a control input. This high voltage-low current source is fed into a 120 to 12 Volt transformer (Tierney Electric, AC 500C-2V23A-L) to provide enough current to cause sufficient heating by the nichrome ribbon wrapped around the combustion cell.

Heating of the oxidation zone is considerably easier since it does not require a change in temperature during a run. The ends of the nichrome heating wire were simply connected via insulated wire to a manual Variac control, and set to the proper voltage, which was about 10V. This setting depends to some degree on how tightly packed the cell is with MnO_2. The temperature of this part of the cell was followed using the type of thermocouple described above. Figure 4-5 shows the set-response capability of the temperature controller, together with the sensitivity of the temperature at the oxidation zone to the setting of the variac.

NDIR CO_2 Gas Analyzer

The CO_2 analyzer is the most important sensor in the system. The system used is a Horiba model PIR-2000 that relies on nondispersive infrared ray absorption for continuously determining the concentration of CO_2 in a gas stream. The sample gas flow rate allowed is between 0.5 and 1.5 L min^{-1} with a limit of detection of 20 ppm, as listed by the manufacturer. Although a range of flow rates is possible, it is important to keep the flow rate the same throughout each experiment, as discussed in the section on flow control. The instrument operates by emitting broadband infrared radiation from a light source which passes through both a sample and reference cell. The cell path length is 200 mm. The light passing through the cells is modulated through a rotating chopper and to a detector. If infrared radiation passing through the sample cell is absorbed by a gas in the sample, there is a corresponding decrease in the amount of IR radiation reaching the sample side of the detector. Since the IR radiation is modulated to only reach one side of the detector at a time, this results in an imbalance between the two sides of the detector. A membrane between the sample and reference cells in the detector produces an

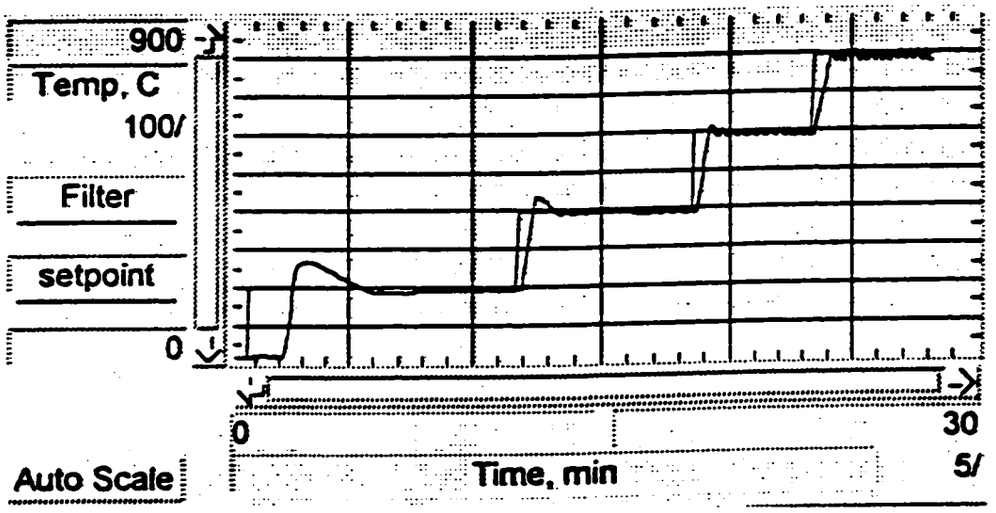

Figure 4-5 Set-response performance of the temperature control system. The temperature setpoint and actual measured temperature are superimposed. There is an approximate one minute lag time between setting a new temperature and relaxation of the system to that temperature.

electrical output, which is amplified and read by the computer system.

LASER TRANSMISSION MEASUREMENT SYSTEM

To observe and correct for charring of organic compounds during the volatilization step, a helium-neon (HeNe) laser is passed through the filter sample during analysis (Melles Griot 05-LHR-151 laser head, 5mW power at 632.8 nm wavelength, 0.8 mm beam diam., 1.00 mrad beam divergence). The light is detected on the other side of the filter by a silicon photodiode detector (Melles Griot 13DSI007, 10mm^2 active area). Because the quartz filter and heating coil emit broadband background radiation at high temperature that interferes with the measurement, a 632.8 nm laser line optical filter is placed in front of the photodetector (Melles Griot 03FIL006, with +0.2, -0 nm tolerance). The important part of this measurement is not the absolute percent transmission, but rather the relative change in transmission throughout the experiment. The level of transmission is noted before heating the sample. As the temperature increases, some organic compounds char and the transmission drops. Transmission continues to decrease until oxygen is introduced into the volatilization part of the cell. This combusts refractory carbon on the filter so the transmission rapidly increases up to the initial level, and higher. The amount of refractory carbon combusted between the time the oxygen is introduced up to when the transmission reaches the initial level is assumed to be equal to the amount of carbon that was produced by charring. The amount of refractory carbon combusted after the transmission has reached this level is therefore due to elemental carbon in the atmospheric aerosol. This scheme is taken into account when calculating the relative amount of organic and refractory material on the filter.

The principle assumption implicit in this treatment is that pyrolytically produced elemental carbon has the same light extinction per unit mass as atmospheric refractory carbon particles. There is no fundamental reason why they should be exactly the same, since elementary carbon is generally thought to be a chemically complex mixture of elemental carbon coated or mixed with organic functional groups at the surface. The other possibility is that the material causing light extinction is actually colored organic

material, which would volatilize during the initial heating. The effect of assuming that all light absorbing species are elemental carbon would cause an error in the initial extinction *due to refractory carbon*, which would lead to an overcorrection using this method. Other important assumptions are that the filters remain stable over the entire temperature range, and that there is no change of light extinction through the sample filter during a routine experiment.

DATA ACQUISITION AND SYSTEM CONTROL

Hardware for data acquisition and control consists of an IBM compatible personal computer (Intel 486 chip) with 32 MB of RAM, running Microsoft Windows 3.11. An analog and digital I/O board with 8 channels of analog to digital and two channels of digital to analog, (two 8-bit bytes) was installed in the computer (Data Translation, model DT2801). This board is wired to a screw terminal that includes cold junction compensation for thermocouples (Data Translation, model DT707-T). Software to collect data, control the moving and heating parts of the instrument, and store and analyze data was provided by HP-VEE (Hewlett Packard Visual Engineering Environment), a graphical programming language with the capability of providing simple computer screens for users while running the instrument.

INSTRUMENTAL RUN SEQUENCE

A single run on the instrument has three principle sections: initialization, measurement, and data analysis. Each of these steps is described in detail in the following subsections.

INITIALIZATION

Daily Setting of Gas Flows

Setting the gas flows is the usual first step at the beginning of every run. The program prompts the user to adjust the gas flows to predetermined settings as it

sequentially opens and closes the proper solenoid valves. This step is done at least once at the beginning of the day, and repeated if it appears the flows have drifted throughout the day. The settings used are listed in the section describing flow control.

Oxidation Zone Temperature Set

The temperature reading of the thermocouple in the oxidation zone of the cell is read and the user is prompted to set the variac at the proper voltage. When that part of the system has come to the proper temperature, the system beeps to let the user know that the rest of the run can proceed. It is important that the gases are flowing at the proper flow rates at this point. At this time all variables used by the program are reset to zero.

Daily System Calibration

The initialization step may or may not include a system calibration, which is generally done at least once per day, or if it appears that there has been instrumental drift throughout the day. Manual calibration takes place by injecting calibration gas (CH_4 10% in helium) through a septum in the gas line. The computer automatically determines the area under the concentration vs. time curve produced from the NDIR analyzer output. The mass of carbon injected is calculated in the program using Equation 4-1:

$$\text{Mass C} = 12(\%CH_4/100)\,(\text{volume injected})/RT \qquad \text{(Eq. 4-1)}$$

The factor of 12 is for the molecular weight of carbon. $\%CH_4$ is the volume percent of methane in the calibration gas, R is the universal gas constant (L-atm mol^{-1}-$^{\circ}K^{-1}$), T is temperature in $^{\circ}K$. In using this equation, it is assumed that the calibration gas behaves as ideal, and that the pressure of the system is 1 atm. The (curve area per mass carbon) ratio is then calculated, which characterizes the system. This process is repeated five times at the beginning of the day to obtain a measurement with the highest precision possible. The injection volume of calibration gas is generally 25 or 50 µL, depending on the aerosol concentration of where the samples were taken. These measurements are precise to within 0.5 % for a single day.

Following manual calibration, the system is auto calibrated by injecting the calibration gas through the Carle injection valve. The signal produced by injecting the fixed volume of the loop is measured 5 times and integrated. The average of the closest three measurements is taken as the usable curve area. This measurement is then divided by the area to mass ratio measured manually to calculate the mass of carbon held in the sample loop of the Carle valve. This mass is used in the autocalibration at the end of every run.

MEASUREMENT

Prompts

The first step in the main part of the instrument run is to prompt the user for the filter identification number, the area of the punch taken from the filter, the volume of air sampled, and the diameter of the quartz filter exposed to the air flow. After the last step of the measurement, this information is used to calculate the concentration of particulate carbonaceous material in the atmosphere.

Preparations

The user is prompted to insert the sample and seal the combustion cell. A five minute purge sequence follows at room temperature to remove any oxygen from the inside of the cell. At this time the initial optical transmission reading is taken.

Heating sequence

The system goes through four identical heating cycles once data collection commences. The temperature is set to increase by 200°C each time, starting with a temperature setting at 200° C. The first step therefore is to set the temperature to 200°C from room temperature. The initial reading from the NDIR analyzer is noted, and the temperature, optical, and NDIR data are all collected at a rate of approximately once per second. The temperature setting increases only after three criteria are met: (1) The temperature must be within 10°C of the temperature setting, (2) There must be at least 5

data points at this temperature setting, and (3) The NDIR reading must have gone down to the initial level, indicating that no additional carbon will be liberated from the filter at this temperature. In this way, the temperature is controlled by the evolution of CO_2, so heavily loaded samples may take longer to analyze than filters with less material to combust.

This temperature program may seem arbitrary, but there was thought put into why to do it in this way. There could not be a simple temperature ramp if the loading and chemical composition of the filters were to have control over the length of the data acquisition of each sample. The issue then becomes the resolution of the data vs. the time it takes to do the analysis. A high thermal resolution is desirable because it allows better indication of the probable molecular forms of the liberated compounds, based on volatility. On the other hand, raising the temperature in small increments increases the length of the analysis, and may not be necessary if the filter is lightly loaded (i.e. the rate temperature rise allowed by the physical configuration of the instrument tends to be slower than the evolution of CO_2 for lightly loaded samples, leading to a nearly linear rise in temperature for these sample types). Because of the very low sample loading for filters collected in a remote marine atmosphere, it was decided to keep the thermal resolution at 200°C.

Refractory carbon analysis

Once the temperature in the volatilization zone reaches 800°C and the NDIR reading returns to baseline, solenoid valves 2 and 4 (as labeled in Figure 4-3) are both actuated to remove 10% of the total flow that is helium and replace it with a flow of 10% O_2 in He. This addition of oxygen causes combustion of any refractory carbon on the filter. This part of the analysis ends when the NDIR reading returns to baseline. All of the data collected gets sent to a file that is automatically named using the filter number.

Autocalibration

Once the sample run is complete, there is an additional calculation of the ratio of

area under curve to carbon mass. This is calculated at the end of every run because the system conditions may change from run to run. This also serves as an internal check that the sensitivity is not drifting throughout the day. Calibration gas is injected through the Carle valve as described in the initialization section. The signal is collected and integrated five times, taking the average as the most representative area under the curve. The area to mass ratio is then calculated from the sample loop mass determined at the beginning of the day.

DATA ANALYSIS

The first step in data analysis is to retrieve the data from the file and integrate the signal produced at each temperature, and for refractory carbon. Once the integration of raw data is complete, the user is prompted if this is a blank run, and if not, what blank value to assume. The raw integration values are calculated into masses using the area to mass ratio determined at the end of the sample run. Once the mass of carbon evolved at each temperature has been determined, the optical correction for charring or organic compounds is calculated. The data points for CO_2 evolving after oxygen is added to the cell and before the transmission returns to the original value are integrated, subtracted from refractory carbon measurement, and added to the organic mass evolved at 800°C. The blank is then subtracted and the masses present on the entire filter are calculated by multiplying by the total filter area and dividing by the area of the sample filter aliquot. The mass concentration per cubic meter air is calculated by dividing this total by the volume of air sampled. Details of filter handling are reported in Chapter 5. Once the calculations are complete, the program generates a report, which is saved as a text file. Graphs showing the evolution of CO_2, temperature, and the laser transmission data are shown to the user.

INSTRUMENT CHARACTERIZATION

OUTPUT

Figure 4-6 shows a typical result for the samples run on this instrument. The graph of evolved CO_2 shows 5 peaks. The first four peaks more or less correspond with the four temperature settings. The fifth peak is due to oxygen being introduced into the cell, where refractory carbon is released from the filter as it is combusted. The pattern in this figure showing the peaks getting progressively smaller with increasing temperature is also typical. The photodetector signal indicates the transmission of the laser beam through the filter, and predictably gets smaller throughout the run until oxygen is introduced. At this point the transmission increases rapidly to a constant value that is higher than the starting transmission.

There are some features specific to these results worth mentioning. The sample filter was loaded heavily enough that there are periods in which temperature remains nearly constant. For very lightly loaded samples, the temperature rise is more of a smooth ramp from 100 °C to 800 °C. The photodetector signal also exhibits flat sections, which on first glance appears to be a mirror image of the temperature profile. Upon closer examination, the photodetector signal is more related to the CO_2 signal, with the largest drops in transmission corresponding to the largest periods of evolution of CO_2 gas. To confirm this observation, the negative of the derivative of the photodetector signal is presented next to the CO_2 signal in figure 4-7. The connection between the two graphs is clear, indicating that the charring of organic material occurs simultaneously with volatilization, i.e. the compounds that volatilize at a particular temperature are the same compounds that char at that temperature. A similar pattern in the transmission signal was seen for all samples collected at the Cheeka Peak field site that were heavily loaded. Chapter 5 covers these samples in detail.

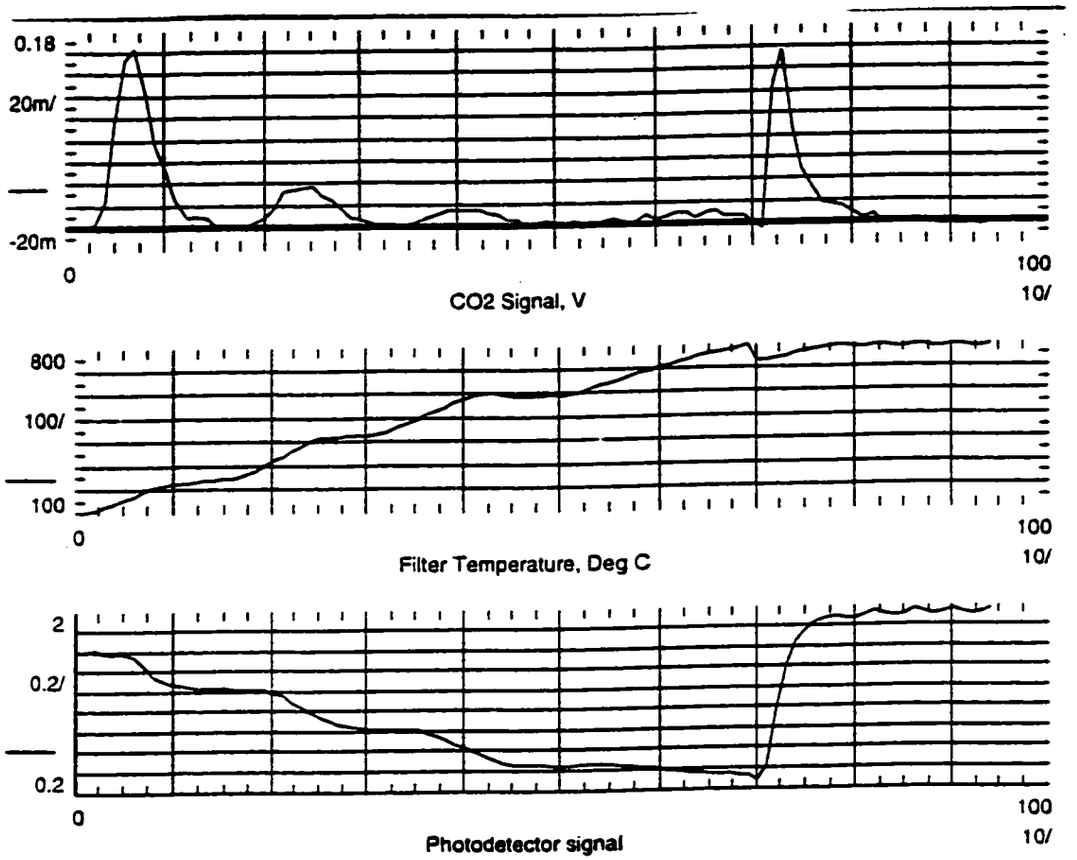

Figure 4-6 Output graphs for a typical sample collected at the Cheeka Peak atmospheric monitoring station. The CO_2 signal is output directly from the NDIR analyzer, and is in units of volts. The filter temperature has units of °C. The photodetector signal is a measure of the transmission of laser light through the filter, and the numbers listed on the y-axis represent the raw output from the photodiode amplifier. This is a relative measurement, so the units are not important to the analysis.

LIMIT OF DETECTION

The classical definition of limit of detection of a concentration of analyte is three times the standard deviation of the instrumental noise (σ_N) above baseline. σ_N is determined by measuring the peak-to-peak noise, and assuming that this quantity is approximately 5 times the standard deviation of the noise. Figure 4-7 shows a graph of the NDIR signal collected when no sample filter was present, but the carrier gas was heated as in a normal experiment. This graph exhibits a peak-to-peak noise of approximately 5 mV. This is typical also for instrumental runs with filter blanks, and during runs while no CO_2 appears to be evolving. The limit-of-detection for the concentration of CO_2 measured would be 3 mV, using the voltage equivalent for the measurement. Since this instrument measures mass of carbon by integrating the concentration measurements, I will integrate this voltage over the minimum number of points allowed by the control program for an instrumental run. There are at least 5 points at each temperature set point, so the equivalent limit-of-detection area under the curve is 0.015 at each temperature set point, or 0.06 for the 4 temperature set points for measuring organic carbon, and 0.015 for the refractory carbon measurement. The total is 0.08 for the entire measurement. The calibration changes daily by small amounts, but the average area-to-mass ratio was 0.65 area units per microgram carbon. Using this figure, the limit-of-detection per temperature setting is 0.12 μg C, corresponding to 0.60 μg organic carbon per analysis, 0.12 μg refractory carbon per analysis, and 0.72 μg total carbon per analysis.

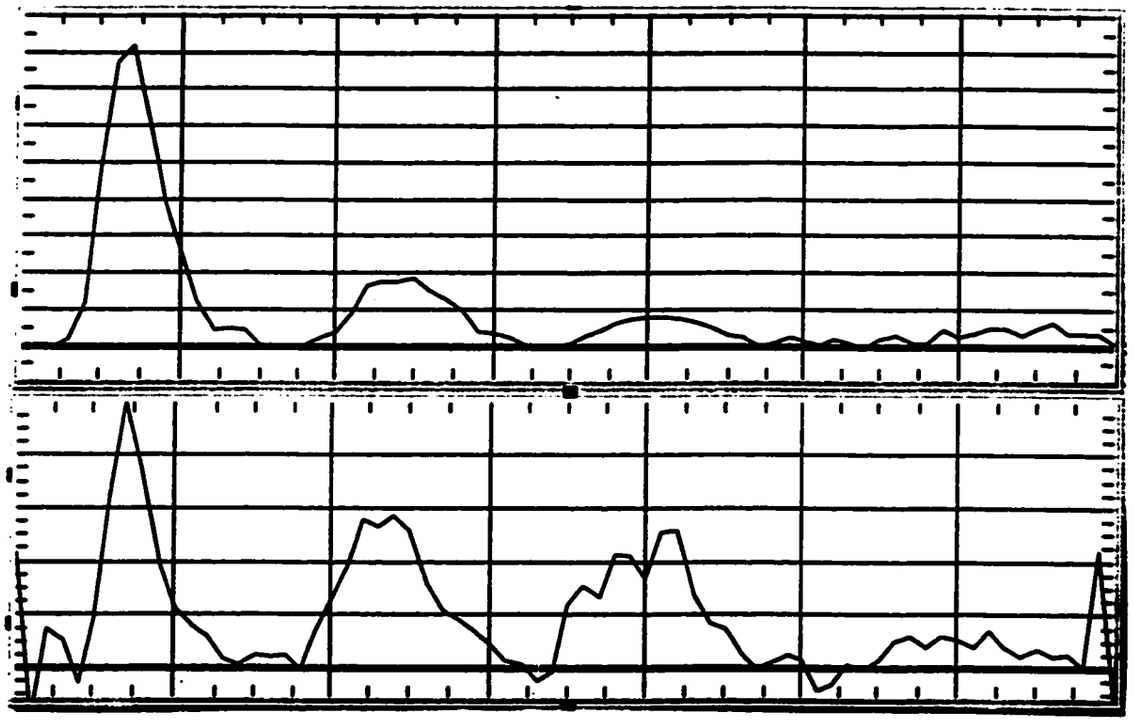

Figure 4-7 Comparison of the graph of evolved CO_2 (top) with the negative derivative of the corresponding photodetector output (bottom). The graphs are shown only up to the point that oxygen is introduced to the cell, because charring is reversed at this point.

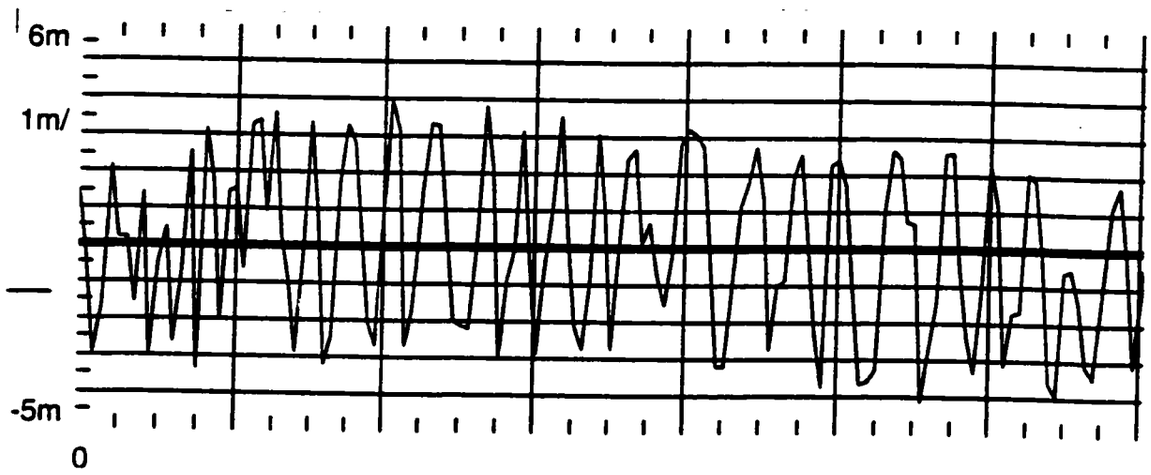

Figure 4-8 Peak-to-peak noise of the NDIR analyzer during a run with no filter sample in the cell. The peak-to-peak noise is taken to be 5 mV.

INSTRUMENTAL ERROR

Although few sample filters had enough exposed area to allow analysis more than two times, an internal check into the repeatability of the instrumental measurements can be determined by examining the measurements of carbon mass from methane in the automatic injection loop that took place daily for calibration of the instrument. These measurements are subject to the same type of manual calibration that each sample filter is compared against, and may experience drift due to changes in oxidizer efficiency or instrumental drift in the NDIR. It is not the ideal measurement of instrumental error because none of the chemical and surface interactions that aerosol particles sitting on quartz filters are subjected to come into play with this measurement. It does, however, provide a controlled means of showing that the instrument did not drift significantly over time. These measurements are summarized in Table 4-1. The average mass of carbon found in the calibration loop was 3.76 μg, with a standard deviation of 0.11 μg. This average mass happens to be very close to the mass of carbon found on the filters collected at Cheeka Peak, as discussed in the following chapter. The standard deviation reported here will be considered to be the carbon analyzer uncertainty for those measurements as well.

Table 4-1 Variation of carbon mass in loop measurement

Date	Mass of carbon in loop (μg)
8/21/96	3.81
8/22/96	3.7
8/26/96	3.72
8/27/96	3.85
8/28/96	3.66
8/30/96	3.56
9/5/96	3.78
9/9/96	3.92
9/10/96	3.84
9/11/96	3.8
9/12/96	3.85
9/16/96	3.83
9/17/96	3.94
9/18/96	3.67
9/20/96	3.72
9/23/96	3.66
9/24/96	3.54
9/26/96	3.6
3/11/97	3.7
3/20/97	3.82
3/26/97	3.83
3/28/97	3.87
Average	**3.76**
Standard Deviation	**0.11**

NOTES TO CHAPTER 4

1. Liousse, C., J.E. Penner, C. Chuang, J.J. Walton, H. Eddleman, and H. Cachier, *A global three-dimensional model study of carbonaceous aerosols.* J. Geophys Res., 1996. **101**(D14): p. 19,411-19,432.

2. Cadle, S., P.J. Groblicki, and D.P. Stroup, *Automated Carbon Analyzer for Particulate Samples.* Analytical Chemistry, 1980. **52**: p. 2201-2206.

3. Huntzicker, J.J., R.L. Johnson, J.J. Shah, and R.A. Cary, *Analysis of organic and elemental carbon in ambient aerosols by a thermal-optical method*, in *Particulate Carbon: Atmospheric Life Cycle*, G.T. Wolff and R.L. Klimisch, Editors. 1982, Plenum Press: New York. p. 79-88.

4. Chow, J.C., J.G. Watson, L.C. Pritchett, W.R. Pierson, C.A. Frazier, and R.G. Purcell, *The DRI Thermal/Optical Reflectance Carbon Analysis System: Description, Evaluation and Applications in U.S. Air Quality Studies.* Atmospheric Environment, 1993. **27A**(8): p. 1185-1201.

CHAPTER 5: CARBONACEOUS AEROSOLS AT CHEEKA PEAK

INTRODUCTION

As discussed in the first two chapters, there is very little information on the concentration and chemical forms of carbonaceous aerosol around the world. Reliable data on these particles are very important for modeling their climatic effects. The information we do have comes mostly from urban areas, particularly Los Angeles and other parts of southern California. There is limited information from rural continental areas, but remote locations are poorly represented, especially remote marine locations. This is probably due to the difficulty and cost making shipboard and aircraft measurements, as well as the extremely low concentrations of organic and elemental carbon in the unpolluted marine atmosphere.

The Cheeka Peak atmospheric monitoring station is located two kilometers inland from the Eastern North Pacific Ocean on the northwest tip of the Olympic Peninsula in Washington State (48°18'N, 124°37' W), at a height of 480 m above sea level. The purpose of the station is to provide a land-based platform from which the marine atmosphere can be studied. Aerosol sampling and gas-phase measurements have taken place here since the mid 1980's, using a 7m tower for sampling. Conditions considered acceptable for sampling marine aerosol at this site are periods when the wind direction indicates on shore flow, the total aerosol number concentration is less than 1000 particles cm^{-3}, the wind speed is greater than 2 m s^{-1}, and when there is no rain or fog. McInnes et al. [1] studied the submicrometer aerosol at this site using gravimetric analysis in combination with ion chromatography in an effort to show consistency (closure) between the two measurements, using the assumption that the major contributors to the submicrometer aerosol mass are sulfate and sea salt particles. The ions analyzed were Na^+, NH_4^+, K^+, Ca^{2+}, Mg^{2+}, Cl^-, NO_3^-, and SO_4^{2-}. Results of this study showed discrepancies between the two measurements; only 40-50% of the mass determined gravimetrically

could be explained by the mass of major ions as measured with ion chromatography (IC). Interestingly, in similar studies involving aerosol collected aboard a ship on cruises in the Pacific, there has been better agreement between the two methods, with 75% or more of the gravimetrically measured mass accountable in the IC analysis. The differences in the results from the two types of platforms led to the suggestion that the samples collected at Cheeka Peak contained additional components not measured by ion chromatography. It was further speculated that these components were most likely organic and aerosol material, but conceivably also refractory carbon and/or mineral dust. Other possibilities included adsorbed or chemically bound water and adsorbed organic gases.

The purpose of the project described in this chapter was to characterize and measure the carbonaceous aerosol at this sampling site to see if better agreement between mass measured gravimetrically and chemically could be obtained by including analysis for carboncaceous components. The instrument used in this study was the thermal/optical carbon analyzer described in Chapter 4. Approximately one year of data is presented here, along with a discussion of the unique sampling challenges associated with this site, as well as some suggestions for future study.

SAMPLING

Field Site Considerations

Studying marine aerosol at the marine:continental interface can be problematic because the aerosol present at this type of location is influenced not only by the marine atmosphere, but also natural continental and anthropogenic emissions. A major assumption in the sampling scheme is that by choosing an acceptable sector between 180°-330° for the wind direction (westerly winds), that the sampled air is derived from a purely marine source, possibly punctuated with ship exhaust. Figure 5-1 shows sample air mass trajectories calculated for Cheeka Peak [2]. As seen in part (a) of this figure, the air mass may have a marine source from many days back. Part (b) shows that the air may

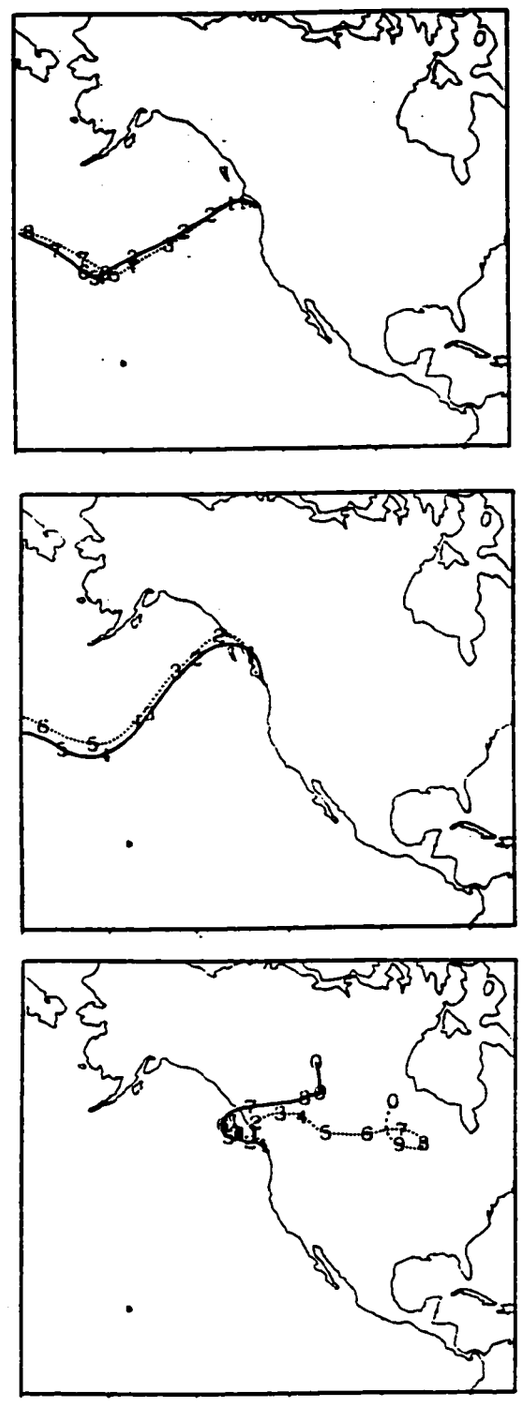

Figure 5-1. Back trajectories for Cheeka Peak (a) Marine air, (b) "modified" marine air (c) continental air, sampled during onshore flow.

sometimes have a marine source, but passes over small areas of coastal land before being sampled at the site. Part (c) shows the "worst case scenario" in which the air mass has a continental source but passes over the sea briefly before being sampled in a flow of westerly wind at the site. Knowledge that this type of air mass has been sampled can be determined after the fact by examination of such trajectories, or possibly during sampling if radon-222 is measured concurrently. This gas appears in higher concentrations in continentally influenced air because it is outgassed from rocks as a product of radioactive decay of radium in the earth's crust, and has been used as a tracer of continental air [3].

Even if air sampled during onshore flow had a completely marine source, there are further complications relating to the low concentrations of aerosol in the marine atmosphere. Past studies of remote marine air at this location have reported concentrations of 0.3-1.9 $\mu g\ m^{-3}$ [1] for submicrometer aerosol at this site. The equipment used to sample size-segregated aerosol in this project imposed a flow rate of 30 $L\ min^{-1}$ and a filter with approximately 7.0 cm^2 of exposed area. Assuming an aerosol concentration of 1.0 $\mu g\ m^{-3}$, onshore flow for 50% of the time in a 24 hour period, a filter concentration of less than 0.3 $\mu g\ cm^{-2}$ of carbon would result for a single day of sampling. For the carbon analyzer, a punch of 1.53 cm^2 is taken from the filter and analyzed. This would result in an analyte sample of less than 0.5 μg of carbon, which is less than the instrumental limit of detection listed in Chapter 4 (0.7 μg of carbon for a single analysis). Although sampling for short periods of time would have been useful for a higher time resolution of the data, collection over one week was the eventual compromise, considering available instrument capabilities, the desire to collect a large data set, and the realistic frequency of possible visits to this remote site.

FILTER SAMPLE CONFIGURATION

Analysis by the thermal-optical method described in Chapter 4 requires a sample substrate that will withstand the heat applied in the analysis and that is not made of carbon-containing material that would contaminate the analysis. Quartz fiber filters have

traditionally been used for this purpose, although glass fiber [4] and silver [5] filters have been mentioned for use when heating to lower temperatures than the method described here. Pallflex QAT-UP filters were used in this study, precombusted at 900 °C for 6 hours in ceramic holders placed in a muffle furnace. This step removed any residual organic compounds from packaging or storage. Filters were allowed to cool overnight in the furnace before additional sample handling took place.

Avoiding sample contamination is very important because of the very low aerosol concentrations at this site. All filters were processed in a class 10 clean room (10 particles per standard cubic foot) environment before sampling. After precombustion, filters were stored in individual sterile plastic petri dishes, lined with aluminum foil that had been heated to 500°C for at least two hours to remove organic material from the surface. Heavy duty teflon tape was wrapped around the outside of the petri dishes to minimize exposure to the outside air. Filters were handled exclusively with stainless steel forceps that were rinsed with methanol prior to each use. At the field site, filters in petri dishes were stored in double ziploc plastic bags and frozen in a portable refrigerator before and after sampling. Filter changes took place in a glove box under a nitrogen atmosphere. The nitrogen entering the glove box was scrubbed for organic vapors by passing through a tube containing activated carbon, followed by a HEPA filter. After sampling, each filter was returned to its original petri dish and resealed with teflon tape before refreezing. Filters were kept cold during transport to and from the field site. Analysis of the filters started in August of 1996, after all samples had been collected. Some of the first samples collected (November of 1994) remained in storage for a year or longer before analysis took place.

Although quartz filters are ideal from an instrumental point of view, there are problems with sampling artifacts. Both volatilization of collected organic particles and adsorption of organic vapors have been discussed [6, 7], which would lead to negative and positive artifacts, respectively. The materials most likely to adsorb to the quartz fibers are polar organic vapors, since the silica in quartz contains has an abundance of active oxygen sites

for binding. The apparent concentration of carbon on a quartz filter has been shown to decrease as the sampling face velocity is increased [8]. (Face velocity is volumetric flow rate divided by the exposed area of the filter.) McDow and Huntzicker [8] presented theoretical thermodynamic calculations to show that the increased pressure drop from higher face velocity would not likely induce volatilization of organic material from collected particles in such a way that can explain the different apparent concentrations. Additional calculations showed that vapor phase adsorption seems to occur on the surface of the quartz, and not as much on the collected particles, based on surface area arguments. However, this calculation did not take into consideration the possible role of organic *ab*sorption into existing particles, as discussed in Chapter 2 (Gas-Particle Partitioning). McDow and Huntzicker conclude that both apparent positive and negative artifacts are due to adsorption of atmospheric vapors on the quartz filter itself. They present additional experiments to show that teflon filters do not efficiently adsorb organic vapors or cause a positive artifact when placed upstream of a quartz filter during sampling. Their results were derived from samples collected in the greater metropolitan Portland area, but it was assumed that the qualitative aspects of their work could be applied to this project. The sampling scheme recommended by McDow and Huntzicker is to collect two parallel samples at the same face velocity. In one sampler there is a quartz filter downstream of a teflon filter (Millipore Zefluor, 2μm pore size). In the other sampler a quartz filter sits by itself. The teflon filter removes particles from the stream, but organic vapors are allowed to pass through to the quartz back filter. The other quartz filter sitting by itself adsorbs organic vapors with an efficiency that is assumed to be equal to that of the other quartz filter, but it also collects particles. The organic carbon due to particles alone, therefore, is supposed to be the carbon on the quartz filter sitting by itself minus the carbon on the quartz back filter. In additional experiments, the authors showed that this difference is nearly unaffected by changes in face velocity. The version of this sampling configuration used for the project at Cheeka Peak is portrayed in Figure 5-2. All filters had a diameter of 29.8 mm of exposed surface and were sampled at 30 L min^{-1}. This translates to a face velocity of about 72 cm s^{-1} for the experiment at Cheeka Peak.

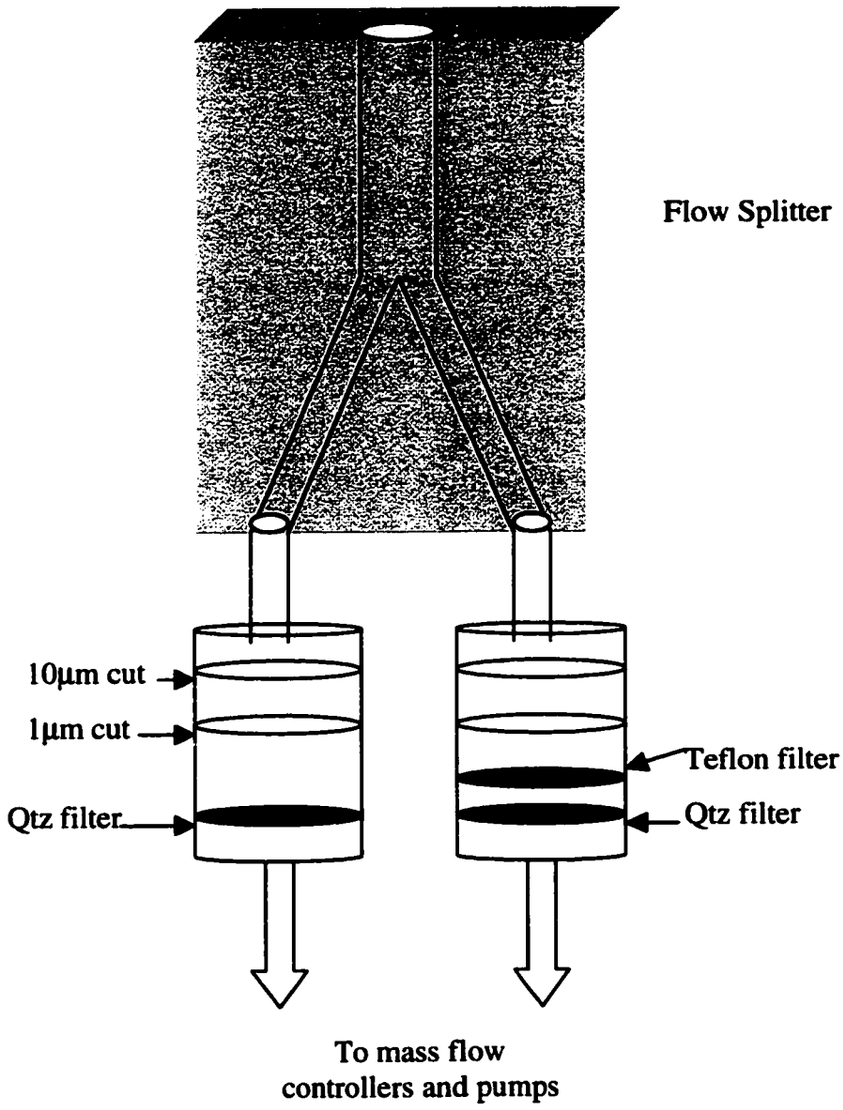

Figure 5-2 Sampling configuration at Cheeka Peak

Two Berner style jet ring impactors with size cuts at 10 μm and at 1.0 μm aerodynamic diameter were used to remove supermicrometer particles. Particles with sizes between 1.0-10 μm were collected onto Tedlar impactor films. Submicrometer particles escape impaction and pass through directly to the teflon or quartz back filters, each mounted inside their respective impactor housing. Silicone gel was used on the first stage of each impactor to avoid particle "bounce" through to the second stage or back filter in the impactor. Field blanks placed in impactors with silicone gel did not seem to be affected compared to blanks not exposed to the silicone.

Flow rates were controlled by mass flow controllers to 30.0 ± 0.1 L min^{-1}. Flows were switched on by automatic computer control when sampling conditions were within preset guidelines (listed above in the introduction to the chapter.) These conditions were checked every 6 seconds, and in order for sampling to be switched on after being turned off, favorable conditions must have been in place for at least one five minute period. Total aerosol number concentration and light scattering of submicrometer aerosol were measured concurrent to filter sampling with a condensation nucleus counter (TSI) and nephelometer (TSI), respectively.

ANALYSIS

Quartz filters were stored at the field site until just before analysis by thermal-optical carbon analysis, described in Chapter 4. Teflon filters were weighed before and after sampling on a Mettler UMT2 balance. The balance was located in a humidity and temperature controlled chamber within a class 100 clean room. Humidity was controlled using a semi-dynamic method [9] which kept relative humidity at $33 \pm 4\%$ by circulating the chamber air over a flat container of saturated $MgCl_2 \cdot 6H_2O$ solution. Prior to reentering the chamber, the air was also scrubbed for ammonia vapor, acidic gases, and organic vapors. Static electricity was minimized in the balance by exposing the filters to a ^{210}Po source. The balance was checked after weighing every 3-4 filters for instrument drift with internal calibration as a standard reference. Each filter was weighed in

triplicate, taking the average as the reported weight. The standard deviation of repeated weighings was approximately ±3 μg per filter, giving a conservative uncertainty of ± 6 μg for particle weights, which would yield an uncertainty of ±0.2 μg m^{-3} air if 30 m^3 air is sampled, which was typical for these samples.

RESULTS AND DISCUSSION

Sampling dates and volume of air filtered are listed in Table 5-1, along with average condensation nucleus (CN) concentrations and light scattering for the periods in which sampling took place. Sampling started at the end (day 306) of 1994, and progressed through the spring (day 100) of 1996. There are short periods for which data from these instruments is not available. Also listed in this table is the mass of particles collected on each teflon filter. Figure 5-3 shows the correlation between particle mass collected and average light scattering. Although crude, it is possible to see a weak linear correlation, that when forced through (0,0), yields a mass scattering efficiency of ca. 3 m^2 g^{-1}. This is the approximate mass scattering efficiency of submicrometer aerosols, and indicates that the particle masses listed are reasonable values and that the one-week sampling durations were detailed enough to show a meager light scatter correlation. There was no similar correlation with CN count, as evidenced in Figure 5-4.

Table 5-1 Sample dates, volumes, particle mass, average light scattering, and average CN counts. Masses are given as difference between initial and end weights of Teflon filters. A * denotes data not applicable or missing. Filters 1-3 were not sampled, and filters 11 and 52 were sampled at the start of 1995 and 1996, respectively.

Teflon Filter #	Sampling start day (doy)	Sampling end day (doy)	Volume Sampled (m^3)	particle wt (μg)	Total fine scattering (green), m^{-1}	Average CN count (particles cm^{-3})
4	306.9	312.1	46.5	80.2	5.05E-06	392
5	312.2	319.9	78.4	150.3	*	355
6	319.0	326.8	114.7	163.7	*	289
7	327.0	333.8	134.5	70.2	*	188
8	333.9	340.9	39.15	21	1.38E-06	179
9	340.9	347.8	35.7	24.7	2.57E-06	263
10	347.9	366.0	99.3	2645.2	*	354
11	20.0	40.8	5.92	14.3	2.26E-06	971
12	40.9	45.8	42.2	132.2	6.60E-06	*
13	46.0	54.7	73.2	26	2.14E-06	141
14	54.7	59.3	22.7	62.7	5.10E-06	*
15	59.9	66.7	54.8	106.6	4.60E-06	587
16	66.9	75.8	40.5	46.3	3.18E-06	204
17	75.9	84.7	95.6	132.6	4.63E-06	420
18	84.9	91.7	227.2	46.9	7.15E-06	685
19	91.8	99.8	113.4	94.9	3.17E-06	433
20	99.9	106.6	22	37.5	5.21E-06	548
21	106.7	112.0	84.2	68.3	3.49E-06	612
22	112.2	120.7	0	19.5	blank	blank
23	120.8	126.0	80.5	93.8	5.88E-06	566
24	126.1	133.7	89.4	265.7	1.01E-05	521
25	133.8	150.9	*	9.9	*	*
26	152.0	153.7	35.8	18.8	*	*
27	153.8	159.7	69.39	104.3	5.03E-06	798
28	160.8	166.7	48.9	54.3	3.14E-06	669
29	166.8	175.8	47	3	1.71E-06	188
30	175.8	187.8	24.4	25.95	3.73E-06	627
31	187.9	194.8	48.8	46.2	6.64E-06	633
32	194.8	199.7	56.2	141.7	9.12E-06	*
33	199.8	208.7	34.4	56.6	8.92E-06	578
34	208.7	218.8	38	69.9	8.31E-06	1038
35	218.9	222.7	20.8	22.1	4.92E-06	457
36	222.8	231.8	61.9	71	4.38E-06	872
37	231.9	237.7	57.5	76.1	5.31E-06	715
38	237.8	243.8	46.7	114.3	8.94E-06	636
39	243.8	257.7	35.9	61.9	4.73E-06	474
40	257.8	265.5	(blank)	(blank)	(blank)	(blank)
41	265.8	274.1	25.2	31.1	4.79E-06	679
42	274.1	279.8	28	41.5	*	*
43	279.8	285.8	87.8	85.5	2.94E-06	601
44	285.8	294.7	73.2	75.8	*	532
45	294.1	299.8	44.9	47.7	4.10E-06	469
46	299.8	306.8	33.7	63.3	3.92E-06	321
47	306.8	312.8	32	26.5	*	*
48	312.8	319.8	*	39.1	*	*
49	319.8	335.8	87.1	12.7	*	*
50	335.8	348.8	97	60.8	*	*
51	348.8	362.7	28.5	35.6	*	*
52	1.0	11.8	60.9	43	*	*
53	11.8	25.8	91.1	77.4	*	*
54	25.8	38.8	29.2	0.8	*	*
55	38.8	52.8	16	37.9	*	*
56	52.8	63.8	34.4	40.1	*	*
57	63.9	78.8	19.7	36.1	*	*
58	78.8	100.8	72.2	124.25	*	*
59	100.8	133.7	47.7	59.6	*	*

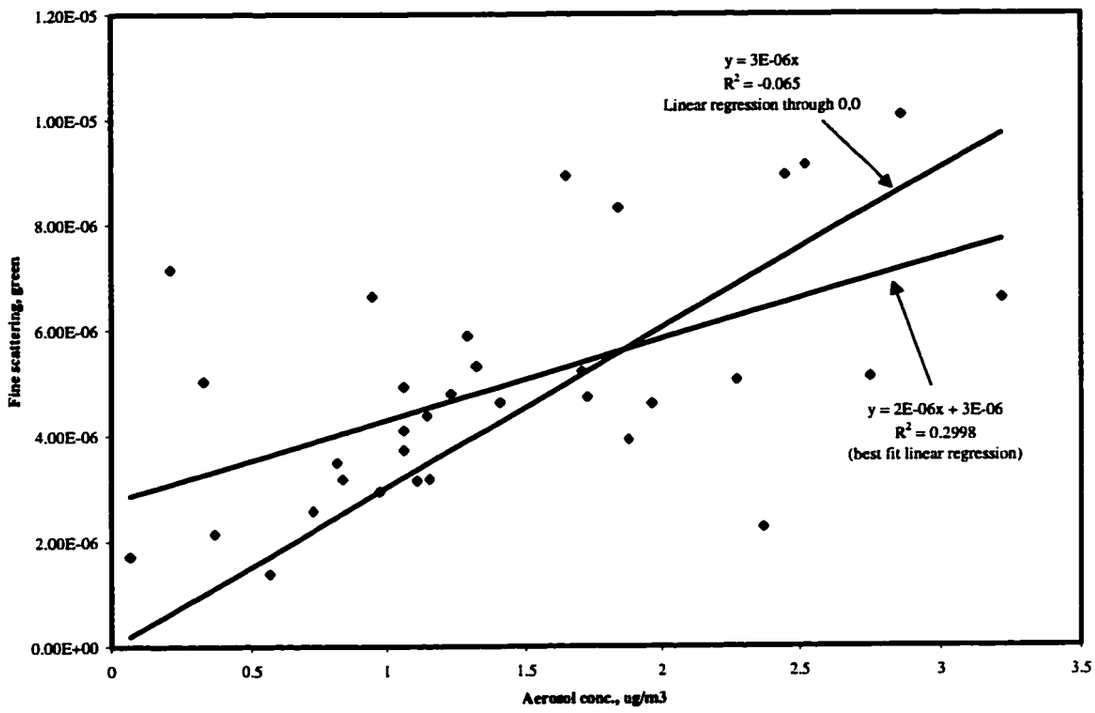

Figure 5-3 Average light scattering (green) vs. gravimetrically measured aerosol concentration on teflon filters. The slope of the fit forced through the origin is the approximate mass scattering efficiency for sulfate aerosols (3 m^2g^{-1}).

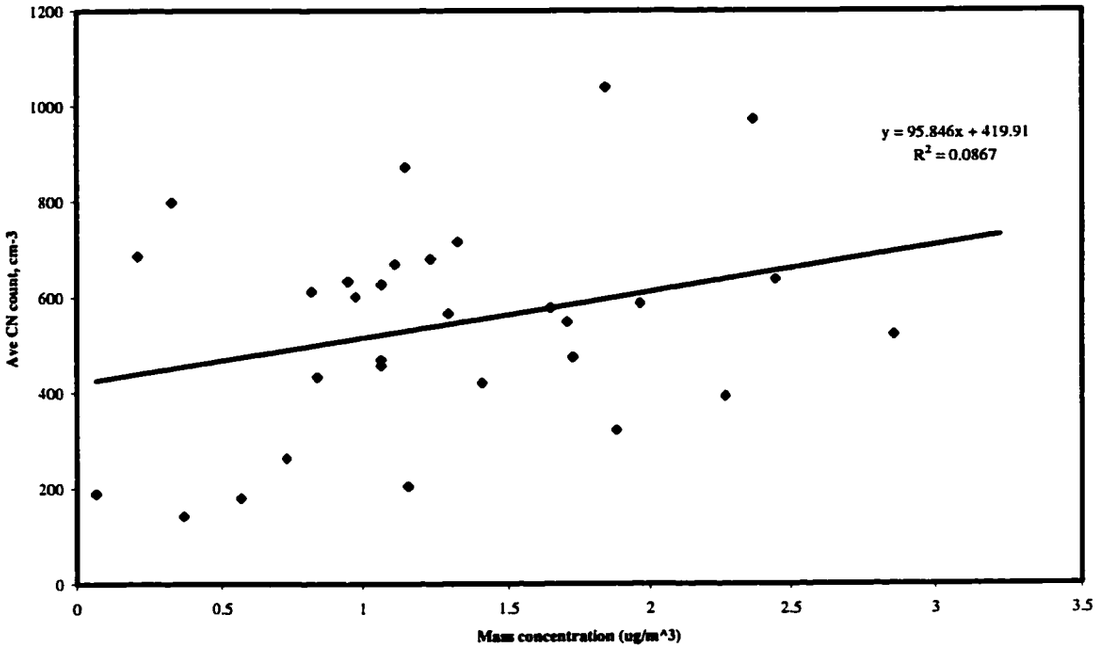

Figure 5-4 Average condensation nucleus count vs. particle mass concentration measured gravimetrically.

CARBON ANALYSIS RESULTS

The raw data from carbon analysis of the samples are listed in Table 5-2. These results are for 1.53 cm^2 punches, which was the largest size punch the analyzer could accommodate. In retrospect, it would have been helpful to have the ability to analyze larger filter sections, since some of the measurements listed are near the detection limit of the instrument. However, this would have caused a trade off in the ability to accurately heat the sample to the correct temperature. The uncertainty assumed for these measurements was 0.133 μg total carbon, which is one standard deviation of the mass of carbon measured daily in the calibration loop of the analyzer. The uncertainty for measurements on filters is likely to be somewhat different, due to variations in analysis temperature, area of filter analyzed, non-uniformity of filter deposit, and variation in the reproducibility of correction for pyrolytically generated elemental carbon. However in the absence of a reliable data set for replicate analyses of filter samples, this number is a good estimate because it takes into account variations in NDIR response, changes in the oxidizing catalyst, and variations in flow rate through the instrument. Observed carbonaceous aerosol concentrations were in the range for which this instrumental uncertainty was significant, as seen in the relative uncertainties listed in Table 5-2.

VAPOR ARTIFACT

Except in a few cases, the amounts of carbon found on the back filters were very close to those found on the front filters. This can be seen graphically in Figure 5-5. In some cases there was more carbon found on the back filter than on the front filter. A listing of the percentage of material on the front filter that was also found on the back filter is found in Table 5-2. An average of 68% of the material on the front filter was also found on the back filter, with a standard deviation of 41%. The amount of carbon on the back filter was over half of the carbon on the front filter for 59% of the sampling periods, and for 18% of the sampling periods there was more material on the back filter than on the front filter. This

Table 5-2 Raw data for organic carbon measured on 1.53 cm^2 filter punches. Absolute uncertainty assumed to be 0.133 µg for all analyses. All carbon on the back filter is assumed to be organic.

Teflon Filt #	Blank corrected organic C on front filter punch, µg	Relative uncertainty, %	Blank corrected organic C on back filter punch, µg	Relative uncertainty, %	Blank corrected soot C on front filter punch, µg	Relative uncertainty, %	Percentage of material on front filter found on back filter
4	0.257	52	0.658	26	0.257	43	95
5	0.693	19	0.540	33	0.504	22	39
6	0.527	25	1.062	14	0.763	14	72
7	0.261	51	0.408	50	0.396	28	49
8	0.195	68	0.314	77	0.151	73	60
9	0.279	48	0.259	112	0.245	45	37
10	0.559	24	0.667	25	0.436	25	57
11	0.193	69	0.542	33	0.155	71	103
12	0.474	28	0.342	66	0.543	20	29
13	0.189	70	0.224	160	0.045	244	54
14	0.527	25	0.795	20	0.254	43	83
15	0.485	27	0.630	27	0.186	59	74
16	0.182	73	0.450	43	0.043	256	111
17	0.226	59	0.544	33	0.322	34	75
18	0.331	40	0.230	148	0.225	49	31
19	0.202	66	1.168	13	0.131	84	228
20	blank	blank	blank	blank	blank	blank	blank
21	0.379	35	0.964	16	0.188	59	129
22	0.621	21	0.683	25	0.140	79	73
23	0.862	15	0.180	339	0.322	34	13
24	1.391	10	0.797	20	0.416	26	40
25	0.173	77	0.270	103	0.058	189	66
26	0.246	54	0.468	41	0.065	169	96
27	0.518	26	0.735	22	0.252	44	78
28	0.202	66	0.645	26	0.129	86	127
29	0.485	27	0.288	91	0.135	81	36
30	0.417	32	0.244	129	0.142	78	33
31	0.797	17	0.413	49	0.102	108	38
32	3.040	4	0.729	23	0.135	81	22
33	0.009	1558	0.689	24	0.295	37	143
34	0.926	14	0.419	48	0.166	66	33
35	0.033	406	0.340	67	0.188	59	85
36	0.531	25	0.000	94	0.115	95	*
37	1.244	11	0.608	28	0.014	762	42
38	0.680	19	0.558	32	0.074	149	60
39	0.909	15	0.854	19	0.030	369	76
40	Balnk	Blank	Blank	Blank	Blank	Blank	blank
41	0.369	36	0.446	44	0.109	101	68
42	0.713	19	0.430	46	0.091	121	44
43	0.623	21	0.584	30	0.111	99	64
44	-0.141	94	0.000	94	-0.038	288	*
45	0.250	53	0.061	168	-0.025	439	15
46	0.074	178	0.338	67	-0.038	288	157
47	0.079	168	0.162	613	0.017	662	59
48	0.160	83	0.226	156	-0.003	3517	67
49	0.066	202	0.257	115	-0.009	1277	109
50	0.294	45	0.349	64	-0.012	924	76
51	0.208	64	0.158	769	-0.038	288	45
52	0.202	66	0.437	45	-0.021	532	121
53	0.522	25	0.162	613	0.002	5140	23
54	0.147	90	0.274	100	-0.009	1277	87
55	0.230	58	0.170	460	-0.006	1985	42
56	0.276	48	0.184	305	0.031	356	38
57	0.397	33	0.186	294	0.016	670	31
58	0.840	16	0.000	94	0.102	108	*
59	0.555	24	0.209	194	-0.023	481	29

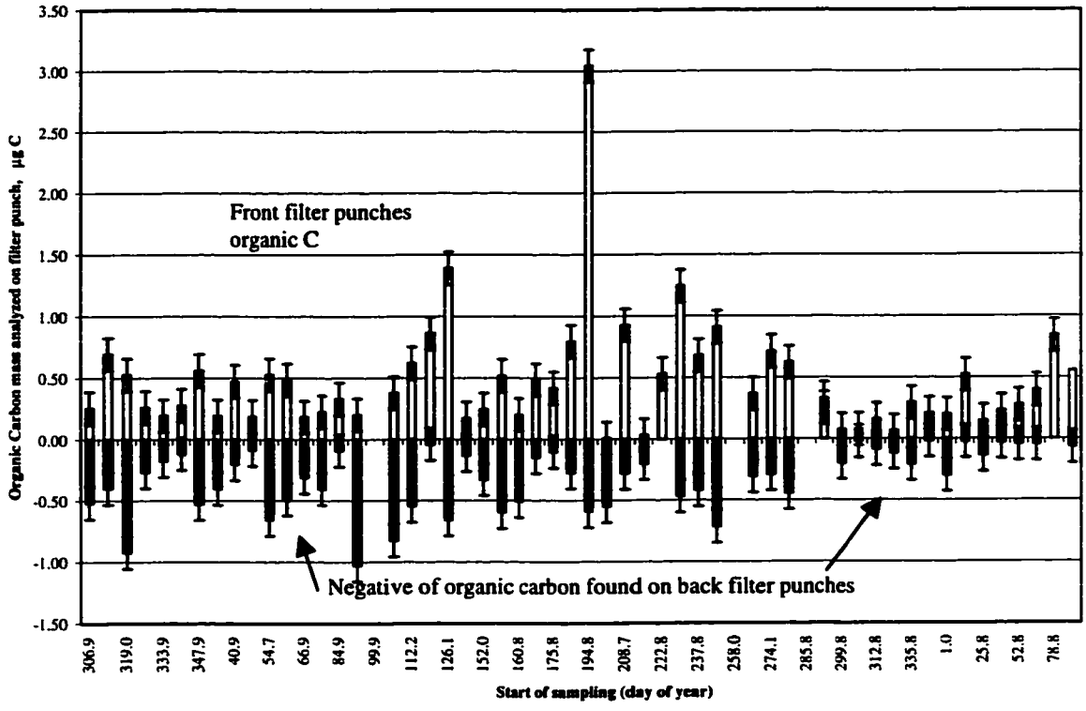

Figure 5-5 Vapor adsorption artifact: material on front filter punch (above) and material on back filter punch (below).

information can be interpreted in three ways. One possibility is that the uncertainty in the analysis was sufficiently large to indicate that more carbon was apparently present on the back filter than there really was. A second explanation is that there was significant volatilization of organic particle material from the teflon filter which was subsequently readsorbed onto the quartz back filter. The third possibility is that during some of the sampling periods, there was a greater abundance of vapor phase organic carbon than particulate organic or refractory carbon, which was preferentially sampled onto the quartz back filter.

The first possibility is likely to explain at least part of the phenomenon of higher concentrations present on the back filter. In all but 5 cases, the listed uncertainty allows for at least an equal amount of carbon to be present on both filters. However, this explanation would not be likely to discount the result that the amount material on the two filters is similar. The second explanation was explored in detail by McDow and Huntzicker [8], who argue that particles sampled at different face velocities would not experience large enough differences in pressure to account for the difference in apparent concentrations found when varying face velocity. Additional evidence against the volatilization explanation can be found by examining the laser transmission records to follow charring during carbon analysis. I present a pair of carbon analyzer outputs in Figure 5-6. Most of the front filters exhibited charring like the one shown in part (a), with a gradual decrease in transmission followed by sharp increase when oxygen was allowed into the volatilization chamber. As discussed in chapter 4, each decrease in transmission corresponds with periods of CO_2 evolution, indicating that the material charring is likely the same material being volatilized at that point. In contrast, none of the back filters analyzed exhibited this type of regular charring—even back filters that were highly loaded. Part (b) of Figure 5-6 shows the companion back filter of the one represented in part (a).

The similarity in the shape, time, and temperature of the first peak in the two plots of evolved CO_2 is striking. Clearly, material that evolves from the filter at the lowest

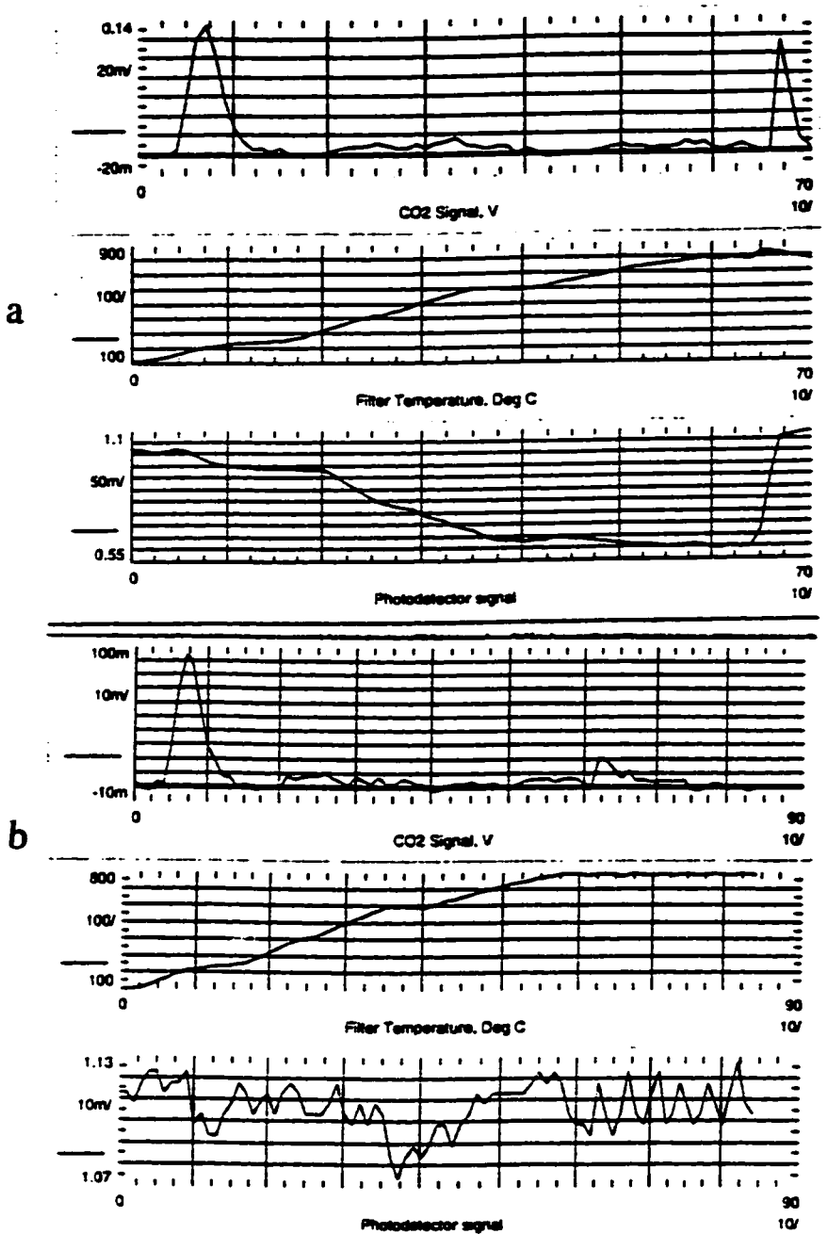

Figure 5-6 Sample carbon analyzer outputs for (a) front filter and (b) back filter exhibiting vapor adsorption artifact. These filters were sampled concurrently, with the same face velocity.

temperature is composed of the most volatile compounds collected, much of which likely to have been collected from vapors. Thus there is probably some overlap in the composition of compounds that are represented in the first peak of the two graphs. However, there is no initial decrease in transmission, associated with evolution of the first peak on the back filter, whereas the front filter shows a clear initial charring. Also, note that the height of the peak from the front filter is about 1.4 times higher than that of the front filter. The simplest explanation is that the additional material present on the front filter is chemically distinct from the vapors collected on the back filter, and that it was these compounds that charred. Another explanation is that the material evolved at this temperature is the same on both filters, but that additional mass was collected on the front filter due to *ad*sorption *onto* or *ab*sorption *into* particles atmospheric particles prior to sampling. From a chemical standpoint, this is a strong possibility, because the polar organic vapors that would adsorb to quartz would also have a high affinity for liquid water, which is plentiful in organic particulate. This mechanism also explains the additional carbon mass on the front filter, but not the different charring behavior. For this mechanism to be plausible, the presence of particles themselves would have to play a part in the formation of refractory carbon in the heating, a theory for which we have no justification. A third possibility is that organic vapors were collected onto or into particles *already* on the filter. This is possible because of the relatively surface area of small particles. For example, assuming 100 μg of collected particles with an average radius of 0.1 μm, the added surface area is approximately 10 cm^2 per filter, which could be significant. Finally, as discussed above, it is possible that material collected on the front (teflon) filter is volatilized and lost to the back (quartz) filter. If volatilization were a principle source of material for the back filter, there would be an equilibrium distribution of identical material between the two filters, and a more similar charring pattern would be expected, assuming no interaction with other particles in the charring mechanism, as discussed above.

ATMOSPHERIC CONCENTRATIONS OF CARBONACEOUS MATERIALS

Table 5-3 lists the atmospheric concentrations of organic, refractory , and total carbon based on the data presented in Table 5-2, and the volume of air sampled according to the equation:

$$C_i = (M_i - X_i)\, A/\alpha\, F\, t \qquad \text{(Eq. 5-1)}$$

where C_i represents the atmospheric concentration of the aerosol of type i, M_i is the mass of i measured on the filter punch, X_i is the instrumental blank for measuring i on the size filter punch used, A is the area of sample filter exposed during sampling, α is the area of the filter punch analyzed, F is the flow rate, and t is the time sampled. For organic carbon, C_i is the apparent concentration of i since the 'true' atmospheric concentration of organic carbon is given as $C_{org,\ front\ filter} - C_{org,\ back\ filter}$, as discussed earlier in the chapter.

The uncertainty in C_i can be calculated by propagation of the errors associated with equation 5-1, such that:

$$(s_C/C_i)^2 = [s_M/(M-X)]^2 + [s_x/(M-X)]^2 + (s_A/A)^2 + (s_\alpha/\alpha)^2 + (s_F/F)^2 + (s_t/t)^2 \qquad \text{(Eq. 5-2)}$$

where s_j is the standard deviation of the j^{th} parameter of equation 5-1. The mass and blank uncertainty have both been mentioned already, and have been considered to come directly from characteristics of the carbon analyzer instrument. Uncertainties in the exposed area of the filter and the area of the punch analyzed are expected to contribute very little to the total uncertainty, so these terms are assumed to be zero in Eq. 5-2. Uncertainty in the flow rate of collection controlled by mass flow controllers is approximately 0.1 L min^{-1} out of a total flow rate of 30 L min^{-1}. Standard deviation of the time sampled, ideally should be at most 6 seconds, since the datalogger at the field site is programmed to collect data every 6 seconds. However, this does not take into account problems with data transfer over phone lines, downed power, and computer problems. In reality this error is likely to be higher than 6 seconds out of the total, but the ideal case

has been assumed here, which makes the error in time sampled nearly zero compared to the other terms in Eq. 5-2.

ATMOSPHERIC CONCENTRATIONS OF CARBONACEOUS COMPONENTS

Table 5-3 lists the atmospheric concentrations of the data listed in Table 5-2. The concentration values listed in Table 5-3 are plotted in Figures 5-7 (atmospheric concentration of organic carbon), 5-8 (atmospheric concentration of refractory carbon), and 5-9 (atmospheric mass concentration of organic material). This last figure mentioned is the combination of the material presented in Figures 5-7 and 5-8, where the vapor-corrected organic concentrations are multiplied by a factor of 1.5 as the assumed (organic compound mass:carbon mass) ratio [10].

CONCENTRATION OF ADSORBED ORGANIC VAPORS

Figure 5-7 is split into two parts. In part (a) the amount of carbon on the front filter (positive values) and the amount of carbon found on the back filter (negative values) are expressed in terms of atmospheric concentration. Concentrations from the back filter are plotted as a negative quantity because they represent the artifact of vapor phase adsorption onto the quartz filters. The sum of the positive and negative concentrations is plotted in part (b) of the figure. The concentration of apparent vapor phase organic material is very similar to the concentration of apparently particle phase material. Measurements of the back filters for the entire data set indicate an average concentration of 0.04 $\mu g\ m^{-3}$ with a standard deviation of 0.05 $\mu g\ m^{-3}$. As mentioned earlier in the chapter, based on high polarity of the silica material in the quartz fibers, the polar organic gases would be the strongest candidates for adsorption. These same types of compounds e.g. formic and acetic acids would also be expected to be found in rainwater, if they are found in the atmosphere.

Samples of cloud water were collected in May of 1993 at Cheeka Peak as part of the first C.A.C.H.E. (cloud and aerosol chemistry experiment) campaign [11]. The polar organic ions formate ($HCOO^-$) and acetate (CH_3COO^-) were measured in the water samples using ion chromatography. Sampling took place over 2-3 hour intervals, with 36 samples being analyzed for both ions. The mean aqueous phase concentration of formate was 6.4 ± 7.3 μeq L^{-1} (microequivalents per liter), while the concentration of acetate was 2.9 ± 4.5 μeq L^{-1}. Using the Junge nucleation scavenging equation [12] to calculate the air equivalent concentration of these two components. The equation states that the cloud liquid water content (L) divided by the nucleation efficiency (ε) is equal to the concentration of a scavenged substance (Y) in air divided by the concentration of sample in rain:

$$L/\varepsilon = [Y]_{air}/[Y]_{rain} \qquad \text{(Eq. 5-3)}$$

The liquid water content was determined to be 0.3 ± 0.2 g m^{-3} during collections. The aqueous concentrations therefore translate to an air equivalent concentration of 2.3 neq m^{-3} (nanoequivalents per cubic meter) for formate and 1.1 neq m^{-3} for acetate, assuming a nucleation efficiency of unity. Multiplication by the molar weight of 45 g mol^{-1} for formate and 59 g mol^{-1} for acetate yields concentrations of 0.1 μg m^{-3} for formate and 0.06 μg m^{-3} for acetate. Given the uncertainty in the measurements, these concentrations are remarkably similar to the vapor adsorption artifact correction, and suggest that these gases are good candidate molecules for the most volatile fraction collected.

Table 5-3 Atmospheric concentrations of organic carbon, refractory carbon, and total carbon

Teflon Filt #	Sampling start day (doy)	Sampling end day (doy)	Concentration of Organic carbon in air (µg/m3)	Error, µg/m^3	Concentration of Refr. carbon in air (µg/m3)	Error, µg/m^3	Concentration of total carbon in air (µg/m3)	Error, µg/m^3
4	306.9	312.1	-0.026	0.018	0.025	0.012	0.000	0.023
5	312.2	319.9	0.017	0.011	0.029	0.007	0.046	0.015
6	319.0	326.8	-0.016	0.007	0.030	0.006	0.015	0.011
7	327.0	333.8	0.000	0.006	0.013	0.009	0.013	0.008
8	333.9	340.9	0.003	0.022	0.018	0.018	0.020	0.026
9	340.9	347.8	0.020	0.024	0.031	0.012	0.052	0.029
10	347.9	366.0	0.002	0.009	0.020	0.008	0.022	0.012
11	20.0	40.8	-0.160	0.145	0.119	0.017	-0.041	0.170
12	40.9	45.8	0.029	0.020	0.059	0.007	0.088	0.028
13	46.0	54.7	0.007	0.012	0.003	0.049	0.009	0.013
14	54.7	59.3	-0.026	0.038	0.051	0.012	0.025	0.047
15	59.9	66.7	0.000	0.016	0.015	0.015	0.015	0.019
16	66.9	75.8	-0.014	0.021	0.005	0.052	-0.009	0.023
17	75.9	84.7	-0.008	0.009	0.015	0.010	0.007	0.011
18	84.9	91.7	0.005	0.004	0.005	0.013	0.009	0.005
19	91.8	99.8	-0.033	0.008	0.005	0.020	-0.028	0.009
20	99.9	106.6	*	*	*	*	*	*
21	106.7	112.0	-0.024	0.010	0.010	0.015	-0.014	0.012
22	112.2	120.7	*	*	*	*	*	*
23	120.8	126.0	0.047	0.011	0.018	0.010	0.065	0.014
24	126.1	133.7	0.037	0.010	0.021	0.008	0.059	0.013
25	133.8	150.9	*	*	*	*	*	*
26	152.0	153.7	-0.010	0.024	0.008	0.036	-0.002	0.027
27	153.8	159.7	-0.005	0.012	0.017	0.012	0.011	0.015
28	160.8	166.7	-0.028	0.018	0.012	0.020	-0.016	0.020
29	166.8	175.8	0.033	0.018	0.013	0.019	0.046	0.021
30	175.8	187.8	0.059	0.035	0.026	0.019	0.085	0.041
31	187.9	194.8	0.049	0.018	0.010	0.024	0.059	0.020
32	194.8	199.7	0.199	0.015	0.011	0.019	0.210	0.018
33	199.8	208.7	-0.072	0.025	0.039	0.011	-0.032	0.031
34	208.7	218.8	0.078	0.023	0.020	0.016	0.098	0.027
35	218.9	222.7	-0.037	0.041	0.041	0.015	0.005	0.049
36	222.8	231.8	0.049	*	0.008	0.022	0.058	*
37	231.9	237.7	0.062	0.015	0.001	0.145	0.063	0.016
38	237.8	243.8	0.026	0.018	0.007	0.032	0.033	0.021
39	243.8	257.7	0.025	0.024	0.004	0.072	0.029	0.026
40	*	*	*	*	*	*	*	*
41	265.8	274.1	0.012	0.034	0.020	0.023	0.031	0.039
42	274.1	279.8	0.069	0.031	0.015	0.027	0.084	0.035
43	279.8	285.8	0.009	0.010	0.006	0.023	0.015	0.011
44	285.8	294.7	*	*	*	*	*	*
45	294.1	299.8	0.033	0.019	-0.003	0.085	0.031	0.021
46	299.8	306.8	-0.017	0.025	-0.005	0.057	-0.022	0.028
47	306.8	312.8	0.008	0.027	0.002	0.126	0.010	0.029
48	312.8	319.8	*	*	*	*	*	*
49	319.8	335.8	-0.003	0.010	0.000	0.239	-0.003	0.011
50	335.8	348.8	0.004	0.009	-0.001	0.174	0.003	0.010
51	348.8	362.7	0.031	0.030	-0.006	0.057	0.024	0.033
52	1.0	11.8	-0.007	0.014	-0.002	0.102	-0.009	0.015
53	11.8	25.8	0.025	0.009	0.000	0.947	0.025	0.010
54	25.8	38.8	0.002	0.029	-0.001	0.239	0.001	0.032
55	38.8	52.8	0.057	0.054	-0.002	0.369	0.056	0.058
56	52.8	63.8	0.031	0.025	0.004	0.070	0.035	0.027
57	63.9	78.8	0.081	0.043	0.004	0.128	0.085	0.047
58	78.8	100.8	0.062	*	0.006	0.024	0.068	*
59	100.8	133.7	0.046	0.018	-0.002	0.093	0.044	0.020

a)

b)

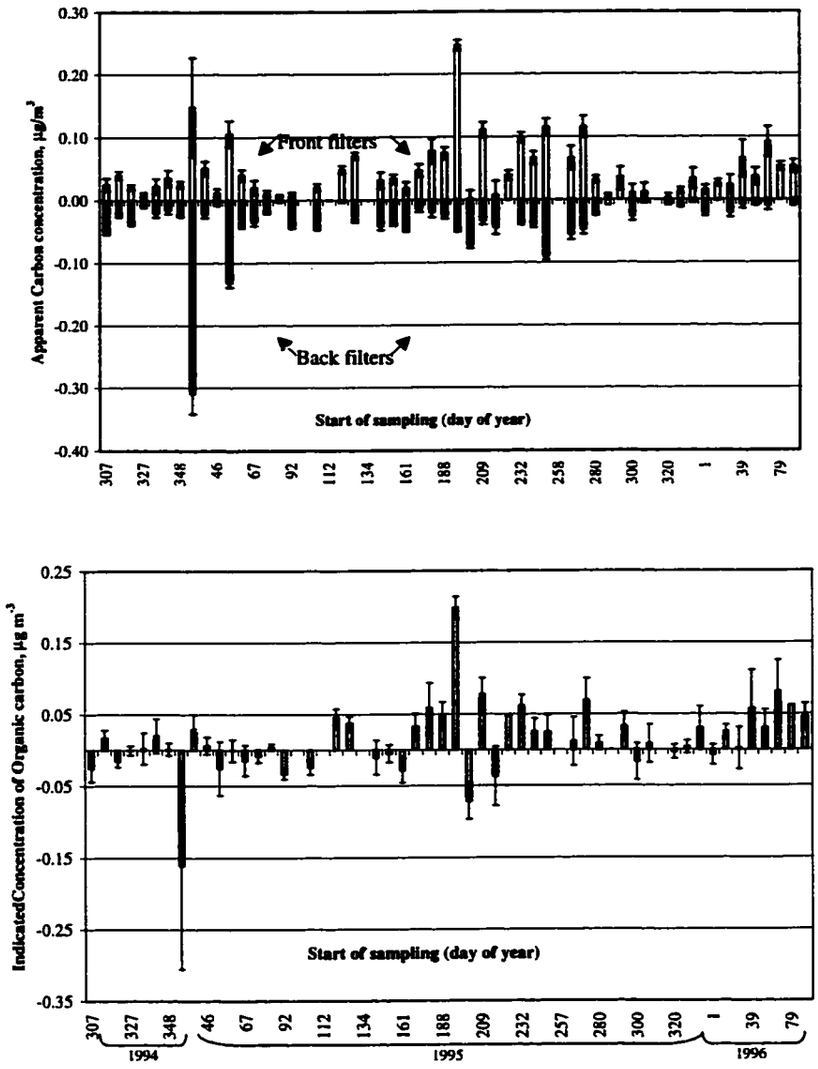

Figure 5-7(a) Apparent concentrations from front filters (positive values) and back filters (negative values) at Cheeka Peak. (b) Resultant indicated concentration of organic carbon at Cheeka Peak. Values in (b) are the sum of the values plotted in (a) and correct for vapor adsorption. Numerical data is in Table 5-3 . Negative values are the result of back filter concentrations that were higher than on the front filter.

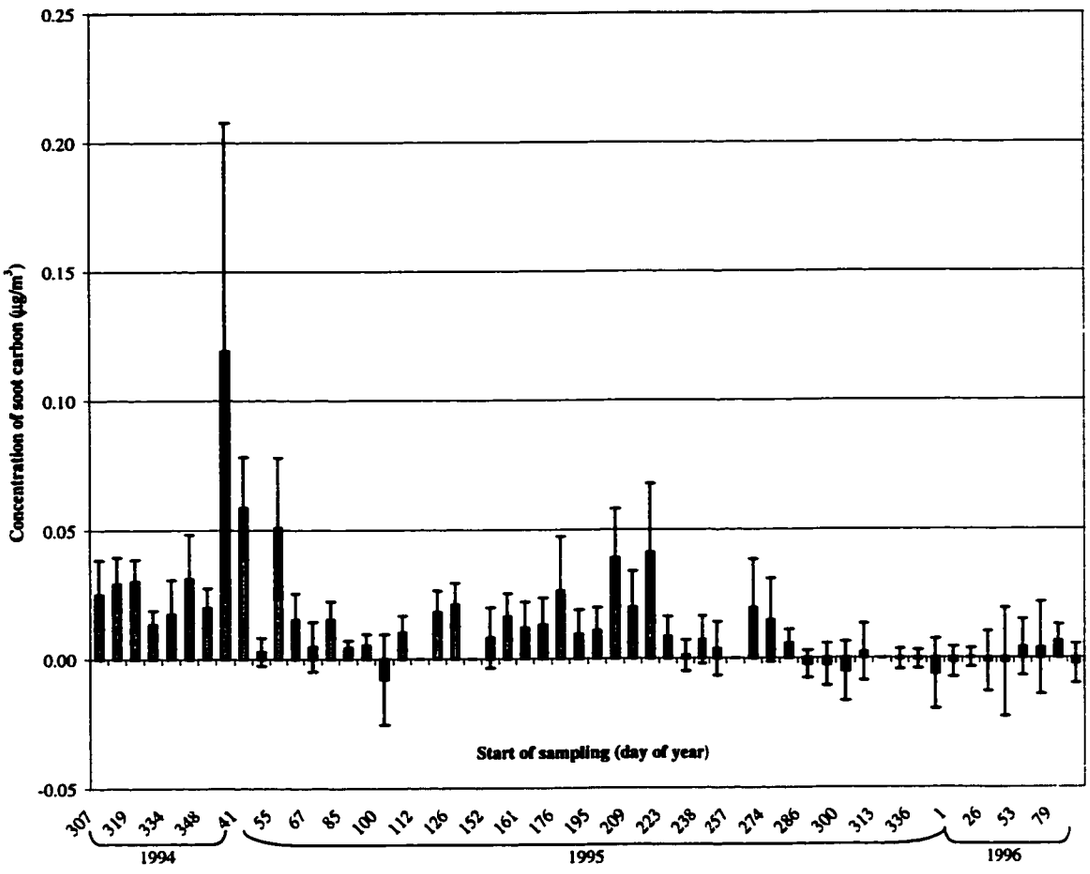

Figure 5-8 Concentration of refractory carbon in air. Negative values indicate that concentration measured on filter was less than the average blank value for refractory carbon.

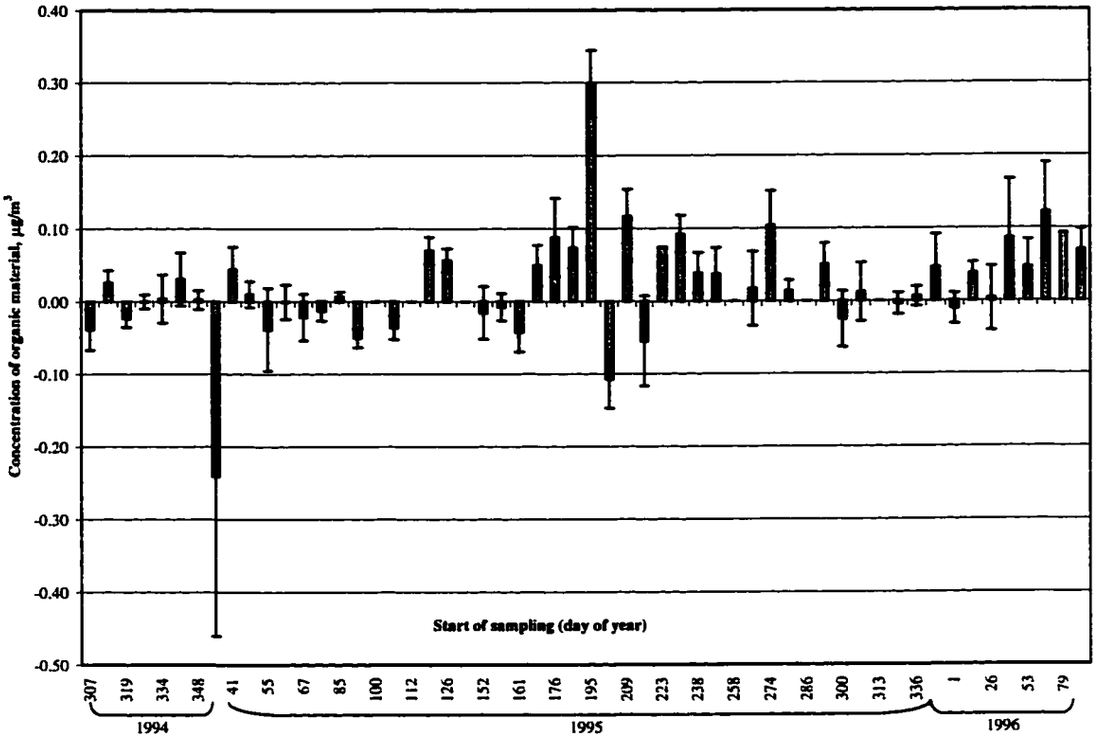

Figure 5-9 Concentration of organic material. The values graphed here are the organic carbon concentrations shown in Figure 5- , multiplied by a factor of 1.5 as the estimation of the average [organic compound mass:organic carbon mass] ratio. The graphed uncertainties take into account an uncertainty of $\pm$ 0.2 for this ratio.

CONCENTRATION OF CARBONACEOUS MATERIAL: MASS BALANCE?

The data listed in Table 5-3 and Figures 5-7, 8, and 9 now seem to give a clearer picture of the concentrations of the different types of carbonaceous material at Cheeka Peak. Without taking an average, the combination of these plots reveal certain conclusions:

- Roughly half of the carbonaceous material collected on the filters seems to come from the gas phase. This gas phase concentration is roughly consistent with organic material (formate and acetate) found in precipitation and cloud water.
- The vapor-corrected organic particulate carbon concentrations are roughly 0.03-0.06 $\mu g\ m^{-3}$.
- The concentrations of refractory carbon range from approximately 0 to 0.04 $\mu g\ m^{-3}$.
- The total concentration of carbon ranges from approximately 0.03 to 0.1 $\mu g\ m^{-3}$.
- When multiplied by factor of 1.5 to account for other elements in organic material, the resultant mass concentration for organic carbon is approximately 0.05-0.12 $\mu g\ m^{-3}$.
- The values listed above are uncertain by about 50%, and meteorology and sources can greatly affect these concentrations.

One of the original questions asked in this chapter is whether carbonaceous particles can provide the additional mass needed to obtain a balance with gravimetric measurements. The data listed in Table 5-4 only begins to answer this question, by comparing the total mass of submicrometer particles collected on each filter with the concentrations listed in Table 5-3. The result is a determination of the mass percentage of particles that are carbonaceous.

Table 5-4 Total particle concentrations and mass percentage of particles that are carbonaceous

Teflon Filt #	Sampling start day (doy)	Sampling end day (doy)	Particle concentration, ug/m3	Mass percentage of particles that are carbonaceous	Uncertainty, mass %
4	306.9	312.1	1.72	-0.8	1.8
5	312.2	319.9	1.92	2.9	1.0
6	319.0	326.8	1.43	0.5	1.0
7	327.0	333.8	0.52	2.5	2.1
8	333.9	340.9	0.54	4.0	6.7
9	340.9	347.8	0.69	8.9	6.2
10	347.9	366.0	26.64	0.1	0.1
11	20.0	40.8	2.42	-5.0	10.0
12	40.9	45.8	3.13	3.3	1.2
13	46.0	54.7	0.36	3.6	5.2
14	54.7	59.3	2.76	0.5	2.3
15	59.9	66.7	1.95	0.8	1.3
16	66.9	75.8	1.14	-1.5	2.9
17	75.9	84.7	1.39	0.2	1.1
18	84.9	91.7	0.21	5.7	3.1
19	91.8	99.8	0.84	-5.3	1.7
20	99.9	106.6	1.70	*	*
21	106.7	112.0	0.81	-3.2	2.2
22	112.2	120.7	*	*	*
23	120.8	126.0	1.17	7.6	1.8
24	126.1	133.7	0.30	26.0	8.5
25	133.8	150.9	*	*	*
26	152.0	153.7	0.53	-1.4	7.2
27	153.8	159.7	1.50	0.6	1.4
28	160.8	166.7	1.11	-2.7	2.6
29	166.8	175.8	0.06	97.5	200.7
30	175.8	187.8	1.06	10.8	6.0
31	187.9	194.8	0.95	8.8	3.3
32	194.8	199.7	2.52	12.3	1.9
33	199.8	208.7	1.65	-4.1	2.7
34	208.7	218.8	1.84	7.4	2.3
35	218.9	222.7	1.06	-1.3	6.4
36	222.8	231.8	1.15	7.2	*
37	231.9	237.7	1.32	7.1	2.1
38	237.8	243.8	2.45	1.9	1.2
39	243.8	257.7	1.72	2.4	2.2
40	257.8	265.5	(blank)	(blank)	(blank)
41	265.8	274.1	1.23	3.0	4.4
42	274.1	279.8	1.48	8.0	3.6
43	279.8	285.8	0.97	2.0	1.6
44	285.8	294.7	1.04	*	*
45	294.1	299.8	1.06	4.5	2.9
46	299.8	306.8	1.88	-1.6	2.1
47	306.8	312.8	0.83	1.8	5.1
48	312.8	319.8	*	*	*
49	319.8	335.8	0.15	-3.0	10.6
50	335.8	348.8	0.63	0.9	2.2
51	348.8	362.7	1.25	3.2	3.8
52	1.0	11.8	0.71	-1.7	3.1
53	11.8	25.8	0.85	4.4	1.8
54	25.8	38.8	0.03	6.3	172.9
55	38.8	52.8	2.37	3.6	3.6
56	52.8	63.8	1.17	4.3	3.4
57	63.9	78.8	1.83	6.9	4.0
58	78.8	100.8	1.72	5.8	*
59	100.8	133.7	1.25	5.4	2.4
			Averages:	2.9	3.4

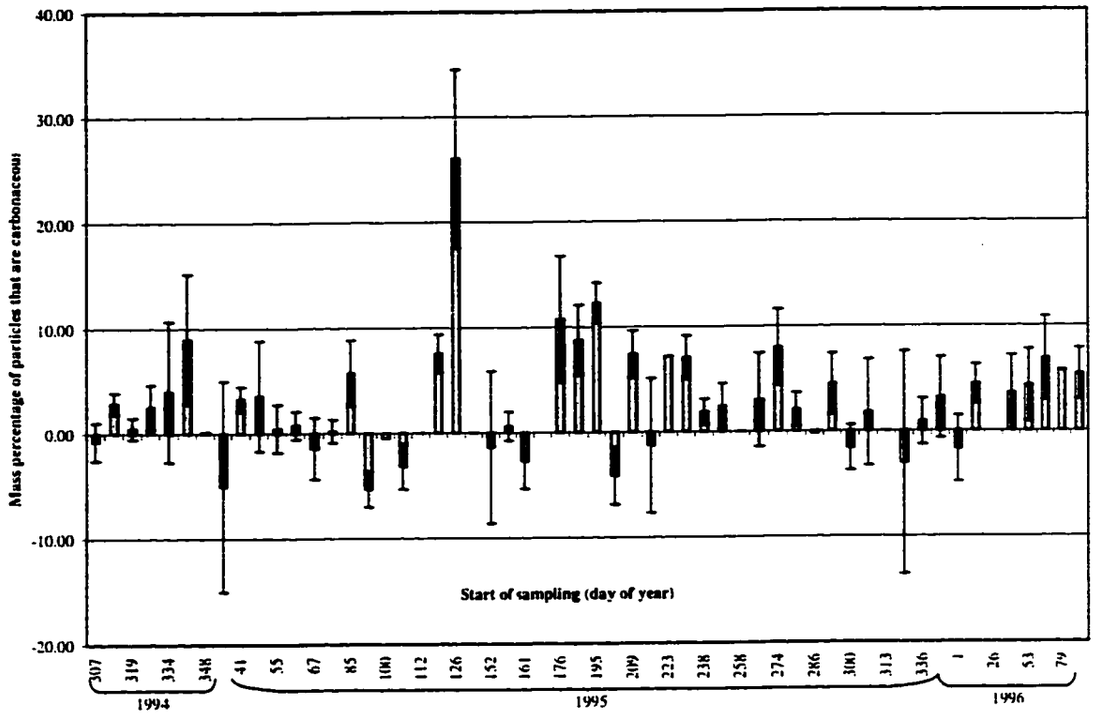

Figure 5-10 Mass percentage of particles that are carbonaceous. Values are those listed in Table 5-4

This calculation also takes into account an assumed value of the organic compound mass:carbon mass ratio to include elements besides carbon in the organics. We see from Table 5-4 that the average contribution of carbonaceous particles to total particle mass is about 3%, with a standard deviation of about 5%. The mass discrepancies between gravimetric and IC analysis listed originally by McInnes et al. was about 40-60%. Therefore the carbonaceous material measured in this project could not balance the unidentified mass reported in this reference. Furthermore, with such small concentrations, we can infer that carbonaceous compounds do not significantly affect light scattering at Cheeka Peak during on shore flow periods.

CONCLUSION AND RECOMMENDATIONS

To recap, the quartz filter samples collected at Cheeka Peak exhibit a very large vapor artifact, which accounts for at least as much carbon as particulate carbon forms. The concentrations of organic material were calculated by subtracting the estimated vapor adsorption artifact. This subtraction lead to large uncertainties because the end result was to subtract one relatively large number from another. Based on the concentration of adsorbed carbon seen on the back filter, I hypothesize that the gases are largely made up of formate and acetate ions. The mechanism for material appearing on the back filters seems to most likely be by gas adsorption, and not volatilization of front-filter material followed by readsorption.

There are some improvements that could be made on the next experiment at this or another clean location dealing with carbonaceous aerosols. The vapor adsorption artifact is large because of the very small concentration of particle carbon at this site. One way to possibly reduce this effect is not to prefire the filters, but to solvent wash them instead. Some groups in Europe have been having luck with this protocol, although their sites are not as pristine as Cheeka Peak [13]. Another possibility would be to try to remove gas phase material upstream of sampling with a series of gas denuders. This

could be followed by duplicate denuders downstream of the particle sampling to measure possible volatilization.

NOTES TO CHAPTER 5

1. McInnes, L.M., P.K. Quinn, D.S. Covert, and T.L. Anderson, *Gravimetric analysis, ionic composition, and associated water mass of the marine aerosol.* Atmos Environ, 1996. **30**(6): p. 869-884.

2. Trajectory analyses run by Dr. Joyce Harris at NOAA CMDL

3. Balkanski, Y.J., D.J. Jacob, R. Arimoto, and M.A. Kritz, *Distribution of 222Rn over the North Pacific: implications for continental influences.* J. Atmos. Chem., 1992. **14**: p. 353-374.

4. Shah, J.J. and J.A. Rau, *Carbonaceous species methods comparison study: Interlaboratory round robin interpretation of results.* 1991.

5. Cadle, S., P.J. Groblicki, and D.P. Stroup, *Automated Carbon Analyzer for Particulate Samples.* Analytical Chemistry, 1980. **52**: p. 2201-2206.

6. Appel, B.R., Y. Tokiwa, and E.L. Kothny, *Sampling of carbonaceous particles in the atmosphere.* Atmos. Environ., 1983. **17**(9): p. 1787-1796.

7. Appel, B.R., W. Cheng, and F. Salaymeh, *Sampling of carbonaceous particles in the atmosphere--II.* Atmos. Environ., 1989. **23**: p. 2167-2175.

8. McDow, S.R. and J.J. Huntzicker, *Vapor adsorption artifact in the sampling of organic aerosol: Face velocity effects.* Atmos. Env., 1990. **24A**(10): p. 2563-2571.

9. Young, J.F., *Humidity control in the laboratory using salt-solutions--A review.* J. Appl. Chem., 1967. **17**: p. 241-245.

10. Liousse, C., J.E. Penner, C. Chuang, J.J. Walton, H. Eddleman, and H. Cachier, *A global three-dimensional model study of carbonaceous aerosols.* J. Geophys Res., 1996. **101**(D14): p. 19,411-19,432.

11. Vong, R.J., B.M. Baker, F.J. Brechtel, R.T. Collier, J.M. Harris, A.S. Kowalski, N.C. McDonald, and L.M. McInnes, *Ionic and trace element composition of cloud water collected on the Olympic Peninsula of Washington State.* Atmos. Env., 1997. **31**(13): p. 1991-2001.

12. Junge, C., *Air Chemistry and Radioactivity.* 1963, New York: Academic Press.

13. Helene Cachier, Personal Communication

CHAPTER 6: CONCLUSION

OVERVIEW

The message of this dissertation is 3-fold: 1) Organic material in atmospheric aerosol is important based on its environmental effects and ubiquity. We should invest more time and effort into understanding it better. 2) Organic aerosol materials, based on solubility, may affect the growth of cloud droplets and optics of clouds in ways that have not been considered until now. 3) There is consistently a very small, but nonzero contribution of organic material in the remote marine atmosphere. Sampling for organic particulate matter at this type of location carries with it certain difficulties based on the low concentrations and relatively high organic vapor concentrations compared to organic material present in particles. I would like to place these conclusions into the larger context what is and is not known about organic atmospheric particles, and make suggestions for future study using these conclusions as a starting point. But, to start with, why is so little known about this important class of atmospheric matter?

OVERSIMPLIFICATION OF THE DESCRIPTION OF ORGANIC MATTER IN THE ATMOSPHERE

A theme that reappears throughout each chapter of this dissertation is that although organic material is an important aerosol fraction, it remains difficult to characterize. Both from the standpoint of sampling (e.g. Chapter 5) and chemical analysis, much less is known about the organic forms of atmospheric aerosol than the inorganic fractions. Because of this lack of basic information on concentration, molecular forms, and molecular properties, there still is no detailed assessment of the relevant climatic and public health effects to which organic aerosol contributes, compared with other atmospheric components. Perhaps the most important reason organic aerosol seems so difficult to understand is that organic compounds have a wide range of physical and chemical properties, whereas other atmospheric aerosol components (like salts) are

more or less uniform in this respect. I have concentrated on two properties in particular in this dissertation: water solubility and volatility. With the inorganic classes of atmospheric aerosols, it is very easy to assume that a component is either "soluble" such as sodium chloride, ammonium sulfate, and ammonium bisulfate, or "insoluble" like most mineral dust and elemental carbon. With few exceptions (most notably calcium sulfate), the generalization fits. The attempt has been made by meteorologists and atmospheric scientists to understand organic components that exist in the atmosphere within a similar framework, which is simply inadequate. Organic molecules have ranges of solubility from not soluble to weakly soluble to very soluble, depending on the functional groups, chain length, and structure of the molecule. These complexities prevent us from including organic matter in cloud and climate models as a single, predictable component. The physical behavior of this material in the atmosphere depends strongly on sources and local meteorological conditions such that one set of properties do not apply universally.

Unfortunately the complexity of organic material in the atmosphere does not end with its range of properties. Many organic compounds are strongly *reactive* in the atmosphere, such that the presence of less than 10 reactive gases can produce hundreds of different compounds in photochemical reactions. Along with the range of properties comes, therefore, a wide and very possibly *changing* set of molecular forms. This complicates our ability to understand the relevance and effects of organic material compared to simpler atmospheric components because the total amount of organic material is only one part of the picture. The amount of each species is the important data to acquire, along with studies of how each of the individual components behaves in the atmospheric environment with oxygen, water, inorganic salts, mineral dust and other organic compounds.

WHAT WE SEE DEPENDS STRONGLY ON HOW WE LOOK

There is some limited information on molecular forms of organic compounds, especially from cities. Unfortunately the presence of certain types of organic material seems to be less related to emissions and atmospheric processes than to the method used for identification. Analytical methods have often been chosen based on what is readily available, or by a dictum of environmental laws. These practices have led to method-specific conclusions. As an example, the principle method used for organic analysis of atmospheric aerosols has been gas chromatography/mass spectrometry from organic solvent extracts of sample filters, revealing the composition of perhaps 20% of the total organic particulate mass in urban areas polluted with car exhaust [1]. Such chemical analysis methods are based on the assumption that all of the organic material on the filter dissolves into the organic solvent and that all of the important compounds elute. It should not be surprising that such methods only identify small fractions of the total organic aerosol. One class of compounds that has been successfully characterized using GC/MS is the polyaromatic hydrocarbons (PAH's). These compounds have received a great deal of attention because they are highly toxic, and seem to be present in measurable concentrations in many areas, especially cities. The contribution of these compounds to the total organic mass is minimal in most cases—not more than a few percent at most. But, these compounds are easily measured by GC/MS, so that is what is seen. A similar situation is the gas adsorption artifact on quartz filters. It is possible (and probable) that many of the concentrations of organic particulate matter reported before the advent of dual filter sampling are erroneously high. Again, what we see depends strongly on how we look. Having stated these shortcomings of analytical chemistry, we can focus on the key remaining scientific questions.

SCIENTIFIC QUESTIONS

Recognizing that ways organic compounds in the atmosphere require a way of thinking that is different from our treatment of other atmospheric components, we can be begin to seriously ask some important scientific questions, some of which appear below:

- What is the spatial distribution of carbonaceous aerosol globally, locally, and vertically?
- What is the fraction of organic vs. elemental carbon?
- What is the size distribution of this aerosol?
- What are the principle sources and fluxes of this aerosol?
- What molecular forms are present in the organic fraction?
- What physical properties do these compounds have? (Index of refraction, water solubility, toxicity, both as individual compounds and as mixtures)
- What is the time variability of these properties?
- What radiative forcings, visibility and cloud effects can be apportioned to this aerosol? (Scattering, absorption, effects on cloud droplet growth, droplet size, etc.)

RECOMMENDATIONS

Based on the questions listed above, there are some specific recommendations that will start the process of gaining more information. These suggestions build on each other, and should be thought of as long-term projections.

TOTAL ORGANIC AND BLACK CARBON MEASUREMENTS

As evidenced by Liousse [2] and Penner [3], a detailed, comparable set of measurements from a wide range of locations around the world would be very helpful for modeling both the biogeochemical transport and climatic effects of carbonaceous aerosols. The current models described in these references utilize data that has very large uncertainties, especially in remote locations. To be useful in such studies, individual measurements must be collected and analyzed according to similar protocol, so planning for measurements should include input from the modeling community. Data such as those presented in Chapter 5 should be used as a starting point, with appropriate changes in protocol based on the problems reported.

WATER SOLUBILITY

Measurement of the degree of water solubility is a relatively simple extension of the total carbon measurement which supplies valuable clues regarding the chemistry of organic aerosol and its interaction with water vapor as described in Chapter 3. The simplest way of determining this fraction is to measure carbon with an analyzer like the one described in Chapter 4, before and after treatment with water. This measurement should be done at least twice per sample: one measurement with a large excess of water and one measurement with approximately the same amount of liquid water available in atmospheric clouds. The excess water experiment provides an analytical estimate of the fraction that would be difficult to characterize using traditional GC/MS analysis. This can be compared to the "unanalyzed fraction" always present in such experiments to attempt mass balance of the type of compounds making up this unknown fraction. The experiment with atmospherically realistic amounts of water roughly gives the mass of organic carbon likely to enter aqueous solution in cloud droplets. The amount of water available is calculated from the average liquid water content (gm^{-3}) multiplied by the volume of air sampled. Physical and chemical variables such as the amount of agitation, exposure to ultrasonic treatment, solution pH, and ionic strength can all affect this measurement.

COMPOSITION OF HIGHLY AND SLIGHTLY SOLUBLE ORGANIC MATERIAL

Organic compounds have successfully been analyzed in rainwater using the wet chemical methods outlined by Likens [4]. In this study more than 80% of dissolved organic carbon could be identified as carboxylic acids, aldehydes, carbohydrates, tannin/lignin, primary amines or phenols in rainwater collected in upstate NY. Although in most cases they do not yield actual molecular form information, these methods can be applied to water extracts from filter samples and give major organic functionality of the water-soluble fraction. Since it is the more polar fractions that are most difficult to analyze using GCMS, a combination of water extraction and this type of wet chemical analysis followed by organic extraction and GCMS on the same filter would provide significant improvement over the traditional protocol which generally calls for organic

extraction/GCMS alone. More advanced methods are slowly becoming more more attractive, as analytical techniques improve. One particularly exciting area is to use HPLC (high performance liquid chromatograpy) in combination with electrospray mass spectrometry. Since reverse-phase HPLC can accommodate aqueous solvents, extraction with pure water is possible directly from the sample filter. This procedure would not be possible with GC/MS. The eluent from the HPLC then enters a charged metal needle. The charge causes the liquid passing through it to break up into very small droplets. The solutes present in the liquid also become ionized in the process. The droplets are evaporated and the ions produced are electrically introduced into a quadrupole mass spectrometer. This method generally produces only parent ions, but an extension of this method is to induce fragmentation in the parent ion using electron impact, followed a second mass spectrometric analysis (HPLC/MS/MS) which allows unambiguous molecular identification in many cases. For exapmle this method has been used for measurement of hydroxymethanesulfonate in rain [5].

Characterization of Major Sources

Although it is very difficult to collect and analyze organic aerosol, especially in clean and remote locations, there are many obvious primary sources of organic and refractory carbon aerosols that have not been thoroughly characterized chemically or isotopically. Biomass burning (both natural and anthropogenic) and fossil fuel combustion are thought to be the major sources of primary organic aerosol and the only sources of black carbon aerosol, as discussed in Chapter 2. Sampling of enough material to analyze from these sources would be comparably simple, and chemical information (especially on the water-soluble fraction) is severely lacking, yet possible to obtain with existing technology. These sources could be sampled and analyzed using the methods outlined above for ambient aerosol: determination of organic/elemental carbon ratio, determination of degree of water solubility with excess and non-excess of water,

determination of major functionality of water-soluble fraction, GCMS analysis of non-soluble fraction, and isotopic analysis (as discussed in the next section and Appendix B).

ISOTOPIC ANALYSIS

Analysis of $^{14}C/^{12}C$ and $^{13}C/^{12}C$ was discussed in section IV. These methods are some of the most powerful tools available for inferring probable sources. The $^{13}C/^{12}C$ ratio of ambient aerosol is especially useful when compared to measurements of suspected sources. Several source regions have been characterized isotopically by Cachier (1987, 1989). This work should be expanded and continued with isotopic measurement of the sources listed the previous section, and coordinated with isotopic measurements and the other measurements listed above for ambient aerosol. The $^{14}C/^{12}C$ ratio is less convenient to measure, but is very helpful in determining whether a sample is composed of fossil or contemporary carbon. This measurement to be done on a more regular basis with concurrent chemical measurements of ambient aerosol as listed above in sections, taking into account the sampling procedures and problems listed in Chapter 5.

MODELING

With implementation of the above recommendations, enough information on molecular form and distribution of material should become available for modeling the environmental effects of organic aerosol based on direct light scattering, cloud optical effects, and some health effects. As more data become available, these models will become more realistic and useful for answering the last few questions listed above.

CONCLUSION

Understanding organic aerosols will not be an easy or short-term task. Many different ways of looking at these particles will be necessary in order to make any useful conclusions about them, in keeping with their physical and chemical complexities. We

must learn to respect the complicated chemical and physical nature of these aerosols and approach them with new analysis techniques and experiments, and understand that the methods used to study the inorganic aerosol fractions will only go a short way in elucidating the interesting characteristics and effects of organic aerosols.

NOTES TO CHAPTER 6

1. Rogge, W.F., M.A. Mazurek, L.M. Hildemann, G.R. Cass, and B.R.T. Simoneit, *Quantification of urban organic aerosols at a molecular level: Indentification , abundance and seasonal variation.* Atmos. Env., 1993. **27A**(8): p. 1308-1330.

2. Liousse, C., J.E. Penner, C. Chuang, J.J. Walton, H. Eddleman, and H. Cachier, *A global three-dimensional model study of carbonaceous aerosols.* J. Geophys Res., 1996. **101**(D14): p. 19,411-19,432.

3. Penner, J.E., C.C. Chuang, and C. Liousse. *The contribution of carbonaceous aerosols to climate change.* in *The Fourteenth International Conference of Nucleation and Atmospheric Aerosols*. 1996. Helsinki, Finland: Pergamon.

4. Likens, G.E., E.S. Edgerton, and J.N. Galloway, *The composition and deposition of organic carbon in precipitation.* Tellus, 1983. **35B**: p. 16-24.

5. Chapman, E.G., C.J. Borinaga, and H.R. Udseth, *Confirmation and quantitation of hydroxymethanesulfonate in precipitation by electrospray ionization-tandem mass spectroscopy.* Atmos. Env., 1990. **24**(12): p. 2951.

BIBLIOGRAPHY

Andreae, M. O. (1991). Biomass burning: Its history, use, and distribution and its impact on environmental quality and global climate. Global Biomass Burning: Atmospheric, Climatic, and Biospheric Implications. J. S. Levine. Cambridge, MA, MIT Press: 3-21.

Andreae, M. O., E. V. Browell, M. Garstang, G. L. Gregory, R. C. Harriss, G. F. Hill, D. J. Jacob, M. C. Pereira, G. W. Sachse, A. W. Setzer, P. L. Silva Dias, R. W. Talbot, A. L. Torres and S. C. Wofsy (1988). "Biomass-burning emissions and associated haze layers over Amazonia." J. Geophys. Res. **93**(D2): 1509-1527.

Andrews, E. and S. M. Larson (1993). "Effect of surfactant layers on the size change of aerosol particles as a function of relative humidity." Environ.Sci.Technol. **27**: 857-865.

Appel, B. R., W. Cheng and F. Salaymeh (1989). "Sampling of carbonaceous particles in the atmosphere--II." Atmos. Environ. **23**: 2167-2175.

Appel, B. R., Y. Tokiwa and E. L. Kothny (1983). "Sampling of carbonaceous particles in the atmosphere." Atmos. Environ. **17**(9): 1787-1796.

Appel, B. R., S. M. Wall and R. S. Knights (1980). "Characterization of carbonaceous materials in atmospheric aerosols by high-resolution mass spectrometric thermal analysis." Adv. Envir. Sci. Technol. **9**: 353-365.

Baker, M. B. and R. J. Charlson (1990). "Bistability of CCN concentrations and thermodynamics in the cloud-topped boundary layer." Nature **345**(6271): 142-145.

Balkanski, Y. J., D. J. Jacob, R. Arimoto and M. A. Kritz (1992). "Distribution of 222Rn over the North Pacific: implications for continental influences." J. Atmos. Chem. **14**: 353-374.

Ballschmiter, K. (1992). "Transport and fate of organic compounds in the global environment." Angew. Chem. Int. Ed. Engl. **31**(5): 487-515.

Balsley, D. R., G. W. Farwell, P. M. Grootes and F. H. Schmidt (1987). "Ion source sample preparation techniques for C-14 AMS measurements." Nucl. Instrum. Methods **B29**: 37-40.

Bigg, E. K. (1986). "Discrepancy between observation and prediction of concentrations of cloud condensation nuclei." Atmos. Res. **20**: 82-86.

Bushby, B., A. Fernandes, D. Wallace and M. Kibblewhite (1993). "Determination of Trace Organic Micropollutants in Atmospheric Deposition." The Science of the Total Environment **135**: 81-94.

Cachier, H. (1989). "Isotopic Characterization of Carbonaceous Aerosols." Aerosol Science and Technology **10**: 379-385.

Cachier, H., M.-P. Bremond and P. Buat-Menard (1989). "Carbonaceous aerosols from different tropical biomass burning sources." Nature **340**: 371-373.

Cadle, S., P. J. Groblicki and D. P. Stroup (1980). "Automated Carbon Analyzer for Particulate Samples." Analytical Chemistry **52**: 2201-2206.

Cautreels, W. and K. Van Cauwenberghe (1977). "Experiments on the distribution of organic pollutants between airborne particulate matter and the corresponding gas phase." Atmos. Env. **12**: 1133-1141.

Chameides, W. L. and D. D. Davis (1983). "Aqueous-phase source of formic acid in clouds." Nature **304**: 427-429.

Chapman, E. G., C. J. Borinaga and H. R. Udseth (1990). "Confirmation and quantitation of hydroxymethanesulfonate in precipitation by electrospray ionization-tandem mass spectroscopy." Atmos. Env. **24**(12): 2951.

Charlson, R. J., J. J. Langner, H. Rodhe, C. B. Leovy and S. G. Warren (1991). "Perturbation of the Northern Hemisphere Radiative Balance by Backscattering from Anthropogenic Sulfate Aerosols." Tellus **43B**: 152-163.

Charlson, R. J., J. E. Lovelock, M. O. Andreae and S. G. Warren (1987). "Oceanic phytoplankton, atmospheric sulphur, cloud albedo and climate." Nature **326**: 655-661.

Charlson, R. J., S. E. Schwartz, J. M. Hales, R. D. Cess, J. J.A. Coakley, J. E. Hansen and D. J. Hofmann (1992). "Climate Forcing by Anthropogenic Aerosols." Science **255**: 423-430.

Chesselet, R., M. Fontugne, P. Buat-Menard, U. Ezat and C. E. Lambert (1981). "The origin of particulate organic carbon in the marine atmosphere as indicated by its stable carbon isotopic composition." Geophys. Res. Lett. **8**(4): 345-348.

Chiou, C. T., D. E. Kile and R. L. Malcolm (1988). "Sorption of vapors of some organic liquids on soil humic acid and its relation to partitioning of organic compounds in soil organic matter." Envir. Sci. Technol. **22**: 298-303.

Chow, J. C., J. G. Watson, L. C. Pritchett, W. R. Pierson, C. A. Frazier and R. G. Purcell (1993). "The DRI Thermal/Optical Reflectance Carbon Analysis System: Description, Evaluation and Applications in U.S. Air Quality Studies." Atmospheric Environment **27A**(8): 1185-1201.

Coplen, T. B., C. Kendall and J. Hopple (1983). "Comparison of stable isotope reference standards." Nature **302**: 235-238.

Council, N. R. (1991). Rethinking the Ozone Problem in Urban and Regional Air Pollution. Washington, D.C., National Academy Press.

Cronn, D. R. (1975). Analysis of Atmospheric Aerosols by High Resolution Mass Spectrometry. Civil Engineering. Seattle, University of Washington.

Cunningham, K. M., M. C. Goldberg and E. R. Weiner (1985). "The aqueous photolysis of ethylene glycol adsorbed on goethite." Photochem. Photobiol. **41**: 409-416.

Duce, R. A. (1978). "Speculations on the budget of particulate and vapor phase non-methane organic carbon in the global troposphere." Pure Appl. Geophys. **116**: 244-273.

Duce, R. A., V. A. Mohnen, P. R. Zimmerman, D. Grosjean, W. Cautreels, R. Chatfield, R. Jaenicke, J. A. Ogren, E. D. Pellizzari and G. T. Wallace (1983). "Organic material in the global troposphere." Rev. Geophys. Space Phys. **21**(4): 921-952.

Edmonds, R. L., Ed. (1979). Aerobiology: The Ecological Systems Approach. Stroudsburg, PA, Dowden, Hutchinson & Ross.

Erel, Y., S. O. Pehkonen and M. R. Hoffmann (1993). "Redox chemistry of iron in fog and stratus clouds." J. Geophys. Res. **98**(D10): 18,423-18,434.

Falconer, R. L. and T. F. Bidleman (1994). "Vapor pressures and predicted particle/gas distributions of polychlorinated biphenyl congeners as functions of temperature and ortho-chlorine substitution." Atmos. Env. **28**(3): 547-554.

Faust, B. C. and M. R. Hoffmann (1986). "Photoinduced reductive dissolution of hematite by bisulfite." Environ. Sci. Technol. **20**: 943-948.

Fehsenfeld, F., J. Calvert, R. Fall, P. Goldman, A. B. Guenther, C. N. Hewitt, B. Lamb, S. Liu, M. Trainer, H. Westberg and P. Zimmerman (1992). "Emissions of volatile organic compounds from vegetation and the implications for atmospheric chemistry." Global Biogeochem. Cycles **6**(4): 389-430.

Folger, D. W. (1970). "Wind transport of land-derived mineral, biogenic and industrial matter over the North Atlantic." Deep Sea Res. **7**: 337.

Fuzzi, S., P. Mandrioli and A. Perfetto (1996). "Fog droplets--An atmospheric source of secondary biological aerosol particles." Atmos. Env **In press**.

Gagosian, R. B., O. C. Zafiriou, E. T. Peltzer and J. B. Alford (1982). "Lipids in Aerosols From the Tropical North Pacific: Temporal Variability." J. Geophys. Res. **87**(C13): 11,133-11,144.

Galloway, J. N., G. E. Likens and E. S. Edgerton (1976). "Acid precipitation in the Northeastern United States: pH and acidity." Science **194**: 722-724.

Galloway, J. N., G. E. Likens, W. C. Keene and J. N. Miller (1982). "The composition of precipitation in remote areas of the world." J. Geophys. Res. **87**: 8771-8786.

Gill, P. S., T. E. Graedel and C. J. Weschler (1983). "Organic films on atmospheric aerosol particles, fog droplets, cloud droplets, raindrops, and snowflakes." Rev. Geophys. and Space Phys. **21**(4): 903-920.

Graedel, T. E. (1979). "Terpenoids in the Atmosphere." Rev. Geophys. and Space Phys. **17**(5): 937-947.

Graedel, T. E. and C. J. Weschler (1981). "Chemistry within aqueous atmospheric aerosols and raindrops." Rev. Geophys. and Space Phys. **19**(4): 505-539.

Gray, H. A., G. R. Cass, J. J. Huntzicker, E. K. Heyerdahl and J. A. Rau (1986). "Characteristics of atmospheric organic and elemental carbon particle concentrations in Los Angeles." Environ. Sci. Technol. **20**: 580-589.

Gribble, G. W. (1992). "Natually occurring organohalogen compounds--a survey." J. Nat. Prod. **55**(10): 1353-1395.

Grosjean, D. (1977). Aerosols. Chapter 3. Ozone and Other Photochemical Oxidants. Washington, D.C., National Academy of Sciences.

Grosjean, D. (1978). Secondary Organic Aerosol: Identification and Mechanisms of Formation. Carbonaceous Particles in the Atmosphere, Berkely, CA.

Grosjean, D. and S. K. Friedlander (1979). Formation of organic aerosols from cyclic olefins and diolefins. The Character and Origins of Smog Aerosols. G. Hidy. New York, John Wiley and Sons. **9**: 435-473.

Grosjean, D. and J. H. Seinfeld (1989). "Parameterization of the formation potential of secondary organic aerosols." Atmos. Env. **23**(8): 1733-1747.

Grosjean, D., J. P. Smith, T. M. Mischke and J. N. Pitts, Jr. (1976). Chemical and physical transformations in urban-suburban transport of air pollutants. Atmospheric Pollution. M. M. Benarie. Amsterdam, Elvesier: 549-563.

Guiang, S. F., III, S. V. Krupa and G. C. Pratt (1984). "Measurements of S(IV) and organic anions in Minnesota rain." Atmos. Environ. **18**: 1677-1682.

Hahn, J. (1979). Organic constituents of natural aerosols. Aerosols: Anthropogenic and Natural, Sources and Transport, New York, The New York Academy of Sciences.

Hänel, G. (1987). "The role of aerosol particles during the condensational stage of cloud: A reinvestigation of numerics and physics." Beitr. Phys. Atmosph. **60**: 321-339.

Hansson, H.-C., M. J. Rood, S. Koloutsou-Vakakis, K. Hameri, D. Orsini and A. Wiedensohler (1997). "NaCl aerosol particle hygroscopicity dependence on mixing with organic compounds." Journal Atmospheric Chemistry (submitted).

Hansson, H.-C., A. Wiedensohler, M. J. Rood and D. S. Covert (1990). "Experimental determination of the hygroscopic properties of organically coated aerosol particles." J. Aerosol Sci. **21S**(1): s241-s244.

Harris, J. .

Hatakeyama, S., M. Ohno, J. Weng, H. Takagi and H. Akimoto (1987). "Mechanism for the formation of gaseous and particulate products from ozone-cycloalkene reactions in air." Envir. Sci. Technol. **21**: 52-57.

Hatakeyama, S., T. Tanonaka, J. Weng, H. Bandow, H. Takagi and H. Akimoto (1985). "Ozone-cyclohexene reaction in air: quantitative analysis of particulate products and the reaction mechanism." Envir. Sci. Technol. **19**: 935-942.

Heintzenberg, J. (1989). "Fine particles in the global troposphere. A review." Tellus **41B**: 149-160.

Hidy, G. M., P. K. Mueller, D. Grosjean, B. R. Appel and J. J. Wesolowski, Eds. (1980). The Character and Origins of Smog Aerosols. Advances in Environmental Science and Technology. New York, John Wiley & Sons.

Hildemann, L. M., M. A. Mazurek, G. R. Cass and B. R. T. Simoneit (1994). "Seasonal trends in Los Angeles ambient organic aerosol observed by high-resolution gas chromatography." Aer. Sci. Technol. **20**: 303-317.

Hildemann, L. M., W. F. Rogge, G. R. Cass, M. A. Mazurek and B. R. T. Simoneit (1996). "Contribution of primary aerosol emissions from vegetation-derived sources to fine particle concentrations in Los Angeles." J. Geophys. Res. **101**(D14): 19,541-19,549.

Hinckley, D. A., T. F. Bidleman and C. P. Rice (1991). "Atmospheric organochlorine pollutants and air-sea exchange of hexachlorocyclohexane in the Bering and Chukchi Seas." J. Geophys. Res. **96**(C4): 7201-7213.

Hoffman, E. J. and R. A. Duce (1976). "Factors influencing the organic carbon content of marine aerosols: A laboratory study." J. Geophys. Res. **81**(21): 3667-3670.

Huntzicker, J. J., R. L. Johnson, J. J. Shah and R. A. Cary (1982). Analysis of organic and elemental carbon in ambient aerosols by a thermal-optical method. Particulate Carbon: Atmospheric Life Cycle. G. T. Wolff and R. L. Klimisch. New York, Plenum Press: 79-88.

Husar, R. B. and W. R. Shu (1975). "Thermal analysis of the Los Angeles smog aerosol." J. Appl. Meteorol. **14**: 1558-1565.

IPCC (1995). Climate Change. Cambridge, Cambridge University Press.

Jaenicke, R. (1988). Aerosol physics and chemistry. Landolt-Bornstein, Numerical Data and Functional Relationships in Science and Technology. K. H. Hellwege. Berlin, Springer-Verlag. **4b**.

Janson (1993). "Monoterpene emissions from scots pine and Norwegian spruce." J. Geophys. Res. **98**(D2): 2839-2850.

Janson, R. (1992). "Monoterpene concentrations in and above a forest of scots pine." J. Atmos. Chem. **14**: 385-394.

Jenkins, B. M., A. D. Jones, S. Q. Turn and R. B. Williams (1996). "Particle concentations, gas-particle partitioning, and species intercorrelations for polycyclic aromatic hydrocarbons (PAH) emitted during biomass burning." Atmos. Environ. **30**(22): 3825-2835.

Johansson, C. and R. W. Janson (1993). "Diurnal cycle of O3 and monoterpenes in a coniferous forest: Importance of atmospheric stability, surface exchange, and chemistry." J. Geophys. Res. **98**(D3): 5121-5133.

Junge, C. (1950). "Das Wachstum der Kondensationskerne mit der relativen Feuchtigkeit." Ann. Met. **3**: 129-135.

Junge, C. (1963). Air Chemistry and Radioactivity. New York, Academic Press.

Junge, C. E. (1977). Basic considerations about trace constituents in the atmosphere as related to the fate of global pollutants. Fate of Pollutants in the Air and Water Environments. I. H. Suffet. New York, John Wiley. **Part 1:** 7-25.

Kawamura, K. and I. R. Kaplan (1983). "Organic compounds in the rainwater of Los Angeles." Envir. Sci. Technol. **17**: 497-501.

Kawamura, K., H. Kasukabe, O. Yasui and L. A. Barrie (1995). "Production of dicarboxylic acids in the artic atmosphere at polar sunrise." Geophys. Res. Lett. **22**(10): 1253-1256.

Kawamura, K., S. Steinberg and I. R. Kaplan (1996). "Concentrations of monocarboxylic and dicarboxylic acids and aldehydes in southern California wet precipitations: Comparison of urban and nonurban samples and compositional changes during scavenging." Atmos. Env. **30**(7): 1035-1052.

Keene, W. C. and J. N. Galloway (1984). "Organic acidity in precipitation of North America." Atmos. Env. **18**(11): 2491-2497.

Köhler, H. (1936). "The nucleus in the growth of hygroscopic droplets." Trans. Far. Soc. **32**: 1152-1161.

Kulmala, M., P. Korhonen, T. Vesala, H.-C. Hansson, K. Noone and B. Svenningsson (1996). "The effect of hygroscopicity on cloud droplet formation." Tellus **48B**: 347-360.

Lee, I. Y., G. Hänel and H. R. Pruppacher (1980). "A numerical determination of the evolution of cloud drop spectra due to condensation on natural aerosol particles." J. Atm. Sci. **37**: 1839-1853.

Legrand, M. R., R. J. Delmas and R. J. Charlson (1988). "Climate forcing implications from Vostok ice-core sulphate data." Nature **34**: 418-420.

Ligocki, M. P. and J. F. Pankow (1989). "Measurements of the gas/particle distributions of atmospheric organic compounds." Environ. Sci. Tech. **23**: 75-83.

Likens, G. E., E. S. Edgerton and J. N. Galloway (1983). "The composition and deposition of organic carbon in precipitation." Tellus **35B**: 16-24.

Liousse, C., J. E. Penner, C. Chuang, J. J. Walton, H. Eddleman and H. Cachier (1996). "A global three-dimensional model study of carbonaceous aerosols." J. Geophys Res. **101**(D14): 19,411-19,432.

Lunde, G., J. Gether, N. Gjos and M. B. S. Lande (1977). "Organic micropollutants in precipitation in Norway." Atmos. Env. **11**: 1007-1014.

Marty, J.-C. and A. Saliot (1982). "Aerosols in Equatorial Atlantic Air: n-Alkanes as a Function of Particle Size." Nature **298**(8 July): 144-147.

Matsumoto, G. and T. Hanya (1980). "Organic constituents in atmospheric fallout in the Tokyo area." Atmos. Env. **14**: 1409-1419.

Matthias-Maser, S. and R. Jaenicke (1991). "A method to identify biological aerosol particles with radius > 0.3 um for the determination of their size distribution." J. Aerosol Sci. **22**(Supp 1): S849-S852.

Matthias-Maser, S. and R. Jaenicke (1994). "Examination of atmospheric bioaerosol particles with radii > 0.2um." J. Aerosol Sci. **25**(8): 1605-1613.

Matthias-Maser, S. and R. Jaenicke (1995). "The size distribution of primary biological aerosol particles with radii > 0.2 um in an urban/rural influenced region." Atmos. Resch. **39**: 279-286.

Mayewski, P. A., W. B. Lyons, M. J. Spencer, M. S. Twickler, C. F. Muck and S. Whitlow (1990). "An ice-core record of atmospheric response to anthropogenic sulphate and nitrate." Nature **346**: 554-556.

Mazurek, M. A., G. R. Cass and B. R. T. Simoneit (1991). "Biological input to visibility-reducing aerosol particles in the remote arid southwestern United States." Environ. Sci. Technol. **25**: 684-694.

McDow, S. R. and J. J. Huntzicker (1990). "Vapor adsorption artifact in the sampling of organic aerosol: Face velocity effects." Atmos. Env. **24A**(10): 2563-2571.

McInnes, L. M., P. K. Quinn, D. S. Covert and T. L. Anderson (1996). "Gravimetric analysis, ionic composition, and associated water mass of the marine aerosol." Atmos Environ **30**(6): 869-884.

McMurray, P. H. and D. Grosjean (1985). "Photochemical Formation of Organic Aerosols: Growth Laws and Mechanisms." Atmospheric Environment **19**(9): 1445-1451.

Munger, J. W., J. J. Collett, B. C. J. Daube and M. R. Hoffmann (1989). "Carboxylic acids and carbonyl compounds in southern California clouds and fogs." Tellus **41B**(3): 230-242.

Noone, K. J., E. Öström, R. A. Pockalny, L. de Bock and R. Van Grieken (1996). The size distribution and chemical compposition of cloud droplet residual particles in marine stratocumulus clouds observed during the MAST experiment. Fourteenth International Conference on Nucleation and Atmospheric Aerosols, Helsinki, Finland, Pergamon.

Novakov, T. and C. E. Corrigan (1996). "Cloud condensation nucleus actuivity of the organic component of biomass smoke particles." Geophys. Res. Lett. **23**(16): 2141-2144.

Novakov, T. and J. E. Penner (1993). "Large Contribution of Organic Aerosols to Cloud-Condensation-Nuclei Concentrations." Nature **365**: 823-826.

O'Brien, R. J., J. R. Holmes and A. H. Bockian (1975). "Formation of photochemical aerosol from hydrocarbons--Chemical reactivity and products." Environ. Sci. Technol. **9**(6): 568-576.

Odum, J. R., T. Hoffmann, F. Bowman, D. Collins, R. C. Flagan and J. G. Seinfeld (1996). "Gas/particle partitioning and secondary organic aerosol yields." Environ. Sci. Technol. **30**: 2580-2585.

Pandis, S. N., R. A. Harley, G. R. Cass and J. H. Seinfeld (1992). "Secondary organic aerosol formation and transport." Atmos. Environ. **26A**(13): 2269-2282.

Pankow, J. F. (1987). "Review and comparative analysis of the theories on partitioning between the gas and aerosol particulate phases in the atmosphere." Atmos. Environ. **21**(11): 2275-2283.

Pankow, J. F. (1993). "A Simple Box Model for the Annual Cycle of Partitioning of Semi-Volatile Organic Compounds Between the Atmosphere and the Earth's Surface." Atmospheric Environment **27A**(7): 1139-1152.

Pankow, J. F. (1994). "An Absorption Model of Gas/Particle Partitioning of Organic Compounds in the Atmosphere." Atmospheric Environment **28**(2): 185-188.

Pankow, J. F. (1994). "An Absorption Model of the Gas/Aerosol Partitioning Involved in the Formation of Secondary Organic Aerosol." Atmospheric Environment **28**(2): 189-193.

Patton, G. W., M. D. Walla, T. F. Bidleman and L. A. Barrie (1991). "Polycyclic aromatic and organochlorine compounds in the atmosphere of Northern Ellesmere Island, Canada." J. Geophys. Res. **96**(D6): 10,867-10,877.

Payne, K. (1982). "Chemistry and Toxicology of PCDDs." Chem. Ind. **9**: 298-300.

Pehkonen, S. O., R. L. Siefert, Y. Erel, S. Webb and M. R. Hoffmann (1993). "Photoreduction of iron oxyhydroxides in the presence of important atmospheric organic compounds." Environ. Sci. Technol. **27**: 2056-2062.

Penner, J. E., C. C. Chuang and C. Liousse (1996). The contribution of carbonaceous aerosols to climate change. The Fourteenth International Conference of Nucleation and Atmospheric Aerosols, Helsinki, Finland, Pergamon.

Penner, J. E., R. E. Dickenson and C. A. O'Neill (1992). "Effects of aerosol from biomass burning on the global radiation budget." Science **256**: 1432-1434.

Prager, M. J., E. R. Stephens and W. E. Scott (1960). "Aerosol formation from gaseous air pollutants." Ind. Eng. Chem. **52**: 521-524.

Prentice, I. C., M. T. Sykes, M. Lautenschlager, S. P. Harrison, O. Denissenko and P. J. Bartlein (1993). "Modelling global vegetation patterns and terrestrial carbon storage at the last glacial maximum." Global Ecol. Biogeogr. Lett. 3: 67-76.

Pruppacher, H. R. and J. D. Klett (1978). Microphysics of Clouds and Precipitation. Dordrecht, D. Reidel.

Quay, P. D., S. L. King, J. Stutsman, D. O. Wilbur, L. P. Steele, I. Fung, R. H. Gammon, T. A. Brown, G. W. Farwell, P. M. Grootes and F. H. Schmidt (1991). "Carbon isotopic composition of atmospheric CH4: Fossil and biomass burning source strengths." Global Biogeochem.Cycles 5(1): 25-47.

Rivera-Carpio, C. A., C. E. Corrigan, T. Novakov, J. E. Penner, C. F. Rogers and J. C. Chow (1996). "Derivation of contributions of sulfate and carbonaceous aerosols to cloud condensation nuclei from mass size distributions." J. Geophys. Res. **101**(D14): 19,483-19,493.

Rogge, W. F., L. M. Hildemann, M. A. Mazurek, G. R. Cass and B. R. T. Simoneit (1993). "Sources of fine organic aerosol. 2. Noncatalyst and catalyst-equipped automobiles and heavy-duty diesel trucks." Environ. Sci. Technol. **27**(4): 636-651.

Rogge, W. F., M. A. Mazurek, L. M. Hildemann, G. R. Cass and B. R. T. Simoneit (1993). "Quantification of urban organic aerosols at a molecular level: Indentification , abundance and seasonal variation." Atmos. Env. **27A**(8): 1308-1330.

Rosen, H., A. D. A. Hansen, L. Gundel and T. Novakov (1978). "Identification of the opticaly absorbing component in urban aerosols." Appl. Optics **17**(24): 3859-3851.

Rubel, G. O. and J. W. Gentry (1985). "Measurement of water and ammonia accommodation coefficients at surfaces with adsorbed monolayers of hexadecanol." J. Aerosol Sci. **16**(6): 571-574.

Sackett, W. M. (1964). "The depositional history and isotopic organic carbon compostion of marine sediments." Mar. Geol. **2**: 173-185.

Satsumabayashi, H. and H. Kurita (1990). "Photochemical formation of particulate dicarboxylic acids under long-range transport in central Japan." Atmos. Env. **24A**(6): 1443-1450.

Satsumabayashi, H., H. Kurita, Y. Yokouchi and H. Ueda (1989). "Mono- and di-carboxylic acids under long-range transport of air polution in central Japan." Tellus **41B**(3): 219-229.

Saxena, P. and L. M. Hildemann (1996). "Water-organics in atmospheric particles: A critical review of the literature and application of thermodynamics to identify candidate compounds." J. Atmos. Chem. **24**: 57-109.

Saxena, P., L. M. Hildemann, P. H. McMurry and J. H. Seinfeld (1995). "Organics alter hygroscopic behavior of atmospheric particles." J. Geophys. Res. **100**(D9): 18,755-18,770.

Schneider, J. K. and R. B. Gagosian (1985). "Particle Size Distribution of Lipids in Aerosols off the Coast of Peru." J. Geophys. Res. **90**(D5): 7889-7898.

Schneider, J. K., R. B. Gagosian, J. K. Cochran and T. W. Trull (1983). "Particle size distributions of n-alkanes and 210-Pb in aeorols off the coast of Peru." Nature **304**: 429-432.

Schuetzle, D. and R. A. Rasmussen (1978). "The molecular composition of secondary aerosol particles formed from terpenes." J. Air Pollut. Cont. Assoc. **28**: 236-240.

Schwartz, S. E. and A. Slingo (1996). Enhanced shortwave cloud radiative forcing due to anthropogenic aerosols. Clouds, Chemistry and Climate. P. Crutzen and V. Ramanathan. Berlin-Heidelberg, Springer-Verlag. **135**.

Sempere, R. and K. Kawamura (1996). "Low molecular weight dicarboxylic acids and related polar compounds in the remote marine rain samples collected from the western Pacific." Atmos. Env. **30**(10/11): 1609-1619.

Shah, J. J. and J. A. Rau (1991). "Carbonaceous species methods comparison study: Interlaboratory round robin interpretation of results." .

Shulman, M. L., M. C. Jacobson, R. J. Charlson, R. E. Synovec and T. E. Young (1996). "Dissolution behavior and surface tension effects of organic compounds in nucleating cloud droplets." Geophys. Res. Lett. **23**(3): 277-280.

Sicre, M.-A., J.-C. Marty and A. Saliot (1990). "n-Alkanes, fatty acid esters, and fatty acid salts in size fractionated aerosols collected over the Mediterranean sea." J. Geophys. Res. **95**(D4): 3649-3657.

Simoneit, B. R. T., R. Chester and G. Eglinton (1977). "Biogenic Lipids in Particulates from the Lower Atmosphere over the Eastern Atlantic." Nature **267**: 682-685.

Simpson, D., A. Guenther, C. N. Hewitt and R. Steinbrecher (1995). "Biogenic emissions in Eruope 1. Estimates and uncertainties." J. Geophys. Res. **100**(D11): 22,875-22,890.

Spencer, W. F., W. J. Farmer and W. A. Jury (1982). "Review: Behavior of organic chemicals at soil, air, water interfaces as related to predicting the transport and volatilization of organic pollutants." Envir. Toxicol. Chem **1**: 17-26.

Stanley, J., R. Ayling, P. Cramer, K. Thornburg, J. Remmus, J. Breen, J. Schwemberger, H. Keng and K. Watanabe (1990). "PCDD and PCDF levels in human adipose tissue in the continental US collected between 1971 and 1987." Chemosphere **20**(7-9): 895-903.

Storey, J. M. E., W. Luo, L. M. Isabelle and J. F. Pankow (1995). "Gas/solid partitioning of semivolatile organic compounds to model atmospheric solid surfaces as a function of relative humidity. 1. Clean quartz." Environ. Sci. Technol. **29**: 2420-2428.

Sugimoto, A. (1996). "GC/GC/C/IRMS system for carbon isotope measurement of low level methane concentration." Geochemical Journal **30**(3): 195-200.

Svenningsson, B., H.-C. Hansson, A. Wiedensohler, K. J. Noone, J. Ogren, A. Hallberg and R. Colvile (1994). "Hygroscopic growth of aerosol particles and its influence on nucleation scavenging in cloud: Experimental results from Kleiner Feldberg." J. Atmos. Chem. **19**: 129-152.

Tanabe, S., H. Tanaka and R. Tatsukawa (1984). "Bioaccumulation of PCBs, DDT and HCH isomers in the North Pacific ecosystem." Arch. Environ. Contam. Toxicol. **13**: 731-738.

Tanabe, S. and R. Tatsukawa (1986). . PCBs and the Environment. J. S. Waid. Florida, CRC Press. **1**: 143-161.

Thibodeaux, L. J., K. C. Nadler, K. T. Valsaraj and D. D. Reible (1991). "The effect of moisture on volatile organic chemical gas-to-particle partitioning with atmospheric aerosols--competitive adsorption theory predictions." Atmos. Environ. **25A**(8): 1649-1656.

Turpin, B. J. and J. J. Huntzicker (1991). "Secondary formation of organic aerosol in the Los Angeles Basin: A descriptive analysis of organic and elemental carbon concentrations." Atmos. Environ. **25A**: 207-215.

Twomey, S. (1977). Atmospheric Aerosols. Amsterdam, Elsevier.

USEPA (1996). Criteria Document on Fine Particles.

Vong, R. J., B. M. Baker, F. J. Brechtel, R. T. Collier, J. M. Harris, A. S. Kowalski, N. C. McDonald and L. M. McInnes (1997). "Ionic and trace element composition of cloud water collected on the Olympic Peninsula of Washington State." Atmos. Env. **31**(13): 1991-2001.

Weathers, K. C., G. E. Likens, F. H. Bormann, S. H. Becknell, B. T. Bormann, B. C. J. Daube, J. S. Eaton, J. N. Galloway, W. C. Keene, K. D. Kimball, W. H. McDowell, T. G. Siccama, D. Smiley and R. A. Tarrant (1988). "Cloudwater chemistry from ten sites in North America." Environ. Sci. Technol. **22**(9): 1018-1026.

Went, F. W. (1960). "Blue hazes in the atmosphere." Nature **187**: 641-643.

White (1990). Section 4 of Visibility: Existing and Historical Conditions--Causes and Effects, J.C. Trijonis, ed. Acid Deposition: State of Science and Technology. P. M. Irving. Washington, D.C., U.S. National Acid Precipitation Assessment Program. **24:** 85-102.

Woodcock, A. H. (1953). "Salt nuclei in marine air as a function of altitude and wind force." J. Meteorol. **10**: 362-271.

Yamasaki, H., K. Kuwata and H. Miyamoto (1982). "Effects of ambient temperature on aspects of airborne polycyclic aromatic hydrocarbons." Environ. Sci. Technol. **16**(4): 189-194.

Young, J. F. (1967). "Humidity control in the laboratory using salt-solutions--A review." J. Appl. Chem. **17**: 241-245.

Zhang, S.-H., M. Shaw, J. H. Seinfeld and R. C. Flagan (1992). "Photochemical aerosol formation from alpha-pinene and beta-pinene." J. Geophys. Res. **97**(D18): 20,717-20,729.

Zhang, X. Q., P. H. McMurry, S. V. Hering and G. S. Casuccio (1993). "Mixing characteristics and water content of submicron aerosols measured in Los Angeles and at the Grand Canyon." Atmos. Environ. **27A**(10): 1593-1607.

Zimmerman, P. R. and R. B. Chatfield (1978). "Estimates of the production of CO and H2 from the oxidation of hydrocarbon emissions from vegetation." Geophys. Res. Lett. **5**: 679-682.

APPENDIX A: DISSOLUTION BEHAVIOR AND SURFACE TENSION EFFECTS OF ORGANIC COMPOUNDS IN NUCLEATING CLOUD DROPLETS

MICHELLE L. SHULMAN, MICHAEL C. JACOBSON, ROBERT J. CHARLSON, ROBERT E. SYNOVEC, AND TOBY E. YOUNG. GEOPHYSICAL RESEARCH LETTERS, VOL. 23 NO. 3, PAGES 277-280, 1996.

Dissolution behavior and surface tension effects of organic compounds in nucleating cloud droplets

Michelle L. Shulman, Michael C. Jacobson, Robert J. Carlson, Robert E. Synovec, and Toby E. Young

Departments of Chemistry and Atmospheric Sciences, University of Washington Seattle

Abstract. Solubilities and surface tensions were measured for difunctional organic acids in various concentrations of $(NH_4)_2SO_4$ and NH_4HSO_4 aqueous solutions. Model results using these data indicate that the organic compounds affect cloud droplet growth by two mechanisms: by gradual dissolution in the growing droplet which affects the shape of the Köhler growth curve, and by lowering of surface tension which decreases the critical supersaturation.

Introduction

Aerosol particles in the atmosphere serve as *cloud condensation nuclei* (CCN) on which water vapor condenses to form cloud droplets [Köhler, 1936]. The size, water solubility, and surface activity of the aerosol particles dictate their ability to act as CCN. Ubiquitous sulfate compounds (e.g. $(NH_4)_2SO_4$) are thought to be the dominant chemical species in CCN [Pruppacher and Klett, 1980] and dissolve readily in water, forming a highly concentrated (typically several molar) saturated aqueous salt solution at deliquescence [Tang *et al.*, 1978].

Cloud condensation nuclei may be chemically mixed [Saxena *et al.*, 1995; Novakov and Penner, 1993; Pruppacher and Klett, 1980; Hänel, 1976], containing surface active organic compounds of variable, often slight solubility in aqueous solutions [Cronn, 1975]. Difunctional acids comprise one class of such organic compounds measured in atmospheric aerosol [Schuetzle *et al.*, 1975; Cronn, 1975; Kawamura *et al.*, 1985; Rogge *et al.*, 1991]. Once droplet growth has been initiated by the deliquescence of the inorganic salt, the physical state of any slightly soluble compound (SSC, e.g. difunctional acid) present is a function of its solubility in the aqueous salt solution, its quantity in the CCN, and the droplet volume. The total amount of dissolved material in the solution droplet and the corresponding surface tension affect the equilibrium vapor pressure of water over the droplet, which determines whether and how rapidly growth occurs. Thus, it is necessary to acquire solubility and surface tension data for compounds that do not readily dissolve.

Modified Köhler Equation

The equilibrium vapor pressure (e') of water over a solution droplet of a given radius (r) relative to the water vapor pressure over a plane surface of water (e_s) is described by a modified form of the Köhler equation:

$$\frac{e'}{e_s} \equiv 1 + \underbrace{\frac{2\sigma M_w}{kT\rho r}}_{\text{Kelvin Effect}} - \underbrace{\frac{3M_w\Phi}{4\pi\rho r^3}\left(\frac{\nu_{ssc}X_{ssc}m_{ssc}}{M_{ssc}} + \frac{\nu_{sulf}m_{sulf}}{M_{sulf}}\right)}_{\text{Raoult Effect}} \quad (1)$$

where σ is the solution surface tension, M_w is the molecular weight of water, k is the Bolzmann constant, T is the temperature, ρ is the solution density, Φ is the osmotic coefficient of the aqueous solution, ν_{dissc} is the number of ions into which a SSC dissociates when dissolved, ν_{sulf} is the number of ions into which sulfate dissociates when dissolved, m_{ssc} is the total mass of SSC, m_{sulf} is the mass of sulfate salt, M_{SSC} is the molecular weight of the SSC, and M_{sulf} is the molecular weight of the sulfate salt. The quantity e'/e_s is governed by both the 'Kelvin Effect' and 'Raoult Effect'. The 'Kelvin Effect' accounts for the enhanced vapor pressure due to droplet curvature, which is affected by droplet surface tension. The 'Raoult Effect' accounts for the reduced vapor pressure due to dissolved material. In using this equation, we make the assumption that only the dissolved fraction of SSC and any additional dissolved material can depress vapor pressure, which is lowered by an amount proportional to the mole fraction of solute dissolved regardless of chemical form so that the effects of sulfate and SSC are simply additive. This assumption may or may not be realistic; however, lacking any data to the contrary (e.g. physical influences of the undissolved second phase) the assumption is necessary in order to assess the respective roles of solubility and surface tension.

The form of Eq. 1 takes into account the possibility that not all of the SSC is dissolved in the droplet at any given radius. The quantity X_{dssc}, is a function of SSC solubility and sulfate concentration, both of which change with droplet radius. If $X_{dssc} = 0$, the Köhler curve takes the standard form and has a single maximum in e'/e_s at some critical radius, r_c and supersaturation (e'/e_s-1) of S_c. However, if X_{dssc} monotonically increases up to a value of unity as the droplet grows, the modified Köhler curves can have two maxima separated by a cusp, as will be illustrated with actual data in the following sections.

Solubility Measurements

Seven difunctional organic oxygenates were chosen as model compounds because of their significant concentrations in the atmosphere, and their range of water solubilities [Seidell, 1941] and surface activities. Five dicarboxylic acids (C_2-C_6), phthalic acid, and cis-pinonic acid were selected. Cis-pinonic acid is an oxidation product of α-pinene, which is emitted from coniferous trees [Schuetzle and Rasmussen, 1978], whereas the other model organic compounds (OC's) are derived from olefins found in fossil fuels [Grosjean *et al.*, 1978].

Paper number 95GL03810
0094-8534/96/95GL-03810$03.00

Solubilities were measured at 0 °C in H_2O and in concentrated aqueous solutions of $(NH_4)_2SO_4$ and NH_4HSO_4 (0.01, 0.1, 1.0, and 3.0 molar) which represent a range of concentrations in the early stages of cloud droplet growth [Ogren and Charlson, 1992]. An excess of pure compound was dissolved in aqueous solution at elevated temperature (~50 °C) and slowly cooled to 0 °C. The resulting precipitate was removed from the saturated solution, and the concentration of the organic solute determined using UV-VIS spectrophotometry. The solubility values are listed in Table 1, and have an uncertainty of approximately ±5%. The results in pure water are comparable to measurements obtained by other investigators [Seidell, 1941].

The general solubility trend observed was malonic > glutaric > succinic > oxalic > adipic > phthalic > cis-pinonic. In most cases, increases in sulfate or bisulfate concentration lead to a decrease in organic solubility, likely due to a 'salting out' effect generally exhibited by solutes in solutions of high ionic strength [Gill *et al.*, 1983]. Model calculations are derived from solubility data of single OC's in solutions of $(NH_4)_2SO_4$ alone. However, it is likely that OC's in the atmosphere would be present as mixtures within CCN and influence each others solubility in growing droplets, due to the similarity of molecular structures.

Model Calculations

We first consider the dissolution behavior of each model compound in a growing, diluting solution drop formed on a CCN consisting of a solute mixture of a single OC and $(NH_4)_2SO_4$ [Fig. 1]. Measured solubilities were expressed as n^{th} order polynomial fits (n=1-3) of sulfate solution concentrations. These functions were used to approximate the concentration of the OC in growing and diluting aqueous droplets, without considering the possible influence of particle size on solubility. Droplets are assumed to be spherical. The mass weighted average density is assumed for dry particles, with linear change in density as water is added to the droplet. The presence of SSC is assumed to have no effect on the deliquescence of the $(NH_4)_2SO_4$.

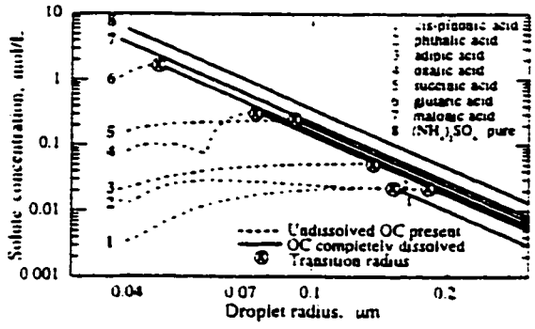

Figure 1. Concentration of OC's in a droplet as a function of radius. The dry particle radius is 0.03 μm, with mass 50% OC and 50% $(NH_4)_2SO_4$ for each of the seven aqueous systems containing an OC. The dry particle radius is 0.03 μm for the curve corresponding to pure sulfate. The size range in the plot is limited to 0.04 μm to just above 0.2 μm to focus on r_T.

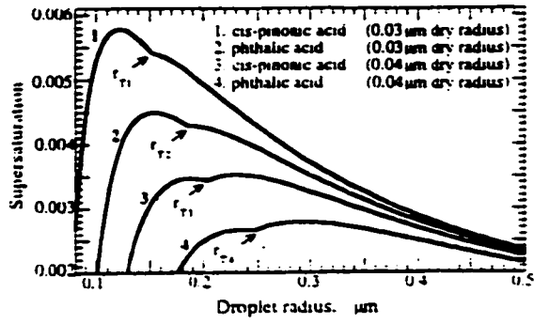

Figure 2. The example calculations are for a dry particle mass of 50% OC and 50% $(NH_4)_2SO_4$. Droplet σ, ambient *T*, Φ, ν_{dissoc}, and ν_{sulf} are assumed to be constant at 76 dynes/cm, 273 K, unity, 2, and 3, respectively. Choosing a constant value for Φ implies solution ideality, which has been shown to introduce only small error in the overall calculation [Young and Warren, 1992]. The size range in the plot is limited in order to focus on the region of droplet activation and the cusp in the curves.

The OC is present in both a saturated solution and an undissolved state (two phases) until the droplet has sufficient aqueous volume to completely dissolve the OC. We refer to the droplet radius at which the OC is completely dissolved as the 'transition radius' (r_T). While the OC is not completely dissolved, two competing effects determine its concentration in the droplet. Droplet growth decreases the concentration by simple dilution, as exhibited by the pure sulfate and malonic acid curves in Fig. 1. However, as the particle grows, the decreasing salt concentration increases the solubility of oxalic, succinic, glutaric, adipic, phthalic, and cis-pinonic acids. For $r > r_T$ the OC concentration drops exponentially. The transition radius increases with decreasing organic solubility for oxalic through phthalic acids. The solubility data were used to calculate e'/e_s for droplets containing a single OC and $(NH_4)_2SO_4$, initially assuming a constant surface tension.

Figure 2 for $m_{SSC} > 0$ indicates that OC's can significantly alter the shape of the Köhler curve and are examples illustrating that there can be *two* radii at which maxima appear in the

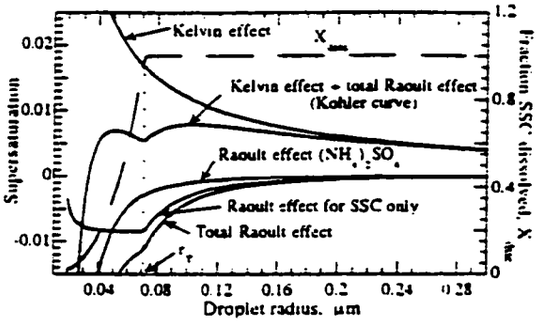

Figure 3. Breakdown of the modified Köhler curve. The conditions for this calculation are: dry radius of 0.05 μm, 80% succinic acid by mass, 20% $(NH_4)_2SO_4$. The values for *T*, Φ, ν_{dissoc}, and ν_{sulf} are the same as those used to generate the curves in Fig. 2.

Köhler curve, separated by a cusp or minimum at the droplet radius $r = r_T$. This result has not been reported previously, and implies that a droplet might partially activate if the second maximum is at a higher supersaturation than the first. Formation of two maxima depends on the solubility (i.e. molecular form) and mass fraction of OC. In most cases, the alteration is most pronounced for the least soluble OC's studied when they are present as a large fraction of CCN mass.

Figure 3 shows the individual terms in the modified Köhler equation and indicates that the cusp caused by SSC's in the curve arises from termination of the dissolution process in the droplet, discontinuously affecting the Raoult term in Eq. 1. This example was chosen to clearly show the consequence of a phase change on the shape of the Köhler curve. At r_T, the SSC completely dissolves and X_{dssc} is 1.0. At sizes up to r_T, the SSC's contribution to the Raoult term increases as the droplet grows, resulting in a depression in e'/e_s relative to that due to the sulfate fraction alone. At the location of r_T, which is compound and mass dependent, the effect of the SSC is maximal, causing the cusp. While all of these model SSC's were organic, some inorganic atmospheric aerosol species would qualitatively yield the same result, e.g. $CaSO_4$ or $CaCO_3$.

Surface Tension Consideration

Surface tensions were measured for the seven OC's in H_2O and in concentrated aqueous solutions of $(NH_4)_2SO_4$ using a droplet volume method [Lima and Synovec, 1995] at room temperature. Droplets emerging from a vertical stainless steel capillary are sized using a laser beam when they detatch from the tip due to gravity. Droplets grow to a size that is proportional to the surface tension of the solution at the capillary tip. An aliquot of 20-100 µl of each OC solution was injected as an undiluted plug into a pure water flow leading to the capillary, causing a measured decrease in droplet radius measured at the tip. Highly concentrated solutions require correction because their densities may be higher than pure water, causing the droplets to detach at a smaller size, which yields a lower apparent surface tension. The limit-of-detection in relative surface tension is $\Delta\sigma/\sigma = 0.0015$. A similiar method has been used by Capel *et al.* [1991] to measure surface tension of fog samples.

Figure 4 shows two trends in surface tension between aqueous solutions of OC's relative to pure water ($-\Delta\sigma/\sigma$): (1) a decrease in surface tension with increasing OC concentration,

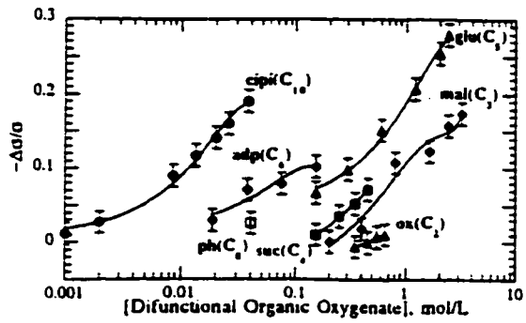

Figure 4. Surface tension data for OC's in H_2O.

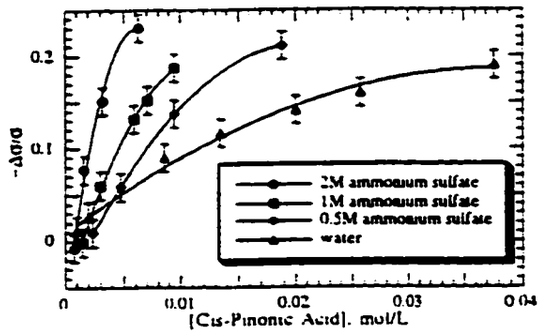

Figure 5. Surface tension data for cis-pinonic acid in H_2O, and three $(NH_4)_2SO_4$ aqueous solutions.

and (2) a decrease in surface tension with increasing carbon number. Phthalic acid and oxalic acid had no apparent effect on the surface tension of pure water. For all of the OC's studied except cis-pinonic acid, increases in $(NH_4)_2SO_4$ concentration had little or no effect on the surface tension of the organic solutions, but for cis-pinonic acid, surface tension change is dependent on both the $(NH_4)_2SO_4$ concentration and the OC concentration, as illustrated in Fig. 5. Addition of $(NH_4)_2SO_4$ to the solution appears to drive the cis-pinonic acid molecules (the least soluble model OC) to the solution surface, thus decreasing droplet surface tension. A bivariate interpolation was generated from the empirical data which allows surface tension to be estimated for any [cis-pinonic]/[$(NH_4)_2SO_4$] mixture.

Surface tension measurements were incorporated into Eq. 1, along with dissolution behavior [Fig. 6]. The radius at which the cusp appears in the Köhler curve does not change due to the surface tension correction, but there is a decrease in the critical supersaturation and an increase in the critical radius.

Conclusion

The calculations presented here indicate that any surface active SSC affects cloud droplet growth by two mechanisms: (1) by gradual dissolution in the growing droplet which affects the

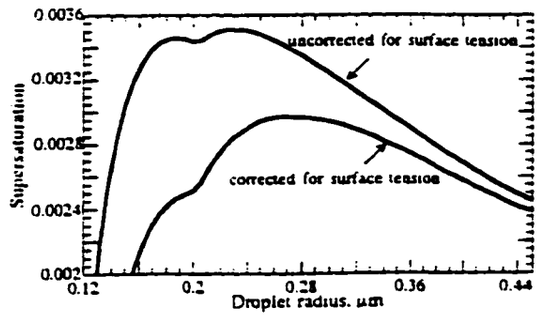

Figure 6. Köhler curves for droplets formed from CCN with 0.04 µm dry radius consisting of 50% dry mass $(NH_4)_2SO_4$ and 50% cis-pinonic acid. The values for T, Φ, v_{dssc}, and v_{sulf} are the same as those used to generate the curves in Fig. 2.

shape of the Köhler curve, and (2) lowering of surface tension which decreases the critical supersaturation. Reduction in the critical supersaturation could *hasten* droplet activation and allow a greater number of CCN [Bullrich and Hänel, 1978; Hänel, 1981]. Slightly soluble compounds would *delay* activation due to the presence of the cusp. Although our study examined systems composed of a single OC and a sulfate salt, a more realistic atmospheric case presumably would have many SSC's existing together in chemically mixed particles. We predict this would yield a series of transition radii and cusps in the growth curve. As a result, there likely would be no steep negative slope allowing rapid growth after activation. Instead, there would be an overall flattening of the curve and a likely metastable size range around the multiple r_c values. The resulting delay in cloud droplet growth expected from multiple cusp formation is consistent with observations in thermal gradient CCN counting chambers when sampling ambient atmospheric particles. This effect was originally attributed to the formation of an insoluble organic coating which impeded the entry of water to the soluble portion of the aerosol [Bigg, 1986]. While coatings may play such a role, our data and calculations suggest a simple chemical explanation for delayed growth without a surface coating: any slightly soluble chemical substance which exists in an ephemeral undissolved phase at a critical stage of droplet growth would be sufficient to alter the growth process.

Acknowledgements. We owe thanks to E. James Davis, David S. Covert, Marcia B. Baker, John H. Seinfeld, and Theodore L. Anderson for critique of the manuscript. Research was supported in part by National Science Foundation grant numbers ATM-9320871 and ATM-9321496, NOAA cooperative agreement number NA37RJ01981 with JISAO contribution number 317.

References

Bigg, E.K., Discrepancy between observation and prediction of concentrations of cloud condensation nuclei, *Atm. Res.*, 20, 82-86, 1986.

Bullrich, K. and G. Hanel, Effects of organic aerosol constituents on extinction and absorption coefficients and liquid water contents of fogs and clouds, *Pure Appl. Geophys.*, 116, 293-301, 1978.

Capel, P.D., C. Leuenberger, and W. Giger, Hydrophobic organic chemicals in urban fog, *Atm. Environ.*, 25A, 1335-1346, 1991.

Cronn, D.R., Analysis of atmospheric aerosols by high resolution mass spectrometry, Ph.D. thesis, 158 pp., University of Washington, Seattle, 1975.

Gill, P.S., T.E. Graedel, and C.J. Weschler, Organic films on atmospheric aerosol particles, fog droplets, cloud droplets, raindrops, and snowflakes, *Rev. Geophys. Space Phys.*, 21, 903-920, 1983.

Grosjean, D., K. Van Cauwenberghe, J.P. Schmid, P.E. Kelley, and J.N. Pitts Jr., Identification of C_3-C_{10} aliphatic dicarboxylic acids in airborne particulate matter, *Environ. Sci. Technol.*, 12, 313-317, 1978.

Hanel, G., The properties of atmospheric aerosol particles as functions of the relative humidity at thermodynamic equilibrium with the surrounding moist air, *Adv. Geophys.*, 19, 73-188, 1976.

Hanel, G., Influences of physical and chemical properties of atmospheric particles on the activation process in fog and clouds, *Contrib. Atm. Phys.*, 54, 159-172, 1981.

Kawamura, K., S. Steinberg, and I.R. Kaplan, Capillary GC determination of short-chain dicarboxylic acids in rain, fog, and mist, *Intern. J. Environ. Anal. Chem.*, 19, 175-188, 1985.

Kohler, H., The nucleus in the growth of hygroscopic droplets, *Trans. Far. Soc.*, 32, 1152-1161, 1936.

Lima, L.R. and R.E. Synovec, Laser-based dynamic surface tension detection for liquid chromatography by probing a repeating drop radius, *J. Chromatogr. A*, 691, 195-204, 1995.

Novakov, T. and J.E. Penner, Large contribution of organic aerosols to cloud-condensation nuclei concentrations, *Nature*, 365, 823-826, 1993.

Ogren, J.A. and R.J. Charlson, Implications for models and measurements of chemical inhomogeneities among cloud droplets, *Tellus*, 44B, 208-225, 1992.

Pruppacher, H.R. and J.D. Klett, *Microphysics of clouds and precipitation*, D. Reidel Publishing Co., Dordrecht, 1980.

Rogge, W.F., M.A. Mazurek, L.M. Hildemann, and G.R. Cass, Quantification of urban organic aerosols at a molecular level: identification, abundance and seasonal variation, *Atm. Environ.*, 27A, 1309-1330, 1991.

Saxena, P., L.M. Hildemann, P.H. McMurry, and J.H. Seinfeld, Organic alter hygroscopic behavior of atmospheric particles, *J. Geophys. Res.*, 100, D9, 18755-18770, 1995.

Schuetzle, D., D.R. Cronn, and A.L. Crittenden, Molecular composition of secondary aerosol and its possible origin, *Environ. Sci. Technol.*, 9, 838-844, 1975.

Schuetzle, D. and R.A. Rasmussen, The molecular composition of secondary aerosol particles formed from terpenes, *J. Air Pollut. Cont. Assoc.*, 28, 236-240, 1978.

Seidell, A., *Solubilities of organic compounds*, 3rd Ed., D. Van Nostrand Co., New York, 1941.

Tang, I.N., H.R. Munkelwitz, and J.G. Davis, Aerosol growth studies-IV. phase transformation of mixed salt aerosols in a moist atmosphere, *J. Aerosol Sci.*, 9, 505-511, 1978.

Young, K.C. and A.J. Warrent, A reexamination of the derivation of the equilibrium supersaturation curve for soluble particles, *J. Atmos. Sci.*, 49, 1138-1143, 1992.

R.J. Charlson, M.C. Jacobson, M.L. Shulman, R.E. Synovec, and T.E. Young, University of Washington, Department of Chemistry, Box 351700, Seattle, WA 98195 (email: jacobsen@u.washington.edu, mishy@u.washington.edu, synovec@chem.washington.edu, tom-cero@u.washington.edu)

(Received: July 11, 1995; revised: November 8, 1995; accepted: December 6, 1995)

APPENDIX B: ISOTOPIC MEASUREMENTS OF CARBON AT CHEEKA PEAK

BACKGROUND

The information in this appendix is late-breaking data on the carbon isotope signatures (^{13}C and ^{14}C) of material collected on quartz filters at Cheeka Peak during the end of the sampling period described in Chapter 5. The aim in performing these isotopic measurements was to determine the likely sources of carbon found at the site. This approach has been used before for carbonaceous aerosol, although ^{13}C has not, to my knowledge, been measured previously with ^{14}C on the same organic samples.

Measurements of the two isotopes provide different types of information. It has long been known that ^{13}C, a stable isotope, is more abundant in marine organic matter than in continental organic matter [1]. It was later shown that the ratio ($^{13}C/^{12}C$) could be used to quantitatively estimate the relative contributions of marine and continental sources in carbonaceous aerosols collected in the marine troposphere [2]. ^{14}C (radiocarbon), which is radioactive, can be used to date a sample of carbon. Since petroleum has a geologic age much greater than the half life (5730 yr) of this isotope, emissions from fossil fuel combustion essentially contain no ^{14}C. However, modern sources of carbon contain a proportion of ($^{14}C/^{12}C$) that is close to the proportion of these isotopes currently in the atmosphere. Measurement of the ($^{14}C/^{12}C$) ratio in atmospheric carbonaceous matter therefore allows inference of the relative amounts of fossil and non-fossil carbon sources.

SAMPLING

Samples were collected on 150 mm quartz fiber filters (Pallflex QAT-UP), that were precleaned by heating to 900°C for 3 hours in a muffle furnace, and allowed to cool overnight before removal. Filters were wrapped in aluminum foil that had also been heated to remove organic material (550 °C for 3 hours). Wrapped filters were placed

together, double-bagged in ziplock bags, and frozen prior to sampling. Sampling took place simultaneously with the samples described in Chapter 5, utilizing the same wind direction, wind speed, particle concentration, and precipitation criteria to obtain marine aerosol. There were no teflon front filters for this project, and only one sample was collected at a time. Filters were placed in a cylindrical filter holder (polypropylene), downstream of 12 cyclone separators (polycarbonate), each with a size cut of 1.0 μm aerodynamic particle diameter when operated at 50 L min^{-1}. The total flow rate through the filter was therefore 600 L min^{-1}. The exposed filter diameter was 130 mm, translating to a face velocity of 75.4 cm s^{-1}. This is approximately the same face velocity as the samples described in Chapter 5, so it should be possible to estimate the amount of adsorbed carbon using those samples. Sampling durations ranged from one to three weeks in order to collect enough material to analyze. The long sampling time precludes analysis for all practical purposes with air mass trajectories. Samples were rewrapped in their original Al foil packaging and refrozen until ready for analysis.

ANALYSIS

Analysis of the quartz filters took place entirely in ampules made of 13mm o.d. Vycor ™ tubing. The ampules were first cleaned by firing at 525 °C for 2-3 hours. Filters were removed from refrigeration, then immediately and expediently rolled and inserted into the ampules. There was no removal process for carbonate from the filters because we assume that the 1 μm cutoff particle diameter elimates this material from the samples. 300 mg of CuO (Baker Chemicals) was also added as an oxidizing agent. Ampules were evacuated using an oil diffusion pump for 2 hours to a final pressure of <1millitorr, before sealing and baking at 900°C for 1 hour in a muffle furnace and cooled slowly overnight while still in the closed furnace. The ampules were cracked open in an evacuated flexible stainless steel and glass chamber (Figure B-1). The glass finger of the chamber was immersed in liquid N_2 to freeze the evolved CO_2 whereupon the trace noncondensable gases were pumped away using the diffusion pump. A dry ice-isopropanol slurry was then applied which allowed removal of the CO_2 into a calibrated

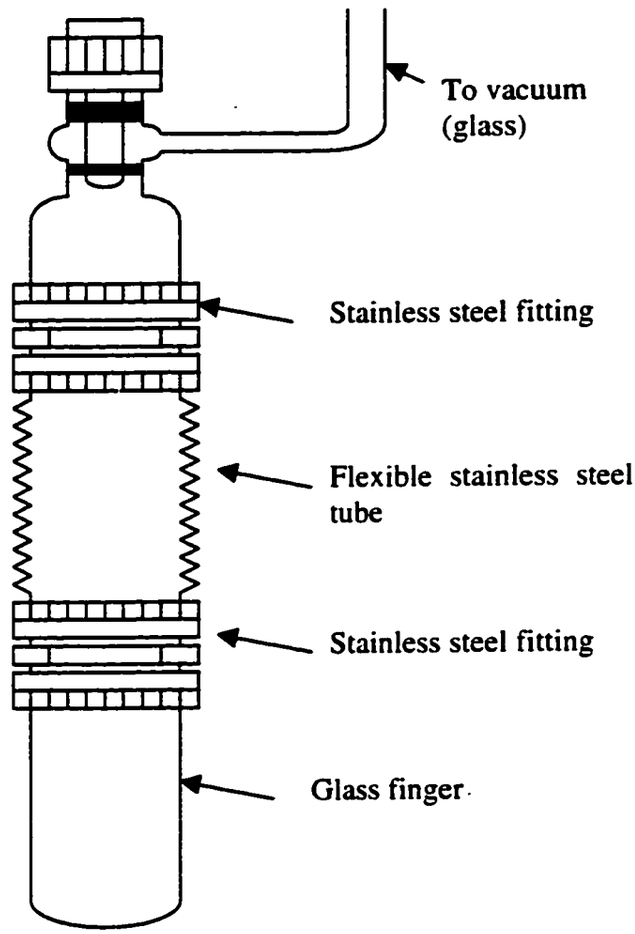

Figure B-1 Flexible cracking device for collection of evolved CO_2.

volume while water evolved during combustion remained frozen in the tip of the chamber. The CO_2 was then warmed to room temperature and its pressure measured using a manometer (MKS Baratron). An aliquot (ca. 20 µL) of CO_2 was transferred cryogenically into a small glass bottle for eventual in-house C^{13}/C^{12} ratio determination on a Finnigan MAT 251 mass spectrometer. The remaining gas was frozen into a ¼ in. pyrex ampule and set aside for accelerator mass spectrometer ^{14}C analysis.

^{14}C analyses were performed at the Center for Accelerator Mass Spectrometry, Lawrence Livermore National Laboratory. The first step in this analysis is to transform the CO_2 in the pyrex ampule into graphite by iron-catalyzed hydrogen reduction and high pressure encapsulation in tantalum [3]. The sample is introduced into an ion accelerator and is bombarded by cesium ions. This releases C^- ions which are extracted and stripped of four electrons to produce $^{14}C^{+3}$ and $^{13}C^{+3}$. The ratio of these ions is then measured by a ΔE/E nuclear detector and a Faraday cup, respectively.

Results of the ^{13}C and ^{14}C analysis are given in Table B-1, and shown in graphical form in Figure B-2. ^{13}C is expressed as $\delta^{13}C$, which is given in parts per thousand (‰, permille) to a standard, such that:

$$\delta^{13}C = \left[\left(\frac{^{13}C_{sample}}{^{12}C_{sample}} / \frac{^{13}C_{std}}{^{12}C_{std}}\right) - 1\right] \times 1000 \qquad \text{(Eq. B-1)}$$

The standard used is a sample of cretaceous belemnite from the Pee Dee formation in North Carolina, which has a defined $\delta^{13}C$ of zero permille. The results listed here are reported using a scale correction derived from values of -1.06 and -41.48 ‰ for the National Bureau of Standards NBS-20 and NBS-16, respectively [4]. All the ^{14}C measurements were made by normalizing the ^{14}C counting rate for each sample to the corresponding ^{13}C ion beamstrength. The $^{14}C/^{13}C$ were converted to the $^{14}C/^{12}C$ accounting for the measured differences in the $\delta^{13}C$ for samples and standards. The radiocarbon

concentration in this table is given as fraction Modern, $\Delta^{14}C$, and conventional radiocarbon age.

Table B-1 Isotopic Data for carbonaceous material collected at Cheeka Peak.

Sample #	Date sampling started	Volume air Sampled (m^3)	Volume of CO2 evolved (μL)	$\delta^{13}C$ (‰)	Percent modern carbon	$\Delta^{14}C$	^{14}C age (years)
1	3/20/96	1440	382	-37.79 ± 0.02	24.3 ± 0.2	-758 ± 2	11370 ± 70
2	4/13/96	954	354	-37.55 ± 0.02	24.0 ± 0.2	-761 ± 2	11450 ± 70
3	5/14/96	974	350	-36.84 ± 0.02	25.3 ± 0.2	-748 ± 2	11030 ± 70
4	6/7/96	1934	528	-29.35 ± 0.02	66.7 ± 0.5	-336 ± 5	3250 ± 60
5	6/18/96	920	149	-36.47 ± 0.02	33.6 ± 0.2	-666 ± 4	8770 ± 110
6	6/27/96	2040	439	-36.85 ± 0.02	19.7 ± 0.3	-803 ± 2	13040 ± 70

Artifacts of sample storage and handling were investigated using blank analyses of filters. Four types of blanks were considered: CO_2 evolved from heating a prefired ampule containing (a) CuO alone, (b) CuO in an ampule that had been prefired together with a filter, (c) CuO together with a prefired filter, (d) CuO with prefired filters that had been stored for various amounts of time in the storage refrigerator where the samples were kept for 400 days. The results of these blank analyses are summarized in Table B-2. These studies suggest that the largest source of laboratory contamination was due to storage in the refrigerator. To check that the sample processing procedure did not introduce isotopic fractionation, a sample of nicotinic acid ($3\text{-}C_5H_4NCO_2H$) that had been previously analyzed on our equipment was combusted and processed in the same way as our samples. This was repeated using different quantities of nicotinic acid both with and without a prefired filter present in the ampule. These results suggest that no fractionation was introduced by the method.

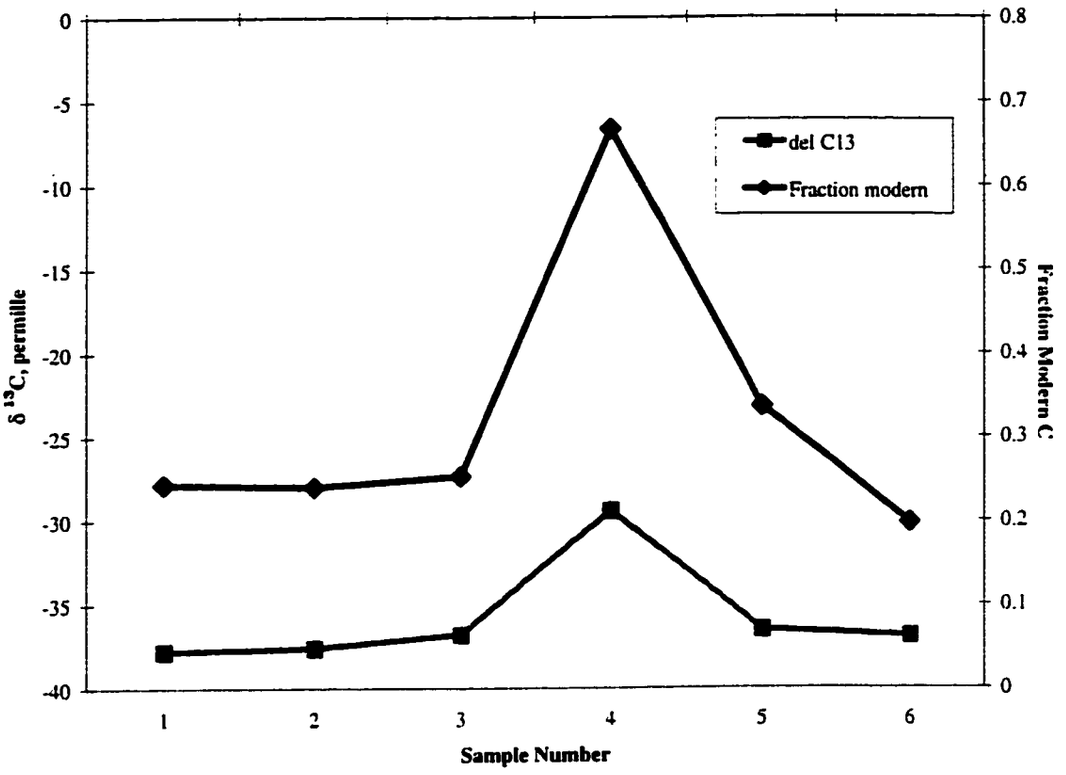

Figure B-2 $\delta^{13}C$ and Fraction Modern carbon as listed in Table B-1.

Table B-2 Effects of blanks on ^{13}C signature.

Blank Description	Volume of CO_2 evolved (μL, STP)	$\delta^{13}C$ (‰ vs. PDB)
CuO Only (Average: n = 2)	2	N/A
Filter fired in ampule prior to sealing	4	N/A
Recently fired filters (average: n = 3)	7	-29.6
Fired filter refrigerated for 20 days (n = 1):	17	-27.2
Fired filter refrigerated for 100 days (n = 4):	18	-28.8
Fired filter refrigerated for 400 days(n = 3)	37	-30.5

DISCUSSION

DEPLETED ^{13}C

The values for $\delta^{13}C$ listed in Table B-1 and shown in Figure B-2 show a depletion in ^{13}C compared to other studies that have examined carbonaceous aerosols in this way. Cachier [5] measured $\delta^{13}C$ for both continental and oceanic samples and found that samples collected in the northern hemisphere were between –25 ‰ and –27 ‰. She found similarity in the isotopic composition of oceanic and continental samples, but

interestingly the samples with the largest depletion were collected in a remote marine location (Enewetak, with –27‰).

The source of the depletion in ^{13}C may not originate on particles, but rather the adsorbed gases collected on the teflon filters. As seen in Chapter 5, the vapor artifact of sampling on quartz filters at this site is over 60% for sampling periods of one week or less. Since the composite $\delta^{13}C$ is the weighted average of the $\delta^{13}C$ from all material on the filter, collection of very depleted vapors such as methane, or products of methane oxidation with a $\delta^{13}C$ of nearly –50‰ [6] could cause a signature of the around –37‰ seen here. The one sample that is enriched in ^{13}C appears to have a different source. Preliminary back trajectory analysis indicates that a significant amount of the air sampled on this filter originated over Alaska. This continental influence may have reduced the relative contribution of adsorbed vapors on the filter, since the isotopic signature is closer to that expected for continental aerosol.

LARGE PERCENTAGE OF FOSSIL CARBON

The relatively low fraction of modern carbon on the samples (ca. 25%) indicates a fossil fuel source dominates. This finding is somewhat difficult to resolve with the explanation involving methane derivatives given for the depletion of ^{13}C, since atmospheric methane measured previously at Cheeka Peak has a radiocarbon content that is 125 % modern [7]. A temporary fossil form of methane from a point source could produce these two signatures together, such as flaming natural gas or a volcanic source such as oceanic "black smokers" but there is no additional evidence at this time supporting such source. A third explanation is that petroleum carbon from the polypropylene sampler leached carbon vapor onto the quartz filter during sampling. Although there was no measurement of the ^{13}C content of this polymer, most petroleum derivatives have a ^{13}C signature that is similar to that of vegetation (~ -26‰) [2]. Furthermore, the consistency in the results seems to point away from contamination during sampling.

CONCLUSION

Isotope measurements of carbonaceous material collected on prefired quartz filters at Cheeka Peak showed consistent depletion in both ^{13}C and ^{14}C. At this time there is no clear explanation for this isotopic signature, but possibilities include adsorbed vapors from a fossil fuel source.

NOTES TO APPENDIX B

1. Sackett, W.M., *The depositional history and isotopic organic carbon compostion of marine sediments.* Mar. Geol., 1964. **2**: p. 173-185.

2. Chesselet, R., M. Fontugne, P. Buat-Menard, U. Ezat, and C.E. Lambert, *The origin of particulate organic carbon in the marine atmosphere as indicated by its stable carbon isotopic composition.* Geophys. Res. Lett., 1981. **8**(4): p. 345-348.

3. Balsley, D.R., G.W. Farwell, P.M. Grootes, and F.H. Schmidt, *Ion source sample preparation techniques for C-14 AMS measurements.* Nucl. Instrum. Methods, 1987. **B29**: p. 37-40.

4. Coplen, T.B., C. Kendall, and J. Hopple, *Comparison of stable isotope reference standards.* Nature, 1983. **302**: p. 235-238.

5. Cachier, H., *Isotopic Characterization of Carbonaceous Aerosols.* Aerosol Science and Technology, 1989. **10**: p. 379-385.

6. Sugimoto, A., *GC/GC/C/IRMS system for carbon isotope measurement of low level methane concentration.* Geochemical Journal, 1996. **30**(3): p. 195-200.

7. Quay, P.D., S.L. King, J. Stutsman, D.O. Wilbur, L.P. Steele, I. Fung, R.H. Gammon, T.A. Brown, G.W. Farwell, P.M. Grootes, and F.H. Schmidt, *Carbon isotopic composition of atmospheric CH4: Fossil and biomass burning source strengths.* Global Biogeochem.Cycles, 1991. **5**(1): p. 25-47.

VITA

Michael Jacobson

University of Washington

1997

Michael Jacobson was born on November 11, 1969 in Shiprock, New Mexico, USA. He is the son of William and Marilyn Jacobson. He grew up in West Lafayette, Indiana, where he graduated from West Lafayette High School. He received his Bachelor of Arts in chemistry from Carleton College, in Northfield, Minnesota. He received a Fulbright fellowship to study for one academic year in Stockholm, Sweden, which he completed in June, 1997. In December, 1997 he completed the requirements for the degree of Doctor of Philosophy in Environmental/Analytical Chemistry at the University of Washington in Seattle, WA, USA.